6D strings and exceptional instantons

Hee-Cheol Kim[1,2,*], Joonho Kim[3,†], Seok Kim,[4,‡] Ki-Hong Lee,[4,§] and Jaemo Park[2,∥]

[1]*Jefferson Physical Laboratory, Harvard University, Cambridge, Massachusetts 02138, USA*
[2]*Department of Physics, Postech, Pohang 790-784, Korea*
[3]*School of Physics, Korea Institute for Advanced Study, Seoul 130-722, Korea*
[4]*Department of Physics and Astronomy and Center for Theoretical Physics, Seoul National University,*
Seoul 151-747, Korea

We propose new ADHM-like methods to compute the Coulomb branch instanton partition functions of 5D and 6D supersymmetric gauge theories, with certain exceptional gauge groups or exceptional matters. We study G_2 theories with $n_7 \leq 3$ matters in $\mathbf{7}$ and $SO(7)$ theories with $n_8 \leq 4$ matters in the spinor representation $\mathbf{8}$. We also study the elliptic genera of self-dual instanton strings of 6D SCFTs with exceptional gauge groups or matters, including all non-Higgsable atomic SCFTs with rank 2 or 3 tensor branches. Some of them are tested with topological vertex calculus. We also explore a D-brane-based method to study instanton particles of 5D $SO(7)$ and $SO(8)$ gauge theories with matters in spinor representations, which further tests our ADHM-like proposals.

I. INTRODUCTION

Instantons are semiclassical representations of nonperturbative quantum phenomena. In Yang-Mills gauge theories, instantons given by self-dual gauge fields on $\mathbb{R}^4$ play important roles in various contexts. For gauge theories in higher dimensions, $d > 4$, they can be solitonic objects rather than vacuum tunneling, being particles in 5D and strings in 6D.

Self-dual Yang-Mills instanton solutions have continuous parameters, which form a moduli space. Understanding the moduli space dynamics is often an important step toward better understanding the physics of instantons. For gauge theories with classical gauge groups, the self-dual solutions and the moduli space dynamics can be described by the ADHM formalism [1]. The ADHM formalism provides gauge theories on the world volume of instantons (1D for particles, 2D for strings), which at low energy reduce to the nonlinear sigma models on the instanton moduli space. In string theory, such gauge theories come from open fundamental strings between Dp-D($p + 4$)

*heecheol1@gmail.com
†joonhokim@kias.re.kr
‡skim@phya.snu.ac.kr
§khlee11812@gmail.com
∥jaemo@postech.ac.kr

branes. This is why only classical gauge groups admit such constructions. Including matters to gauge theories also affects the moduli space dynamics of instantons. Open strings can engineer matters in the fundamental or rank 2 product representations. This gives the notion of "classical matters," whose inclusion to the instanton moduli space dynamics still admits ADHM description. But matters in other representations, like higher rank product representations or spinor representations of $SO(N)$, cannot be engineered using open strings. We shall call them "exceptional matters."

Yang-Mills instantons also play crucial roles in supersymmetric gauge theories. Among others, in 4d $\mathcal{N} = 2$ theories, the Seiberg-Witten solution [2] in the Coulomb branch acquires all order multi-instanton contributions. It can be microscopically derived by computing the instanton partition function [3] on $\mathbb{R}^4$ with the so-called Omega deformation. The uplifts of this partition function to 5D $\mathcal{N} = 1$ gauge theories on $\mathbb{R}^4 \times S^1$, and to 6D $\mathcal{N} = (1, 0)$ gauge theories on $\mathbb{R}^4 \times T^2$, are also important observables of 5D/6D superconformal field theories (SCFTs). The computation of this partition function in [3] relies on the ADHM method, applicable only to classical gauge theories. However, exceptional gauge theories are also important in various situations. For instance, one often uses various (p, q) 7-branes wrapped on 2-cycles to engineer 6D $\mathcal{N} = (1, 0)$ SCFTs, which admit exceptional gauge groups and matters rather generically.

In this paper, we develop ADHM-like formalisms of instantons for a small class of exceptional gauge groups or matters, which can be used to study the instanton partition

functions in the Coulomb phase. Namely, we provide 1D/2D gauge theories which we suggest to describe certain aspects of exceptional instanton particles and strings. We managed to find such formalisms for G_2 theories with matter hypermultiplets in **7** and for $SO(7)$ theories with exceptional matters in the spinor representation **8**. We also expect their 0D reductions to describe exceptional instantons of 4D gauge theories, although we do not study them here. In 5D, we can describe G_2 theories with $n_7 \leq 3$ matters in **7** and $SO(7)$ instantons with $n_8 \leq 4$ matters in **8**. In 6D, gauge anomaly cancellations restrict our setup to $n_7 = 1$ and $n_8 = 2$.

Our constructions have the following features. The correct instanton moduli space has G_r isometry for gauge group G_r of rank r. However, our gauge theories realize the symmetry only in a subgroup H_r with same rank. We always take H_r to be a classical group, say $H_r = SU(r+1)$. The moduli space of G_r instantons contains that of $H_r \subset G_r$ instantons as a subspace. Our 1D/2D gauge theories only realize the latter correctly. Away from this subspace, only the dimensions of moduli space agree. So, we *do not expect* that our gauge theories capture the full moduli space dynamics of the exceptional G_r instantons. In the Coulomb branch, the instanton size and the G_r gauge orbit parts of the moduli space are lifted to a set of isolated points (which are nondegenerate after Omega deformation). We propose that our gauge theories correctly compute the Coulomb branch observables of G_r instantons. In fact, the supersymmetry (SUSY) partition functions of our models in the Coulomb branch exhibit full G_r symmetry. More precisely, since we turn on r Coulomb vacuum expectation values (VEVs), we find that the Weyl symmetry of H_r enhances to that of G_r. Since the UV gauge theory flows to the nonlinear sigma model on the moduli space, this is a kind of IR symmetry enhancement.

Our ADHM-like descriptions are found based on trials-and-errors. We start from H_r classical ADHM construction, and add more world volume matters and interactions to suit the physics. In particular, they are motivated by [4], where 2D gauge theories were found for the instanton strings of non-Higgsable 6D $SU(3)$ gauge theories. Although $SU(3)$ is a classical group, 6D non-Higgsable $SU(3)$ gauge theory cannot be engineered by using just D-branes. Rather, it is engineered by using mutually nonlocal 7-branes wrapping a 2-cycle, in precisely the same way as engineering exceptional gauge theories. Incidentally, the naive ADHM description for $SU(3)$ instantons is sick, by having 2D gauge anomalies. The correct gauge theories for the $SU(3)$ instanton strings were found in [4]. Its reduction to 1D provides a novel alternative ADHM-like description for $SU(3)$ instantons. The ADHM-like descriptions of this paper extend these results, related by Higgsings $SO(7) \xrightarrow{\text{VEV of } \mathbf{8}} G_2 \xrightarrow{\text{VEV of } \mathbf{7}} SU(3)$.

In 6D, G_2 and $SO(7)$ theories with matters are somewhat important, as they appear in the "atomic" constituents of 6D

SCFTs [5,6].[1] Roughly speaking, in the list of atomic 6D SCFTs, there are nine of them with rank 1 tensor branches. They are constructed by putting F-theory on an elliptic Calabi-Yau threefold, whose base is given by the $O(-n) \rightarrow \mathbb{P}^1$ bundle with $n = 1, 2, \ldots, 8, 12$ [7–9]. Also, there are three more atomic SCFTs with higher rank tensor branches called "32," "322," and "232" [10]. Constructing more complicated 6D SCFTs is basically forming "quivers" of these atoms [5,6,10]. The last three atomic SCFTs with higher rank tensor branches contain $G_2 \times SU(2)$ or $SO(7) \times SU(2)$ gauge symmetries with half-hypermultiplets in $(\mathbf{7}, \mathbf{2})$ or $(\mathbf{8}, \mathbf{2})$, respectively. See Sec. IV for a summary. Our descriptions of G_2 and $SO(7)$ instantons allow us to study the instanton strings of such SCFTs. Collecting recent studies and new findings of this paper, one now has 2D gauge theory methods to study the strings of the following 6D atomic SCFTs: $O(-1)$ theory [11,12], $O(-2)$ theory [13], $O(-3)$ theory [4], $O(-4)$ theory [14], and all three higher rank theories (this paper). Quivers of these 2D theories are also explored in [4,12,13,15]. Among others, these gauge theories can be used to study the elliptic genera of the strings. These elliptic genera were also studied using other approaches, including the topological vertex methods [16] and the modular bootstraplike approach [17–20].

We test the BPS spectra of our ADHM-like models using various alternative approaches. Among others, in Sec. III, we develop a D-brane-based approach to study exceptional instanton particles in 5D gauge theories. This approach is applicable to G_2 instantons, and $SO(7)$ or $SO(8)$ instantons with matters in spinor representations. For G_2 and $SO(7)$ cases, the Witten indices computed from this approach test our ADHM-like proposals. Also, a 5D description for the circle compactified 232 SCFT [10] has been found in [16], using 5-brane webs. This allows us to compute the BPS spectrum of its strings using topological vertices. We do this calculus in Sec. IV and find agreement with our new gauge theories.

We leave a small technical remark on $SO(7)$ instantons. The canonical ADHM description for k $SO(7)$ instantons (without matters in **8**) is given by an $Sp(k)$ gauge theory. Its partition function is given by a contour integral [21,22], yielding a complicated residue sum. Unlike $SU(N)$ instanton partition functions, in which case closed form expressions for the residue sums are known [3], such expressions have been unknown for $SO(N)$. In this paper, using our alternative ADHM-like description, we find a closed form residue sum expression for $SO(7)$.

The rest of this paper is organized as follows. In Sec. II, we sketch the basic ideas. We then present the ADHM-like

---

[1]There are closely related but slightly different notions in the literature, such as atomic SCFTs, "minimal" SCFTs, non-Higgsable clusters, and so on. We are not very careful about the distinctions here.

descriptions of instantons for $SO(7)$ theories with matters in **8** and G_2 theories with matters in **7**. In Sec. III, we explore alternative D-brane descriptions to study certain exceptional instanton particles and use them to test our proposals. In Sec. IV, we construct the 2D gauge theories for the strings of 6D atomic SCFTs with rank 2 or 3 tensor branches, with $G_2 \times SU(2)$, $G_2 \times SU(2) \times \{\}$, $SU(2) \times SO(7) \times SU(2)$ gauge groups. We test the last one with topological vertices. Section V concludes with various remarks.

II. EXCEPTIONAL INSTANTON PARTITION FUNCTIONS

Our proposal is based on the following ideas: (1) we are interested in the Coulomb phase partition functions of exceptional instantons, not in the symmetric phase. (2) In the Coulomb phase, the instanton moduli space is lifted by massive parameters, to saddle points lying within the moduli space of instantons with classical subgroups. (3) Thus, we only seek for a formalism to study the massive fluctuations around the last saddle points, accomplished by extending ADHM formalisms for classical instantons. We elaborate on these ideas in some detail.

A. Coulomb phase.— We are interested in the gauge theory in the Coulomb branch. Suppose that the gauge group G_r has rank r. We turn on nonzero VEV v of the scalar in the vector multiplet, which breaks G_r to $U(1)^r$. In 6D, vector multiplet does not contain scalars. In this case, we consider the theory compactified on circle, with nonzero holonomy playing the role of Coulomb VEV. In the symmetric phase, instantons develop a moduli space, part of which being gauge orientations and instanton sizes. In

the Coulomb phase, there appears nonzero potential on the instanton moduli space, proportional to v^2. This potential lifts the size and orientation 0-modes. There are extra $4k$ position moduli of k instantons on $\mathbb{R}^4$, which will also be lifted in the Omega background. The moduli space is then completely lifted to points. So, we expect that it suffices to understand the quantum dynamics of instantons near these points.

B. ADHM on a subspace.— The second idea is that one can use the ADHM formalism of instantons when G_r is a classical group. In d-dimensional gauge theory, the ADHM formalism can be understood as a $(d-4)$-dimensional gauge theory living on the instanton solitons. For classical G_r, the low energy moduli space of $(d-4)$-dimensional gauge theory is the instanton moduli space, so one expects in IR to get nonlinear sigma models on the instanton moduli space. When G_r is exceptional, no such formalisms are known. However, it is often possible to find a classical subgroup $H_r \subset G_r$ of the given exceptional group G_r with same rank. Then, we try to describe the (massive) quantum fluctuations around the saddle points by expanding the H_r ADHM formalism, adding more $(d-4)$-dimensional fields. This is where we need educated guesses, in the spirit of model buildings. We want a subgroup H_r with same rank as G_r, partly because we wish our formalism to see all $U(1)^r$ in the Coulomb phase. Possible G_r and H_r are given in Table I, when H_r is a simple group. To study exceptional matters of $SO(7)$, we shall also consider $H = SU(4)$ for $G = SO(7)$.

For example, consider the case with $H_{r=N-1} = SU(N)$. The $SU(N)$ ADHM description of k instantons has $U(k)$ gauge symmetry and the following fields:

$$\text{Chiral:}\ (q, \psi) \in (\mathbf{k}, \overline{\mathbf{N}}), \qquad (\tilde{q}, \tilde{\psi}) \in (\bar{\mathbf{k}}, \mathbf{N}), \qquad (a, \Psi), (\tilde{a}, \tilde{\Psi}) \in (\mathbf{adj}, \mathbf{1})$$
$$\text{Vector} \sim \text{Fermi:}\ (A_\mu, \lambda_0) \in (\mathbf{adj}, \mathbf{1}), \qquad (\lambda) \in (\mathbf{adj}, \mathbf{1}). \tag{2.1}$$

The fields are organized into 2D $\mathcal{N} = (0, 2)$ supermultiplets, and we have shown the representations in $U(k) \times SU(N)$. Fields in a parenthesis denote bosonic/fermionic ones in a multiplet, while (λ) denotes a Fermi multiplet.

These fields combine to $\mathcal{N} = (0, 4)$ vector multiplet and hypermultiplets. The instanton moduli space is obtained from the scalar fields, subject to the complex ADHM constraint and the D-term constraint (real ADHM constraint),

$$q\tilde{q} + [a, \tilde{a}] = 0, \quad qq^\dagger - \tilde{q}^\dagger \tilde{q} + [a, a^\dagger] + [\tilde{a}, \tilde{a}^\dagger] = 0, \tag{2.2}$$

TABLE I. Possible choices of H_r for various G_r, when H_r is a simple group.

G_r	H_r	Branching rules
G_2	$SU(3)$	$\mathbf{14} \to \mathbf{8} \oplus \mathbf{3} \oplus \bar{\mathbf{3}},\ \mathbf{7} \to \mathbf{3} \oplus \bar{\mathbf{3}} + \mathbf{1}$
F_4	$SO(9)$	$\mathbf{52} \to \mathbf{36} \oplus \mathbf{16},\ \mathbf{26} \to \mathbf{1} \oplus \mathbf{9} \oplus \mathbf{16}$
E_7	$SU(8)$	$\mathbf{133} \to \mathbf{63} \oplus \mathbf{70},\ \mathbf{56} \to \mathbf{28} \oplus \overline{\mathbf{28}}$
E_8	$SU(9)$	$\mathbf{248} \to \mathbf{80} \oplus \mathbf{84} \oplus \overline{\mathbf{84}}$
E_8	$SO(16)$	$\mathbf{248} \to \mathbf{120} \oplus \mathbf{128}$
$SO(7)$	$SU(4)$	$\mathbf{21} \to \mathbf{15} \oplus \mathbf{6},\ \mathbf{8} \to \mathbf{4} \oplus \bar{\mathbf{4}}$

and after modding out by the $U(k)$ gauge orbit. More precisely, the nonlinear sigma model on the instanton moduli space is obtained from the gauged linear sigma model at low energy. This part is the standard ADHM construction of $SU(N)$ instantons. Now we should add extra light fields, including more scalars to describe G_r

instantons' extra moduli. d-dimensional vector multiplet in G_r decomposes in H_r as

$$\mathbf{adj}(G) \rightarrow \mathbf{adj}(H)\bigoplus_i \mathbf{R}_i(H), \qquad (2.3)$$

where $\mathbf{R}_i(H)$ are suitable representations of H_r in Table I. Vector multiplet in $\mathbf{adj}(H)$ induces the standard instanton moduli, described in UV by the above ADHM description. Vector multiplets in $\mathbf{R}_i$ introduce further moduli, whose real dimension is $4kT(\mathbf{R}_i)$. $T(\mathbf{R})$ is the Dynkin index of $\mathbf{R}$. When $\mathbf{R}_i$ is a fundamental representation or rank 2 product representations, we managed to find the extra fields. We are technically motivated by the mathematical constructions of [23], but will simply present them as our "ansatz" for the UV uplift of these zero modes. From Table I, one finds that $\mathbf{R}_i$'s are product representations with ranks less than or equal to 2 only for $G_2 \supset SU(3)$ and $SO(7) \supset SU(4)$. For these, the adjoint representations of G_r decompose as

$$SU(3) \subset G_2 \colon \mathbf{14} \rightarrow \mathbf{8} \oplus \mathbf{3} \oplus \bar{\mathbf{3}} = \mathbf{8} \oplus \mathbf{3} \oplus \mathbf{anti}(\mathbf{3} \otimes \mathbf{3})$$

$$SU(4) \subset SO(7) \colon \mathbf{21} \rightarrow \mathbf{15} \oplus \mathbf{6}. \qquad (2.4)$$

We shall present extra chiral and Fermi multiplets with suitable interactions in the next subsections, which extends the moduli space in $\sum_i 4kT(\mathbf{R}_i)$ new directions.

C. When it fails.— We made similar trials with other exceptional gauge groups and matters, which failed. It may be worthwhile to briefly report the reasons of failure. A typical reason is that the UV theory has extra branch of moduli space that does not belong to our instanton moduli space at low energy. Namely, apart from the exceptional instanton's moduli space, one sometimes has extra branch which cannot be lifted by supersymmetric potentials.

For instance, we tried to extend the ADHM construction of $H = SU(8), SU(9)$ to get those for $G = E_7, E_8$. In these cases, $\mathbf{R}_i$'s are product representations of rank 4 and 3, respectively. We made several trials to realize the extra moduli with right dimensions, especially without unwanted extra branches of moduli space which may spoil the instanton calculus. We however failed to get the precise descriptions, despite finding models which partly exhibit the right physics of instantons and instanton strings. See Sec. V for more discussions.

We also suspect that some choice of $H_r \subset G_r$ may miss certain small instanton saddle points. To clearly understand this issue, we should find more examples than we have now.

There are simpler examples in which our new formalism fails. For instance, we consider our alternative $SO(7)$ ADHM (Sec. II A) and try to add zero modes from matters in $\mathbf{7}$ (vector representation). Zero modes of $\mathbf{7}$ are well known in the standard $SO(N)$ ADHM, which form an $Sp(k)$ fundamental Fermi multiplet. In our $SU(4) \times U(k)$ formalism, $\mathbf{7}$ is regarded as $\mathbf{7} \rightarrow \mathbf{6} + \mathbf{1}$. We can ignore the

singlet if the gauge orientation of instantons is along $SU(4)$. $\mathbf{6}$ is the rank 2 antisymmetric representation. According to [23], and in D-brane engineerings, the ADHM fields induced by matters in bulk antisymmetric representation include scalars in rank 2 symmetric representation of $U(k)$. This creates an extra branch of moduli space which is unphysical in the instanton calculus, but is present only in the UV uplifts. Even in ADHM models engineered by string theory, there are often such extra branches. In [22], the contributions from these branches are factored out, mainly guided by string theory. However, including this extra branch in our $SO(7)$ ADHM-like model, we find it difficult to properly identify and separate the extra contributions. Similarly, we cannot do an ADHM-like calculus for the 5D G_2 $\mathcal{N} = 1^*$ theory.

Now, we explain examples that turn out to work.

A. $SO(7)$ instantons and matters in 8

The adjoint representation of $SO(7)$ decomposes in $SU(4)$ as $\mathbf{21} \rightarrow \mathbf{15} + \mathbf{6}$. We first seek for an alternative ADHM-like formalism of pure $SO(7)$ instantons, extending $SU(4)$ ADHM. We explain it as the quantum mechanics of instanton particles in 5D $\mathcal{N} = 1$ Yang-Mills theory.

The quantum mechanics for k $SU(4)$ instantons has $U(k)$ gauge symmetry. It has following fields: $\mathcal{N} = (0, 4)$ $U(k)$ vector multiplet, consisting of 1D reduction of 2D gauge fields $A_\mu = (A_0, \varphi = A_1)$, and fermions λ_0, λ; hypermultiplets with bosonic fields $q_i, \tilde{q}^i$ in $(\mathbf{k}, \bar{\mathbf{4}}) + (\bar{\mathbf{k}}, \mathbf{4})$, where $i = 1, 2, 3, 4$; hypermultiplets with bosonic fields $a, \tilde{a}$ in $(\mathbf{adj}, \mathbf{1})$. In IR, one imposes

$$D \sim qq^\dagger - \tilde{q}^\dagger \tilde{q} + [a, a^\dagger] + [\tilde{a}, \tilde{a}^\dagger] = 0,$$
$$J_\lambda \sim q\tilde{q} + [a, \tilde{a}] = 0 \qquad (2.5)$$

by D-term or J-term potentials in the $\mathcal{N} = (0, 2)$ language. See [4,24,25] for the notations and reviews. These constraints and modding out by $U(k)$ gauge orbit eliminate $2k^2$ complex variables from $2k^2 + 8k$ components of $q, \tilde{q}, a, \tilde{a}$. So, one finds $8k$ complex moduli.

With extra vector multiplet fields in $\mathbf{6}$, there are extra bosonic zero modes. A vector multiplet in rank 2 antisymmetric representation of $SU(N)$ induces $2kT(\mathbf{anti}_2) = k(N - 2)$ complex bosonic zero modes in k instanton background. So, we should add extra fields in UV and modify interactions, to get extra $2k$ complex bosonic modes at $N = 4$. We find that the following extra fields, taking the forms of $\mathcal{N} = (0, 2)$ chiral or Fermi multiplets, yield the right physics[2] (only bosonic fields shown for the chiral multiplets):

---

[2]Our motivation behind introducing this ansatz for the UV theory is described below (2.2). All involved technical steps in identifying extra zero modes are summarized in the Appendix.

Chiral ϕ_i: $(\bar{\mathbf{k}}, \bar{\mathbf{4}})_{J=\frac{1}{2}}$

Chiral $b, \tilde{b}$: $(\overline{\mathbf{anti}}_2, \mathbf{1})_{J=\frac{1}{2}}$

Fermi $\hat{\lambda}$: $(\mathbf{sym}_2, \mathbf{1})_{J=0}$

Fermi $\check{\lambda}$: $(\mathbf{sym}_2, \mathbf{1})_{J=-1}$. $\qquad$ (2.6)

$\mathbf{sym}_2, \mathbf{anti}_2$ denote rank 2 (anti)symmetric representations of $\mathbf{k}$, and the charge J in the subscript will be explained shortly. We introduced extra $4k + 2 \cdot \frac{k^2-k}{2}$ complex bosonic fields. Using the extra Fermi fields $\hat{\lambda}, \check{\lambda}$, we introduce the following interactions. As noted in [4], the desired interactions should be nonholomorphic in the chiral multiplet fields, which is possible only with $\mathcal{N} = (0,1)$ SUSY. Therefore, we regard all these fields as $(0,1)$ superfields, as explained in [4], and turn on the following $\mathcal{N} = (0,1)$ superpotential:

$$J_{\hat{\lambda}}^{(0,1)} \sim (\phi_i q^{i\dagger})_S + (ba^\dagger + \tilde{b}\tilde{a}^\dagger)_S,$$
$$J_{\check{\lambda}}^{(0,1)} \sim (\phi_i \tilde{q}^i)_S + (\tilde{b}a - b\tilde{a})_S. \qquad (2.7)$$

The subscripts S denote symmetrization of the $k \times k$ matrices. We want (2.7) to be the only source of breaking (0,2) SUSY to (0,1) in the classical action. The D-term is given by

$$D \sim qq^\dagger - \tilde{q}^\dagger \tilde{q} - \phi^\dagger \phi + [a, a^\dagger] + [\tilde{a}, \tilde{a}^\dagger] - 2b^\dagger b - 2\tilde{b}^\dagger \tilde{b}. \qquad (2.8)$$

Then, since $|J|^2$ appear in the bosonic potential for each J, one imposes at low energy extra $k^2 + k$ complex constraints from the new superpotentials. Collecting all, one finds

$$3 \cdot 4k + 2 \cdot k^2 + 2 \cdot \frac{k^2-k}{2} - 2k^2 - 2 \cdot \frac{k^2+k}{2} = 10k \qquad (2.9)$$

complex bosonic zero modes. This agrees with the dimension $2kc_2$ of $SO(7)$ instanton moduli space, where $c_2(SO(2N+1)) = 2N - 1$. The $SU(4)$ ADHM quantum mechanics with extra charged fields given by (2.6) is our proposed ADHM-like formalism for $SO(7)$ instantons.

We explain the symmetries of this model. All symmetries we explain below are compatible with the superpotentials. It first has $SU(4)$ symmetry. There is also a $U(1)_J$ symmetry, whose charges J we already listed above when we introduced fields. There is also $SU(2)_l$, which rotates $a, \tilde{a}$ and also $b, \tilde{b}$ as doublets. The charges and representations are summarized in Table II. This system has only $\mathcal{N} = (0,1)$ supersymmetry and $SU(4)$ global symmetry in UV. We assert that they enhance to (0,4) SUSY and $SO(7)$ in IR, when we compute the Coulomb branch partition functions. $SO(7)$ enhancement will be visible as $SO(7)$ character expansions of the partition functions. In the

TABLE II. Charges/representations of fields in our $SO(7)$ ADHM-like model.

Fields	$U(k)$	$SU(4)$	$U(1)_J$	$SU(2)_l$
$(q_i, \tilde{q}^i)$	$(\mathbf{k}, \bar{\mathbf{k}})$	$(\bar{\mathbf{4}}, \mathbf{4})$	$\frac{1}{2}$	**1**
$(a, \tilde{a})$	$\mathbf{adj}$	**1**	$\frac{1}{2}$	**2**
(λ_0, λ)	$\mathbf{adj}$	**1**	$(0, -1)$	**1**
ϕ_i	$\bar{\mathbf{k}}$	$\bar{\mathbf{4}}$	$\frac{1}{2}$	**1**
$(b, \tilde{b})$	$\overline{\mathbf{anti}}_2$	**1**	$\frac{1}{2}$	**2**
$(\hat{\lambda}, \check{\lambda})$	$\mathbf{sym}_2$	**1**	$(0, -1)$	**1**

context of SUSY enhancement, we claim that $U(1)_J$ enhances to $SU(2)_r \times SU(2)_R$, where $SO(4) = SU(2)_r \times SU(2)_l$ rotates the spatial $\mathbb{R}^4$ on which particles can move, and $SU(2)_R$ is the 5D R-symmetry. J is identified as $J = \frac{J_r + J_R}{2}$, where J_r, J_R are the Cartans of $SU(2)_r, SU(2)_R$. One Cartan is not visible in UV. The index of our models will agree with different computations whose settings manifestly preserve (0,4) SUSY.

We study the moduli space, with and without 5D Coulomb VEV. For technical reasons, let us just consider the case with $k = 1$. At $k = 1$, the fields $b, \tilde{b}$ are absent, and $a, \tilde{a}$ are free fields for the center-of-mass motion. First, consider the symmetric phase at $v = 0$. One should solve the following equations:

$$|q_i|^2 - |\tilde{q}^i|^2 - |\phi_i|^2 = 0, \quad q_i \tilde{q}^i = 0,$$
$$\phi^{\dagger i} q_i = 0, \quad \tilde{q}^i \phi_i = 0. \qquad (2.10)$$

At $\phi_i = 0$, this is the equation for the $SU(4)$ instantons. This subspace is the cone over $SU(4)/U(2)$. Away from $\phi_i = 0$, although the dimension of the moduli space is same as the relative moduli space of an $SO(7)$ instanton, the two moduli spaces are different. The proper $SO(7)$ instanton moduli space is the cone over the $SO(7)/(SU(2) \times SO(3))$ coset, whose metric is given by the homogeneous metric. However, we find no $SO(7)$ isometry on our moduli space.

In the Coulomb branch and with the Omega deformation, the moduli space lifts to isolated points, on the $SU(4) \subset SO(7)$ instanton moduli space. To see this, we expand the studies of [26]. The Coulomb VEV v_i $(i = 1, \ldots, 4)$ satisfying $\sum_i v_i = 0$ couples to the 1D fields as follows. Let us denote by $\varphi \equiv A_1$ the scalar in the 1D vector multiplet. v is a traceless diagonal matrix, with eigenvalues v_i. Nonzero v changes the coupling to φ as follows:

$$|\varphi q|^2 + |\tilde{q}\varphi|^2 + |\phi\varphi|^2$$
$$\to |\varphi q - qv|^2 + |v\tilde{q} - \tilde{q}\varphi|^2 + |v\phi + \phi\varphi|^2. \qquad (2.11)$$

This is because φ, v are scalars in the 1D vector multiplet of $U(k) \times SU(4)$, where v is a background field, and fields

couple to them according to their representations in $U(k) \times SU(4)$. Note that the relative $-$ signs for $q, \tilde{q}$ appear because they are in the bifundamental representations $(\mathbf{k}, \bar{\mathbf{4}})$ or its conjugate, while relative $+$ sign for ϕ is because it is in $(\bar{\mathbf{k}}, \bar{\mathbf{4}})$. We set all complete square terms to zero at energies lower than 1D gauge coupling. One should also minimize the following D-term potential at $k = 1$:

$$V \leftarrow (|q|^2 - |\tilde{q}|^2 - |\phi|^2 - \xi)^2. \qquad (2.12)$$

Here, since we have a $U(k)$ gauge theory, we have turned on a Fayet-Iliopoulos (FI) parameter, ξ, which we take to be positive $\xi > 0$ for convenience. ξ can also be taken to be negative, without changing the Coulomb phase partition function, as we shall see below. However, physics is easier to interpret with $\xi > 0$. So we set (at $k = 1$)

$$v_i q_i = \varphi q_i, \quad v_i \tilde{q}^i = \varphi \tilde{q}^i, \quad v_i \phi_i = -\varphi \phi_i, \qquad (2.13)$$

where $i = 1, 2, 3, 4$ indices are not summed over, and

$$|q_i|^2 - |\tilde{q}^i|^2 - |\phi_i|^2 = \xi > 0. \qquad (2.14)$$

Equation (2.13) is not eigenvector equation for the matrix v, whose eigenvalues are φ for $q, \tilde{q}$ to be nonzero, and $-\varphi$ for ϕ to be nonzero. From (2.14), one should have $q_i \neq 0$, which means that φ is set equal to one of the v_i's. Then one can have nonzero q_i at the saddle point, whose value is tuned to meet (2.14). At generic values of v_i's, one should set $\phi_i = 0$, meaning that we are forced to stay in the $SU(4)$ instanton moduli space.[3] So, in the Coulomb branch calculus, ϕ provides massive degrees of freedom living on the $SU(4)$ instanton moduli space.

The Witten index of the quantum mechanics preserving (0,4) SUSY is defined by

$$Z_k(\epsilon_{1,2}, v_i) = \text{Tr}_k[(-1)^F e^{-\epsilon_1(J_1+J_R)} e^{-\epsilon_2(J_2+J_R)} e^{-v_i q_i} e^{-m_a F_a}], \qquad (2.15)$$

where trace is over states in the k instanton sector. J_1, J_2 are the two Cartans of $SO(4)$ which rotate the spatial $\mathbb{R}^4$, where they rotate mutually orthogonal $\mathbb{R}^2$ factors. They are related to $J_{l,r}$ by $J_r = \frac{J_1+J_2}{2}, J_l = \frac{J_1-J_2}{2}$. J_R is the Cartan of $SU(2)_R$ coming from the 5D R-symmetry. Note that only the combination $J_r + J_R = 2J$ appears, so our UV model can fully detect them. q_i are the r electric charges in $U(1)^r \subset G_r$, which is $SO(7)$ here. F_a denote other flavor symmetries, which is absent now but introduced for later purpose. The measures are chosen to commute with two

---

[3]At this stage, $\tilde{q}^i$ can also be nonzero by solving the same eigenvector equation as q_i. However, as shown in the Appendix of [26], the eigenvector equations for q_i and $\tilde{q}^i$ become different with nonzero Omega background parameter. Therefore, in the fully Omega-deformed background, only q_i is nonzero.

Hermitian supercharges $Q^{A\dot{\alpha}} = Q^{+\dot{-}}, Q^{-\dot{+}}$. See, e.g., [22] for the notations. These two supercharges are mutually Hermitian conjugate, which we write as $Q, Q^\dagger$. They form a pair of fermionic oscillators, pairing a set of bosonic and fermionic states. Such a pair of states is not counted in the index, as their contributions cancel due to the factor $(-1)^F$. Such a Hilbert space interpretation will hold with as little as (0,2) SUSY. In our UV (0,1) system, we abstractly interpret the partition function as a SUSY path integral of the Euclidean quantum field theory (QFT) on T^2. 1 Hermitian SUSY in UV is enough to derive the formula for Z_k available in the literatures. Its path integral should agree well with the index (2.15), possibly up to an overall prefactor.

For gauge theories, this index can be evaluated by a residue sum [22,27,28] (see also [29,30]). Note that [31] also discussed the diagrammatic classification of Jeffrey-Kirwan (JK)-residues (Res) in the 4D version of the SO gauge theory. The formula was discussed in the context of (0,2) theories, but it applies with one Hermitian supercharge as well [4]. In our model, the contour integral takes the following form[4]:

$$Z_k = \frac{1}{k!} \oint \prod_{I=1}^k \frac{d\phi_I}{2\pi i}$$

$$\cdot \frac{\prod_{I\neq J} 2\sinh\frac{\phi_{IJ}}{2} \cdot \prod_{I,J} 2\sinh\frac{2\epsilon_+ - \phi_{IJ}}{2}}{\prod_{I=1}^k \prod_{i=1}^4 2\sinh\frac{\epsilon_+ \pm (\phi_I - v_i)}{2} \cdot \prod_{I,J} 2\sinh\frac{\epsilon_{1,2} + \phi_{IJ}}{2}}$$

$$\times \frac{\prod_{I\leq J}(2\sinh\frac{\phi_I+\phi_J}{2} \cdot 2\sinh\frac{\phi_I+\phi_J-2\epsilon_+}{2})}{\prod_I \prod_i 2\sinh\frac{\epsilon_+ -\phi_I - v_i}{2} \cdot \prod_{I<J} 2\sinh\frac{\epsilon_{1,2} - \phi_I - \phi_J}{2}}.$$

$$(2.16)$$

Here, $\phi_{IJ} \equiv \phi_I - \phi_J$, and 2 sinh factors with repeated signs or subscripts (like $\pm$ or $\epsilon_{1,2}$) are all multiplied. The $SU(4)$ chemical potentials satisfy $\sum_{i=1}^4 v_i = 0$. We also used $\epsilon_\pm \equiv \frac{\epsilon_1 \pm \epsilon_2}{2}$. The integrand on the first line comes from the $SU(4)$ ADHM fields $q, \tilde{q}, a, \tilde{a}$ and $U(k)$ vector multiplet fermions. The second line comes from the extra fields.

The integral can be performed as follows. The nonzero residue contributing to Z_k is called the JK-residue. To define this, one first picks up an auxiliary vector η in the k-dimensional charge space ("conjugate" to the integral variables ϕ_I). Possible poles in the integrand are given by hyperplanes of the form $\rho_\alpha \cdot \phi + \cdots = 0$, where the expression on the left-hand side comes from the argument of the sinh factors $2\sinh\frac{\rho_\alpha \cdot \phi + \cdots}{2}$ in the denominator of (2.16). One can in general pick $d(\geq k)$ charge vectors ρ_α, $\alpha = 1, \ldots, d$ and hyperplanes to specify a pole. In our systems, all relevant poles satisfy $d = k$. With chosen η, JK-

---

[4]The overall signs of Z_k are fixed by requiring agreement with the index for the $Sp(k)$ ADHM theory [21].

Res may be nonzero only if η is spanned by the k charge vectors $\rho_1, \rho_2, \ldots, \rho_k$ with positive coefficients. Here, the choice $\eta = (1, \ldots, 1)$ simplifies the evaluation [22]. Since the charges appearing in the denominator of the second line are all negative in (2.16), one can show (combined with the fact that charges on the first line take the form of e_I or $e_I - e_J$) that JK-Res should always be zero by definition if one of the charges from the second line is chosen in ρ_α. This implies that the poles with nonzero residues are always chosen from the first line only, which are already classified in [3,22,32,33]. The pole locations for ϕ_I are classified by the colored Young diagrams with k boxes, meaning a collection of four Young diagrams $Y = (Y_1, \ldots, Y_4)$ whose box numbers sum to k. Let us denote by $s = (m, n)$ the box of a Young diagram Y_i, which is the box on the m'th row

and n'th column of Y_i. s running over possible k boxes replaces $I = 1, \ldots, k$ index of ϕ_I. We specify the pole location associated with Y as $\phi(s)$. The result is [3,22,32,33]

$$\phi(s) = v_i - \epsilon_+ - (n-1)\epsilon_1 - (m-1)\epsilon_2,$$
$$s = (m, n) \in Y_i \qquad (i = 1, \ldots, 4). \tag{2.17}$$

(This corrects a typo in [22], exchanging $m \leftrightarrow n$.) Had there been only the first line in (2.16), the residues were computed in [22,32,33]. Plugging in $\phi(s)$ into the second line of (2.16), one obtains an extra factor for each residue. The residue sum is given by

$$Z_k = \sum_{\vec{Y};|\vec{Y}|=k} \prod_{i=1}^{4} \prod_{s \in Y_i} \frac{2\sinh(\phi(s)) \cdot 2\sinh(\phi(s) - \epsilon_+)}{\prod_{j=1}^{4} 2\sinh\frac{E_{ij}(s)}{2} \cdot 2\sinh\frac{E_{ij}(s) - 2\epsilon_+}{2} \cdot 2\sinh\frac{\epsilon_+ - \phi(s) - v_j}{2}}$$
$$\times \prod_{i \le j}^{4} \prod_{s_{i,j} \in Y_{i,j}; s_i < s_j} \frac{2\sinh\frac{\phi(s_i) + \phi(s_j)}{2} \cdot 2\sinh\frac{\phi(s_i) + \phi(s_j) - 2\epsilon_+}{2}}{2\sinh\frac{\epsilon_{1,2} - \phi(s_i) - \phi(s_j)}{2}}, \tag{2.18}$$

where

$$E_{ij}(s) = v_i - v_j - \epsilon_1 h_i(s) + \epsilon_2(v_j(s) + 1). \tag{2.19}$$

Here and below, $s_i < s_j$ means $(i < j)$ or $(i = j$ and $m_i < m_j)$ or $(i = j$ and $m_i = m_j$ and $n_i < n_j)$. $h_i(s)$ denotes the distance from s to the right end of the diagram Y_i by moving right. $v_j(s)$ denotes the distance from s to the bottom of the diagram Y_j by moving down. See, e.g., [26]. Equation (2.18) is our proposal for the partition function of k $SO(7)$ instantons. This is quite novel for the following reason. $SO(7)$ instantons have standard

ADHM formulation, using $Sp(k)$ gauge theories for k instantons. The pole classification is unknown for the $Sp(k)$ index. On the other hand, (2.18) is an explicit formula.

Before adding matters in **8**, we first check that (2.18) is indeed the correct $SO(7)$ instanton partition function. We checked the equivalence of (2.16), or (2.18), and the index of $Sp(k)$ ADHM gauge theory [21,22], up to $k \le 3$ (turning off all chemical potentials except ϵ_+ at $k = 3$). Here we explain the case with $k = 1$ in detail, which is already nontrivial. For the purpose of illustration, we directly start from the contour integral. At $k = 1$, one finds

$$\left(2\sinh\frac{\epsilon_{1,2}}{2}\right) Z_1 = \oint d\phi \frac{2\sinh\epsilon_+}{\prod_{i=1}^{4} 2\sinh\frac{\epsilon_+ \pm (\phi - v_i)}{2}} \cdot \frac{2\sinh\phi \cdot 2\sinh(\phi - \epsilon_+)}{\prod_{i=1}^{4} 2\sinh\frac{\epsilon_+ - \phi - v_i}{2}} \tag{2.20}$$

from our model. Taking the residues at $\phi = v_i - \epsilon$, for $\eta > 0$, one finds

$$\left(2\sinh\frac{\epsilon_{1,2}}{2}\right) Z_1 = \sum_{i=1}^{4} \frac{1}{\prod_{j(\neq i)} 2\sinh\frac{v_{ij}}{2} \cdot 2\sinh\frac{2\epsilon_+ - v_{ij}}{2}} \cdot \frac{2\sinh(2\epsilon_+ - v_i)}{\prod_{j(\neq i)} 2\sinh\frac{2\epsilon_+ - v_i - v_j}{2}}. \tag{2.21}$$

This is a special case of (2.18). To check this result is correct, we study the $SO(7)$ single instanton partition function obtained from the standard $Sp(1)$ ADHM formalism [21,22],

$$\left(2\sinh\frac{\epsilon_{1,2}}{2}\right) Z_1^{\text{standard}} = \frac{1}{2} \oint d\phi \frac{2\sinh\epsilon_+ \cdot 2\sinh(\epsilon_+ \pm \phi) \cdot 2\sinh(\pm\phi)}{\prod_{a=1}^{3} 2\sinh\frac{\epsilon_+ \pm \phi \pm u_a}{2} \cdot 2\sinh\frac{\epsilon_+ \pm \phi}{2}}. \tag{2.22}$$

Residues are taken at $\phi = \pm u_a - \epsilon_+$ and $-\epsilon_+$ for $\eta > 0$, but the last residue is 0. u_a and v_i are related by

$$v_1 = \frac{u_1 + u_2 + u_3}{2}, \qquad v_2 = \frac{u_1 - u_2 - u_3}{2}, \qquad v_3 = \frac{-u_1 + u_2 - u_3}{2}, \qquad v_4 = \frac{-u_1 - u_2 + u_3}{2}. \qquad (2.23)$$

The residue sum is given by

$$\left(2\sinh\frac{\epsilon_{1,2}}{2}\right) Z_1^{\text{standard}} = \frac{1}{2}\sum_{a=1}^{3}\sum_{s=\pm}\frac{2\cosh\frac{su_a}{2}\cdot 2\cosh\frac{2\epsilon_+ - su_a}{2}\cdot 2\sinh(\pm(su_a - \epsilon_+))}{2\sinh(su_a)\cdot 2\sinh(\epsilon_+ - su_a)\prod_{b(\neq a)}2\sinh\frac{su_a\pm u_b}{2}\cdot 2\sinh\frac{2\epsilon_+ - su_a\pm u_b}{2}}. \qquad (2.24)$$

Despite very different looks, one can show (say, by using computer) that

$$Z_1(v_i) = Z_1^{\text{standard}}(u_a) \qquad (2.25)$$

after the identification (2.23). This identity and similar ones at higher k's imply that Z_k exhibits $SU(4) \to SO(7)$ enhancement, since Z_k^{standard} has manifest $SO(7)$ Weyl symmetry.

Now we discuss the inclusion of ADHM fields coming from the hypermultiplet matters in **8**. We continue to study the instanton particles of 5D SYM. **8** decomposes in $SU(4)$ as

$$\mathbf{8} \to \mathbf{4} + \bar{\mathbf{4}}. \qquad (2.26)$$

In the original ADHM formalism of $SO(7)$ instantons, it is unclear how to UV uplift the fermion zero modes caused by these hypermultiplets in the instanton background. One may even feel it impossible, since the standard $SO(7)$ ADHM cannot see 4π rotations in $Spin(7)$. However, viewing it as $SU(4)$ instantons with certain extensions, each hypermultiplet in **4** (or $\bar{\mathbf{4}}$) induces a Fermi multiplet which is fundamental (or antifundamental) in $U(k)$. So, in our new description, we naturally guess that the effect of $n_\mathbf{8}$ hypermultiplets is adding $n_\mathbf{8}$ pairs of Fermi multiplets of the following form:

$$\Psi_a, \tilde{\Psi}_a: \; (\mathbf{k}, \mathbf{1}) + (\bar{\mathbf{k}}, \mathbf{1}) \quad (a = 1, \dots, n_\mathbf{8}). \qquad (2.27)$$

It has been known [34] that the 5D $SO(7)$ SYM has a UV completion to a 5D SCFT for $n_\mathbf{8} \leq 4$. Recently, it was discussed that 5D SCFTs can exist till $n_\mathbf{8} \leq 6$ [35]. See also [36]. Our construction provides good descriptions of instantons for $n_\mathbf{8} \leq 4$. It will be easiest to explain this point after we discuss the index below. The flavor symmetry for $\Psi_a, \tilde{\Psi}_a$ may naively appear to be $U(2n_\mathbf{8})$. This is because we do not have any superpotential for these Fermi fields. They interact with other fields through gauge coupling only, so that one can rotate $\Psi_a, \tilde{\Psi}_a^\dagger$ with $U(2n_\mathbf{8})$. However, these fermions can couple to 5D background bulk fields, including the hypermultiplet fields in **8**. (Even in ADHM models based on D-brane engineerings, it sometimes happens that the soliton quantum mechanics is ignorant

on the bulk symmetry, in a similar manner.) These couplings will only preserve $U(n_\mathbf{8}) \subset Sp(n_\mathbf{8})$. See the beginning of the next subsection for this coupling to the bulk fields.

Adding these fermions, our ADHM-like description can be easily generalized. Namely, the extra Fermi fields are given standard kinetic term, whose derivatives are covariantized with 1D $U(k)$ vector multiplet fields. Its Witten index $Z_k^{n_\mathbf{8}}(\epsilon_{1,2}, v_i, m_a)$ with $a = 1, \dots, n_\mathbf{8}$ is defined with extra factors $e^{-m_a F_a}$ inserted in its definition, where F_a are the Cartans of $Sp(n_\mathbf{8})$. The contour integral expression for the Witten index takes the form of (2.16), with the following extra integrand multiplied for the new Fermi fields:

$$\prod_{a=1}^{n_\mathbf{8}}\prod_{I=1}^{k} 2\sinh\frac{m_a + \phi_I}{2}\cdot 2\sinh\frac{m_a - \phi_I}{2}. \qquad (2.28)$$

The extra factor (2.28) does not create new poles at finite ϕ, but may create new poles at infinity $\phi_I \to \pm\infty$. We first discuss the last possibility.

Here, first note that ϕ_I originates from the eigenvalues of the 1D $U(k)$ vector multiplet fields, $\phi \equiv \varphi + iA_\tau$, where A_τ is the vector potential on the Euclidean time. The contour integrand $Z_{\text{one-loop}}$ comes from one-loop path integral of 1D fields in the background of constant ϕ_I. So $V(\phi) \sim -\log Z_{\text{one-loop}}$ is the one-loop potential energy for ϕ_I. Before multiplying (2.28), the integrand of (2.16) converges to zero at $|\phi_I| \to \infty$ for any I, since there are more bosonic fields than fermionic fields. More concretely, consider the case with $k = 1$. One obtains $Z_{\text{one-loop}}^{n_\mathbf{8}=0} \sim e^{-4|\phi|}$, implying that the linear potential $V(\phi) = 4|\phi|$ confines the eigenvalues to $\phi = 0$. In other words, although ϕ classically develops a continuum to $\phi \to \pm\infty$, one-loop effect lifts this continuum by an attractive force. In ADHM models with brane engineering, this can be visualized as the instantons being attracted to the locations of 5D SCFTs [22]. The $U(k)$ vector multiplet fields are clearly extra degrees of freedom that enter while making a UV completion of the nonlinear sigma model. If there is a continuum created by ϕ, this represents states that do not belong to 5D QFT. The confinement from $V(\phi) = 4|\phi|$ signals that such obvious extra states may not be present in the quantum system.

Now, we extend these studies to $n_8 > 0$. At $k = 1$, one obtains $V(\phi) = (4 - n_8)|\phi|$. So at $n_8 \leq 3$, the quantum potential still confines the instanton. At $n_8 = 4$, ϕ generates a flat direction. This branch has extra states which is an artifact of UV completion, not belonging to the 5D QFT Hilbert space. So strictly speaking, $n_8 \leq 3$ is the bound in which our ADHM-like model is reliable. Fortunately, there are well-developed empirical ways of factoring out such extra states' contribution to the index. So we believe that our approach will be useful till $n_8 = 4$. At $n_8 \geq 5$, the quantum potential is repulsive, and it is not clear whether

one can use this theory to study 5D QFT at all. (However, see [37] for some progress.) In the contour integral like (2.16) or its extension with (2.28), the absence of continuum means the absence of poles at infinity. This implies that the choice of η in the JK-residue evaluation does not change the final result [22,27]. This is the case for $n_8 \leq 3$.

For $n_8 \leq 3$, the pole classification that we explained earlier for pure $SO(7)$ instantons still holds, labeled by $SU(4)$ colored young diagrams. We only need to multiply the value of (2.28) at the pole to the residue. The resulting index is given by

$$
Z_k = \sum_{\vec{Y};|\vec{Y}|=k} \prod_{i=1}^{4} \prod_{s \in Y_i} \frac{2 \sinh(\phi(s)) \cdot 2 \sinh(\phi(s) - \epsilon_+)}{\prod_{j=1}^{4} 2 \sinh \frac{E_{ij}(s)}{2} \cdot 2 \sinh \frac{E_{ij}(s) - 2\epsilon_+}{2} \cdot 2 \sinh \frac{\epsilon_+ - \phi(s) - v_j}{2}}
$$
$$
\times \prod_{i \leq j} \prod_{s_{i,j} \in Y_{i,j}; s_i < s_j} \frac{2 \sinh \frac{\phi(s_i) + \phi(s_j)}{2} \cdot 2 \sinh \frac{\phi(s_i) + \phi(s_j) - 2\epsilon_+}{2}}{2 \sinh \frac{\epsilon_{1,2} - \phi(s_i) - \phi(s_j)}{2}} \cdot \prod_{i=1}^{4} \prod_{s \in Y_i} \prod_{a=1}^{n_8} 2 \sinh \frac{m_a \pm \phi(s)}{2}. \tag{2.29}
$$

The partition functions (2.29) will be tested in Secs. III and IV at $n_8 = 1$, 2 using alternative descriptions, which include no guess works but are more elaborate in calculations. For instance, the indices at $k = 1$ divided by the center-of-mass factor $\hat{Z}_1 \equiv (2 \sinh \frac{\epsilon_{1,2}}{2}) Z_1$ are given by

$$
\hat{Z}_1^{n_8=1} = \prod_{i<j} \frac{t^2}{(1 - t^2 b_i^{\pm} b_j^{\pm})} [\chi_{\mathbf{2}}^{Sp(1)} f_0(v) + f_1(v)], \tag{2.30}
$$

$$
\hat{Z}_1^{n_8=2} = \prod_{i<j} \frac{t^2}{(1 - t^2 b_i^{\pm} b_j^{\pm})} [\chi_{\mathbf{5}}^{Sp(1)} f_0(v) + \chi_{\mathbf{4}}^{Sp(2)} f_1(v) + f_2(v)], \tag{2.31}
$$

$$
\hat{Z}_1^{n_8=3} = \prod_{i<j} \frac{t^2}{(1 - t^2 b_i^{\pm} b_j^{\pm})} [\chi_{\mathbf{14'}}^{Sp(3)} f_0(v) + \chi_{\mathbf{14}}^{Sp(3)} f_1(v) + \chi_{\mathbf{6}}^{Sp(3)} f_2(v) + f_3(v)], \tag{2.32}
$$

where

$$
\begin{aligned}
f_0(v) &= \chi_{\mathbf{9}}^{SU(2)} + \chi_{\mathbf{7}}^{SU(2)}(\chi_{\mathbf{7}}^{SO(7)} + 1) + \chi_{\mathbf{5}}^{SU(2)}(-\chi_{\mathbf{35}}^{SO(7)} + \chi_{\mathbf{7}}^{SO(7)} + 1) \\
&\quad + \chi_{\mathbf{3}}^{SU(2)}(-\chi_{\mathbf{35}}^{SO(7)} + \chi_{\mathbf{27}}^{SO(7)} + 1) + \chi_{\mathbf{105}}^{SO(7)} - \chi_{\mathbf{21}}^{SO(7)} + \chi_{\mathbf{7}}^{SO(7)} \\
f_1(v) &= -\chi_{\mathbf{8}}^{SU(2)}\chi_{\mathbf{8}}^{SO(7)} - \chi_{\mathbf{6}}^{SU(2)}\chi_{\mathbf{8}}^{SO(7)} + \chi_{\mathbf{4}}^{SU(2)}\chi_{\mathbf{112}}^{SO(7)} - \chi_{\mathbf{2}}^{SU(2)}\chi_{\mathbf{168}}^{SO(7)} \\
f_2(v) &= \chi_{\mathbf{7}}^{SU(2)}\chi_{\mathbf{35}}^{SO(7)} - \chi_{\mathbf{5}}^{SU(2)}(\chi_{\mathbf{7}}^{SO(7)} - \chi_{\mathbf{35}}^{SO(7)} + \chi_{\mathbf{105}}^{SO(7)}) - \chi_{\mathbf{3}}^{SU(2)}(\chi_{\mathbf{21}}^{SO(7)} + \chi_{\mathbf{27}}^{SO(7)} - \chi_{\mathbf{35}}^{SO(7)} \\
&\quad - \chi_{\mathbf{77}}^{SO(7)} + \chi_{\mathbf{168'}}^{SO(7)} + 1) - \chi_{\mathbf{7}}^{SO(7)} + \chi_{\mathbf{21}}^{SO(7)} + \chi_{\mathbf{27}}^{SO(7)} - \chi_{\mathbf{105}}^{SO(7)} + \chi_{\mathbf{189}}^{SO(7)} + \chi_{\mathbf{330}}^{SO(7)} \\
f_3(v) &= -\chi_{\mathbf{112'}}^{SO(7)}\chi_{\mathbf{6}}^{SU(2)} + (\chi_{\mathbf{48}}^{SO(7)} - \chi_{\mathbf{112'}}^{SO(7)} + \chi_{\mathbf{512}}^{SO(7)})\chi_{\mathbf{4}}^{SU(2)} - (\chi_{\mathbf{112'}}^{SO(7)} + \chi_{\mathbf{448}}^{SO(7)})\chi_{\mathbf{2}}^{SU(2)}.
\end{aligned} \tag{2.33}
$$

Here $t \equiv e^{-\epsilon_+}$. $\chi_{\mathbf{R}}^{SU(2)}$ is the character of diag$[SU(2)_R \times SU(2)_r]$ in representation **R**, in the convention $\chi_{\mathbf{2}}^{SU(2)} = t + t^{-1}$. $b_i \equiv e^{-v_i}$, and $(1 - t^2 b_i^{\pm} b_j^{\pm})$ means that all four factors with different signs are multiplied. The convention on representations (e.g., primes) all follow [38]. The numerators are invariant under $SO(7) \times Sp(n_8)$ Weyl symmetry, being character sums. Since the denominators are products with all

possible $\pm$ signs, they are also invariant under $SO(7)$ Weyl group which flips $b_i \to b_i^{-1}$. So $\hat{Z}_1^{n_8}$ is invariant under the Weyl group of $SO(7) \times Sp(n_8)$.

We expect our quantum mechanics to work also at $n_8 = 4$. Here, the 1D Coulomb branch with nonzero ϕ_I has a continuum. There may appear extra contribution from this continuum to the index [22], apart from (2.29).

(For conceptual simplicity, we consider the problem at zero FI parameter $\xi = 0$.) The extra contribution from the 1D Coulomb continuum is neutral in $SO(7) \times Sp(4)$. This is because the extra states in the 1D Coulomb branch come from the region with large ϕ_I, where all $U(k)$ charged fields acquire large masses. The charged fields are those which

see $SO(7) \times Sp(4)$. So the extra continuum does not see these charges. Here we shall only test the $SO(7) \times Sp(4)$ symmetry enhancements at $n_8 = 4$. So we simply ignore the extra contribution and show that (2.29) exhibits $SO(7) \times Sp(4)$ Weyl symmetry. The result at $k = 1$, showing $SO(7) \times Sp(4)$ Weyl symmetry, is given by

$$\hat{Z}_1^{n_8=4} = \prod_{i<j} \frac{t^2}{(1 - t^2 b_i^{\pm} b_j^{\pm})} [\chi_{42}^{Sp(4)} f_0(v) + \chi_{48}^{Sp(4)} f_1(v) + \chi_{27}^{Sp(4)} f_2(v) + \chi_{8}^{Sp(4)} f_3(v) + f_4(v)], \qquad (2.34)$$

with $f_{0,1,2,3}(v)$ given by (2.33), and

$$
\begin{aligned}
f_4(v) = &-\chi_{13}^{SU(2)} + \chi_{11}^{SU(2)}(\chi_{21}^{SO(7)} - \chi_{7}^{SO(7)}) + \chi_{9}^{SU(2)}(\chi_{7}^{SO(7)} - \chi_{21}^{SO(7)} - \chi_{27}^{SO(7)} + \chi_{35}^{SO(7)} + \chi_{105}^{SO(7)} - \chi_{189}^{SO(7)} - 1) \\
&- \chi_{7}^{SU(2)}(2\chi_{7}^{SO(7)} - 2\chi_{21}^{SO(7)} - 2\chi_{27}^{SO(7)} + \chi_{35}^{SO(7)} + \chi_{77}^{SO(7)} + 2\chi_{105}^{SO(7)} - \chi_{168'}^{SO(7)} - \chi_{189}^{SO(7)} - \chi_{294}^{SO(7)} \\
&- \chi_{330}^{SO(7)} + \chi_{378}^{SO(7)} - 1) - \chi_{5}^{SU(2)}(-3\chi_{7}^{SO(7)} + 3\chi_{21}^{SO(7)} + 3\chi_{27}^{SO(7)} - \chi_{35}^{SO(7)} - 2\chi_{77}^{SO(7)} - 4\chi_{105}^{SO(7)} \\
&+ 2\chi_{168'}^{SO(7)} + \chi_{182}^{SO(7)} + 2\chi_{189}^{SO(7)} - \chi_{294}^{SO(7)} + 2\chi_{330}^{SO(7)} - \chi_{378}^{SO(7)} - \chi_{616}^{SO(7)} - \chi_{693}^{SO(7)} + \chi_{1617}^{SO(7)} + 1) \\
&- \chi_{3}^{SU(2)}(3\chi_{7}^{SO(7)} - 4\chi_{21}^{SO(7)} - 4\chi_{27}^{SO(7)} + 2\chi_{35}^{SO(7)} + 3\chi_{77}^{SO(7)} + 6\chi_{105}^{SO(7)} - 3\chi_{168'}^{SO(7)} - \chi_{182}^{SO(7)} \\
&- 2\chi_{189}^{SO(7)} - \chi_{294}^{SO(7)} - 4\chi_{330}^{SO(7)} + \chi_{378}^{SO(7)} + 2\chi_{616}^{SO(7)} + 2\chi_{693}^{SO(7)} + \chi_{819}^{SO(7)} - \chi_{825}^{SO(7)} - \chi_{1560}^{SO(7)} - 2) \\
&+ (4\chi_{7}^{SO(7)} - 4\chi_{21}^{SO(7)} - 5\chi_{27}^{SO(7)} + 2\chi_{35}^{SO(7)} + 4\chi_{77}^{SO(7)} + 7\chi_{105}^{SO(7)} - 3\chi_{168'}^{SO(7)} - \chi_{182}^{SO(7)} - 3\chi_{189}^{SO(7)} - 5\chi_{330}^{SO(7)} \\
&+ 2\chi_{378}^{SO(7)} + 2\chi_{616}^{SO(7)} + 3\chi_{693}^{SO(7)} + 2\chi_{819}^{SO(7)} - \chi_{1617}^{SO(7)} - \chi_{1911}^{SO(7)} - 1).
\end{aligned}
\qquad (2.35)
$$

Now we consider the instanton strings of 6D super-Yang-Mills theories with $SO(7)$ gauge group and matters in **8**. The number n_8 of hypermultiplets cannot be arbitrary, due to gauge anomalies [6,39]. Without matters in other representations, one should have $n_8 = 2$ [6]. Incidentally, the 6D consistency requirement $n_8 = 2$ is also reflected in our ADHM-like construction, uplifted to 2D for instanton strings. This comes from 2d $U(k)$ gauge anomaly cancelation. First, consider the $SU(k)$ anomaly, proportional to $D_{\mathbf{R}} = \pm 2T(\mathbf{R})$ for right-/left-moving fermions. From $D_{\mathbf{k}} = 1$, $D_{\mathbf{adj}} = 2k$, $D_{\mathbf{sym_2}} = k + 2$, $D_{\mathbf{anti_2}} = k - 2$, one obtains

$$
\begin{aligned}
&-2 \cdot 2k + 2 \cdot 4 \cdot 1 + 2 \cdot 2k + 4 \cdot 1 + 2 \cdot (k - 2) \\
&- 2 \cdot (k + 2) - n_8 \cdot 2 \cdot 1 = 2(2 - n_8).
\end{aligned}
\qquad (2.36)
$$

These terms come from fermions in the multiplets (λ_0, λ), $(q, \tilde{q})$, $(a, \tilde{a})$, ϕ, $(b, \tilde{b})$, $(\hat{\lambda}, \check{\lambda})$, $(\Psi_a, \tilde{\Psi}_a)$, respectively. The $SU(k)$ anomaly cancels only at $n_8 = 2$. The overall $U(1)$ anomaly is proportional to the square of charges. The net anomaly is given by

$$
\begin{aligned}
&2 \cdot 4k \cdot 1^2 + 4k \cdot 1^2 + 2 \cdot \frac{k^2 - k}{2} \cdot 2^2 - 2 \cdot \frac{k^2 + k}{2} \cdot 2^2 \\
&- n_8 \cdot 2k \cdot 1^2 = 2k(2 - n_8).
\end{aligned}
\qquad (2.37)
$$

This again cancels at $n_8 = 2$. So, our ADHM-like quiver consistently uplifts to 2D at $n_8 = 2$.

As a basic test of our 2D gauge theories, we study the 't Hooft anomalies of global symmetries. The full 2D symmetry is expected to be $SO(7) \times Sp(2) \times SU(2)_l \times SU(2)_r \times SU(2)_R$. From our UV description, we can only study $SU(4) \times U(2) \times SU(2)_l \times U(1)_J$. There is an alternative way of computing the anomalies on the strings, using anomaly inflow [4,40]. By comparing two calculations, we shall provide a test of our gauge theories.

Using the inflow method, the 2D anomaly can be computed as follows. We first compute the anomaly polynomial 8-form of the 6D SCFT with a tensor multiplet, $SO(7)$ vector multiplet, and half-hypermultiplets in $\frac{1}{2}(\mathbf{8}, \mathbf{4})$ of $SO(7) \times Sp(2)$. The anomaly polynomial in the tensor branch consists of one-loop contribution $I_{\text{one-loop}}$, coming from massless tensor/vector/hyper-multiplets, and the classical Green-Schwarz contribution I_{GS} [41,42]. The two contributions should partly cancel for the terms containing $SO(7)$ gauge fields [43,44]. $I_{\text{one-loop}}$ is given by

$$
\begin{aligned}
I_{\text{one-loop}} = &-\frac{3}{32}[\text{Tr}(F_{SO(7)}^2)]^2 + \frac{1}{16}\text{Tr}(F_{SO(7)}^2)[2\text{tr}_4(F_{Sp(2)}^2) \\
&- 20c_2(R) - p_1(T)] + \cdots \\
= &-\frac{3}{2}\left[\frac{1}{4}\text{Tr}(F_{SO(7)}^2) + \frac{1}{12}(20c_2(R) + p_1(T) \right. \\
&\left. - 2\text{tr}_4(F_{Sp(2)}^2))\right]^2 + \cdots,
\end{aligned}
\qquad (2.38)
$$

where $\cdots$ denote terms independent of the $SO(7)$ field strength $F_{SO(7)}$. Following [44], we use the notation $\mathrm{Tr} \equiv \frac{1}{h^\vee}\mathrm{tr}_{\mathbf{adj}}$, and $\mathrm{tr}_{\mathbf{adj}}(F^4) = -\mathrm{tr}_{\text{fund}}(F^4) + 3(\mathrm{Tr}(F^2))^2$, $\mathrm{tr}_{\mathbf{8}}(F^4) = -\frac{1}{2}\mathrm{tr}_{\text{fund}}(F^4) + \frac{3}{8}(\mathrm{tr}(F^2))^2$, $\mathrm{tr}_{\mathbf{8}}(F^2) = \mathrm{Tr}(F^2)$, $\mathrm{tr}_{\mathbf{adj}}(F^2) = 5\mathrm{Tr}(F^2)$ for $SO(7)$. To cancel the one-loop $SO(7)$ anomaly, one should have the following Green-Schwarz 8-form [44]:

$$I_{\mathrm{GS}} = \frac{3}{2}I^2,$$

$$I \equiv \frac{1}{4}\mathrm{Tr}(F^2_{SO(7)}) + \frac{1}{12}(20c_2(R) + p_1(T) - 2\mathrm{tr}_{\mathbf{4}}(F^2_{Sp(2)})).$$
(2.39)

This takes the form of $I_{\mathrm{GS}} = \frac{1}{2}\Omega^{ij}I_i I_j$ with i, j running over just 1, so that $I_1 = I$ and $\Omega^{11} = 3$. Ω^{11} may be fixed from the fact that it comes from $O(-3) \to \mathbb{P}^1$ geometry in F-theory, with self-intersection number of $\mathbb{P}^1$ being 3. Knowing I_i appearing in $I_{\mathrm{GS}} = \frac{1}{2}\Omega^{ij}I_i I_j$, one can determine the 2D anomaly 4-form on the strings, from inflow. The formula is [4,40]

$$I_4 = -\Omega^{ij}k_i\left[I_j + \frac{1}{2}k_j\chi(T_4)\right],$$
(2.40)

where k_i is the string number in the i'th gauge group (or i'th tensor multiplet). We decomposed the 6D tangent bundle T to $T_2 \times T_4$, along/normal to the strings. From this formula, one finds

$$I_4 = -\frac{3}{2}k^2\chi(T_4)$$
$$- 3k\left[\frac{1}{4}\mathrm{Tr}(F^2_{SO(7)}) + \frac{5}{3}c_2(R) + \frac{p_1(T)}{12} - \frac{1}{6}\mathrm{tr}_{\mathbf{4}}(F^2_{Sp(2)})\right]$$
(2.41)

for the $SO(7)$ instanton strings at $n_{\mathbf{8}} = 2$, with topological number k.

Now, we compute I_4 from our gauge theory. A chiral fermion's anomaly 4-form is given by

$$I_4 = \pm\left[\frac{1}{2}\mathrm{tr}(F^2) + \frac{p_1(T_2)}{24}\right],$$
(2.42)

where $\pm$ signs are for left-/right-moving fermions, respectively, in our convention. F collectively denotes all background gauge fields for the global symmetries acting on the fermion. Here it is for $SU(4) \times U(1)_J \times SU(2)_l \times U(2)_F$. We can only study the anomalies of the symmetries surviving in UV and check the consistency with (2.41). Fermi and vector multiplets have left-moving fermions, while chiral multiplets have right-moving fermions. Each multiplet contributes to terms of the form (2.42) with a suitable sign. First, contributions from fields neutral in $SU(4) \times U(2)$ are already computed in [4],

$(\lambda_0, \lambda) + (a, \tilde{a})$: $k^2(c_2(r) - c_2(l))$

$$\check{\lambda}, \check{\check{\lambda}}: (k^2 + k)\left[\frac{F^2_R}{8} + \frac{c_2(r)}{2} + \frac{p_1(T_2)}{24}\right]$$

$$b, \tilde{b}: -(k^2 - k)\left[\frac{F^2_R}{8} + \frac{c_2(l)}{2} + \frac{p_1(T_2)}{24}\right].$$
(2.43)

R is the $U(1)$ Cartan of $SU(2)_R$. Here and later, we shall often use expressions like $c_2(r)$, $c_2(R) = \frac{F^2_R}{4}$ assuming symmetry enhancement, but only the $U(1)_J$ part is to be kept in UV. Namely, one first keeps the Cartan parts of the field strengths for J_r, J_R. Then they are all replaced by J and its field strength F_J. We present the results using $c_2(R)$ and $c_2(r)$ since this may suggest possible patterns of IR symmetry enhancement. (See also [4].) The fields charged under $SU(4) \times U(2)$ contribute to I_4 as follows:

$$q, \tilde{q}, \phi: -3k\left[\frac{1}{4}\mathrm{Tr}(F^2_{SU(4)}) + 4\cdot\frac{F^2_R}{8} + 4\cdot\frac{p_1(T_2)}{24}\right]$$

$$\Psi_a, \tilde{\Psi}_a: 2k\left[\frac{1}{2}\mathrm{tr}_2(F^2_{U(2)}) + 2\cdot\frac{p_1(T_2)}{24}\right].$$
(2.44)

Adding all, and using $p_1(T) = p_1(T_2) - 2c_2(l) - 2c_2(r)$, one obtains

$$I_4 = \frac{3}{2}k^2(c_2(r) - c_2(l))$$
$$- 3k\left[\frac{1}{4}\mathrm{Tr}(F^2_{SU(4)}) + \frac{5}{3}\cdot\frac{F^2_R}{4} + \frac{p_1(T)}{12} - \frac{1}{3}\mathrm{tr}_2(F^2_{U(2)})\right].$$
(2.45)

Here and below, we shall frequently use the fact that $\mathrm{Tr}(F^2)$ remains the same after restricting F to a subalgebra if a long root of the original algebra is kept, so that unit instanton charge $\frac{1}{4}\int\mathrm{Tr}(F^2)$ remains the same [44]. Here it applies to $SU(4) \subset SO(7)$. As for $U(2) \subset Sp(2)$, or more generally $U(n) \subset Sp(n)$, the embedding is such that $\mathrm{tr}_{2n} \to 2\mathrm{tr}_n$. Taking these into account, (2.45) agrees with (2.41) upon restricting (2.41) to $SU(4), U(2), SU(2)_r \times SU(2)_R \to J$, and using $\chi(T_4) = c_2(l) - c_2(r)$. Their mixed anomalies with $U(k)$ also vanish.

One can study the elliptic genera Z_k of k instanton strings, whose spatial direction wraps S^1. The definition is almost identical to (2.15), except that there is another factor $e^{2\pi i\tau P}$ inside the trace, where P is the left-moving momentum on S^1. The basic formula is given in [29,30]. The result is obtained by simply replacing all $2\sinh$ functions in (2.16), (2.28), (2.29) by $2\sinh\frac{z}{2} \to \frac{i\theta_1(\tau|\frac{z}{2\pi i})}{\eta(\tau)} \equiv \theta(z)$. For instance, at $k = 1$, one obtains

$$Z_1(\tau, \epsilon_{1,2}, v_i, m_a)$$

$$= \frac{1}{\theta(\epsilon_{1,2})} \sum_{i=1}^{4} \frac{\theta(4\epsilon_+ - 2v_i) \prod_{a=1}^{2} \theta(m_a \pm (v_i - \epsilon_+))}{\prod_{j(\neq i)} \theta(v_{ij}) \theta(2\epsilon_+ - v_{ij}) \theta(2\epsilon_+ - v_i - v_j)},$$

(2.46)

where $v_{ij} \equiv v_i - v_j$. Some tests of these formulas will be given in Sec. IV B.

B. G_2 instantons and matters in 7

With a hypermultiplet in **8**, one can Higgs $SO(7)$ to G_2. Decomposing the scalar to $\mathbf{8} \to \mathbf{7} \oplus \mathbf{1}$ in G_2, **1** is given VEV and decouples in IR. **7** is eaten up by the broken part of the $SO(7)$ gauge fields, since $\mathbf{21} \to \mathbf{14} \oplus \mathbf{7}$. The matter consists of two half hypermultiplets, forming a doublet of flavor symmetry $Sp(1)_F$. The scalar can be written as $[\Phi_{Aa}]_{(s_1,s_2,s_3)}$, where $A = 1, 2$ is the doublet index of $SU(2)_R$ R-symmetry, $a = 1, 2$ is that of $Sp(1)_F$, and $s_{1,2,3} = \pm\frac{1}{2}$ labels the components of **8**. It satisfies the reality condition $(\Phi^*)^{Aa}_{(s_1,s_2,s_3)} = \epsilon^{AB}\epsilon^{ab}(\Phi_{Bb})_{(s_1,s_2,s_3)}$. Let us take $\Phi_{Aa} \equiv [\Phi_{Aa}]_{(+,+,+)} + [\Phi_{Aa}]_{(-,-,-)}$, satisfying $(\Phi^*)^{Aa} = \epsilon^{AB}\epsilon^{ab}\Phi_{Bb}$. One takes $\Phi_{Aa} = \epsilon_{Aa}\Phi$, with a pure imaginary VEV Φ. This preserves a diagonal subgroup of $SU(2)_R \times Sp(1)_F$, which is the $SU(2)_R$ symmetry after Higgsing. At general n_8, we give VEV to the last hypermultiplet scalar, $a = n_8$. One should lock the chemical potentials as

$$m_{\text{last}} - \epsilon_+ \pm v_4 = 0, \qquad (2.47)$$

with both signs, not to rotate the scalar VEV. So, we should take $m_{\text{last}} - \epsilon_+ = 0$, $v_4 = 0$. The former condition turns off the $Sp(1) \subset Sp(n_8)$ chemical potential m_{last}, and the latter reduces the rank of gauge group by 1. As the index is invariant under the RG flow triggered by the scalar VEV, one can get the IR G_2 index by constraining the $SO(7)$ index.

In our $SU(4)$ formalism, the bulk scalars are written as $Q_i, \tilde{Q}^i$, where $i = 1, 2, 3, 4$. Giving VEV to **1** amounts to turning on $Q_4 = \tilde{Q}^4 = M \neq 0$ (real), where we take the

unbroken $SU(3) \subset G_2$ to be labeled by $i = 1, 2, 3$. In 1D, the background fields couple to the 1D fields as

$$J_{\Psi_{\text{last}}} \sim Q_i \tilde{q}^i, \qquad J_{\tilde{\Psi}_{\text{last}}} \sim \tilde{Q}^i q_i. \qquad (2.48)$$

The second potential $|J_{\tilde{\Psi}_{\text{last}}}|^2 \sim M^2 |q_4|^2$ gives mass to q_4, while the first one gives mass to $\tilde{q}^4$.[5] The $SU(4)$ ADHM fields reduce to the $SU(3)$ ADHM fields at low energy. Among the extra fields, ϕ_i with $i = 1, 2, 3, 4$ decomposes into ϕ_i with $i = 1, 2, 3$ in $(\bar{\mathbf{k}}, \bar{\mathbf{3}})$, and ϕ_4 in $(\bar{\mathbf{k}}, \mathbf{1})$. If $n_8 \geq 2$, one still has $n_7 = n_8 - 1$ pairs of Fermi multiplets $\Psi_a, \tilde{\Psi}_a$ left in $(\mathbf{k}, \mathbf{1}) + (\bar{\mathbf{k}}, \mathbf{1})$, $a = 1, ..., n_7$. To summarize, one first has the $SU(3)$ ADHM fields,

$$A_\mu, \lambda_0, \lambda: \mathcal{N} = (0, 4) \ U(k) \text{ vector multiplet}$$
$$q_i, \tilde{q}^i: (\mathbf{k}, \bar{\mathbf{3}}) + (\bar{\mathbf{k}}, \mathbf{3}) \quad (i = 1, 2, 3)$$
$$a, \tilde{a}: (\mathbf{adj}, \mathbf{1}). \qquad (2.49)$$

In addition, one has

$$\phi_i, \phi_4: \text{Chiral in } (\bar{\mathbf{k}}, \bar{\mathbf{3}})_{J=\frac{1}{2}} + (\bar{\mathbf{k}}, \mathbf{1})_{J=\frac{1}{2}}$$
$$b, \tilde{b}: \text{Chiral in } (\overline{\mathbf{anti}}_2, \mathbf{1})_{J=\frac{1}{2}}$$
$$\hat{\lambda}: \text{Fermi in } (\mathbf{sym}_2, \mathbf{1})_{J=0}$$
$$\check{\lambda}: \text{Fermi in } (\mathbf{sym}_2, \mathbf{1})_{J=-1}. \qquad (2.50)$$

For $n_7 \leq 3$ hypermultiplet matters in representation **7**, there are extra Fermi multiplets,

$$\Psi_a, \tilde{\Psi}_a: (\mathbf{k}, \mathbf{1}) + (\bar{\mathbf{k}}, \mathbf{1}), \quad a = 1, ..., n_7. \qquad (2.51)$$

The $\mathcal{N} = (0, 1)$ action follows from a construction similar to $SO(7)$ in Sec. II A.

The index Z_k for k G_2 instantons can either be obtained from the Witten index of the above gauge theory, or by taking the Higgsing condition of the $SO(7)$ index, $m_{n_8} = \epsilon_+$, $v_4 = 0$. It may be more illustrative to write both the contour integral expression and the residue sum. The contour integral expression for the index is given by

$$Z_k = \frac{1}{k!} \oint \prod_{I=1}^{k} \frac{d\phi_I}{2\pi i} \cdot \frac{\prod_{I \neq J} 2\sinh\frac{\phi_{IJ}}{2} \cdot \prod_{I,J} 2\sinh\frac{2\epsilon_+ - \phi_{IJ}}{2}}{\prod_{I=1}^{k} \prod_{i=1}^{3} 2\sinh\frac{\epsilon_+ \pm (\phi_I - v_i)}{2} \cdot \prod_{I,J} 2\sinh\frac{\epsilon_{1,2} + \phi_{IJ}}{2}}$$

$$\times \frac{\prod_{I \leq J}(2\sinh\frac{\phi_I + \phi_J}{2} \cdot 2\sinh\frac{\phi_I + \phi_J - 2\epsilon_+}{2})}{\prod_I (\prod_{i=1}^{3} 2\sinh\frac{\epsilon_+ - \phi_I - v_i}{2} \cdot 2\sinh\frac{\epsilon_+ - \phi_I}{2}) \cdot \prod_{I < J} 2\sinh\frac{\epsilon_{1,2} - \phi_I - \phi_J}{2}} \cdot \prod_{I=1}^{k} \prod_{a=1}^{n_7} 2\sinh\frac{m_a \pm \phi_I}{2}. \qquad (2.52)$$

The residue sum, labeled by $SU(3)$ colored Young diagrams, is given by

---

[5]One may more generally take $J_\Psi \sim \alpha Q_i \tilde{q}^i + \beta \tilde{Q}^i \phi_i$, compatible with $U(k) \times SU(4)$. However, with $SU(4)$ broken to $SU(3)$, $\tilde{q}^4$ and ϕ_4 have same charges in unbroken symmetries, and α, β does not affect the IR physics.

$$Z_k = \sum_{\vec{Y};|\vec{Y}|=k} \prod_{i=1}^{3} \prod_{s \in Y_i} \frac{2\sinh(\phi(s)) \cdot 2\sinh(\epsilon_+ - \phi(s))}{\prod_{j=1}^{3}\left(2\sinh\frac{E_{ij}(s)}{2} \cdot 2\sinh\frac{E_{ij}(s)-2\epsilon_+}{2} \cdot 2\sinh\frac{\epsilon_+ - \phi(s)-v_j}{2}\right) \cdot 2\sinh\frac{\epsilon_+ - \phi(s)}{2}}$$

$$\cdot \prod_{i \le j} \prod_{s_{i,j} \in Y_{i,j};s_i < s_j} \frac{2\sinh\frac{\phi(s_i)+\phi(s_j)}{2} \cdot 2\sinh\frac{\phi(s_i)+\phi(s_j)-2\epsilon_+}{2}}{2\sinh\frac{\epsilon_{1,2}-\phi(s_i)-\phi(s_j)}{2}} \cdot \prod_{i=1}^{3}\prod_{s \in Y_i}\prod_{a=1}^{n_7} 2\sinh\frac{m_a \pm \phi(s)}{2}, \tag{2.53}$$

where $\phi(s)$ and $E_{ij}(s)$ are defined in (2.17) and (2.19).

We first study the case with $n_7 = 0$. We can test the results against known G_2 instanton partition functions of [45]. We tested (2.53) till $k \le 3$. First, at $k = 1$, it will be illustrative to make a basic presentation, directly from the contour integral. Equation (2.52) at $k = 1$ is given by

$$\left(2\sinh\frac{\epsilon_{1,2}}{2}\right)Z_1 = \oint d\phi \frac{2\sinh\epsilon_+ \cdot 2\sinh\phi \cdot 2\sinh(\phi - \epsilon_+)}{\prod_{i=1}^{3}\left(2\sinh\frac{\epsilon_+ \pm (\phi-v_i)}{2} \cdot 2\sinh\frac{\epsilon_+ - \phi - v_i}{2}\right) \cdot 2\sinh\frac{\epsilon_+ - \phi}{2}}. \tag{2.54}$$

At $\eta > 0$, the poles are chosen at $\phi = v_i - \epsilon_+$, $i = 1, 2, 3$. So, one obtains

$$\left(2\sinh\frac{\epsilon_{1,2}}{2}\right)Z_1 = \sum_{i=1}^{3} \frac{2\sinh(v_i - 2\epsilon_+)}{\prod_{j(\ne i)}\left(2\sinh\frac{v_{ij}}{2} \cdot 2\sinh\frac{2\epsilon_+ - v_{ij}}{2} \cdot 2\sinh\frac{2\epsilon_+ + v_{ij}}{2}\right) \cdot 2\sinh\frac{v_i - 2\epsilon_+}{2}}, \tag{2.55}$$

where we used $v_1 + v_2 + v_3 = 0$. Each residue only exhibits Weyl symmetry of $SU(3)$, given by 3! permutations of v_1, v_2, v_3. However, the sum of three residues exhibits enhanced Weyl symmetry of G_2, the dihedral group D_6 of order 12. The extra transformation generating full D_6 is $v_i \to -v_i$ for all $i = 1, 2, 3$, $SU(3)$ charge conjugation. One can show that Z_1 is given by

$$\left(2\sinh\frac{\epsilon_{1,2}}{2}\right)Z_1 = \frac{t^3(1+t^2)(1+t^2\chi_7^{G_2}(v)+t^4)}{\prod_{i<j}(1-t^2 e^{v_{ij}})(1-t^2 e^{-v_{ij}})} = t^3 \sum_{n=0}^{\infty} \chi_{(0,n)}^{G_2}(v)t^{2n}, \tag{2.56}$$

where $t \equiv e^{-\epsilon_+}$. $\chi_7^{G_2} = 1 + \chi_3^{SU(3)} + \chi_{\bar{3}}^{SU(3)} = 1 + \sum_{i=1}^{3}(e^{v_i} + e^{-v_i})$ is the character of **7**. $\chi_{(0,n)}^{G_2}$ is the character of the irrep $(0,n)$ of G_2, which is the n'th symmetric product of the adjoint representation **14**. (2.56) is known as the correct G_2 instanton partition function at $k = 1$ [45].

At $k = 2$, Z_2 can be rearranged into (where $t = e^{-\epsilon_+}$, $u = e^{-\epsilon_-}$)

$$\left(\prod_{n=1}^{2} 2\sinh\frac{n\epsilon_{1,2}}{2}\right)Z_2 = \frac{t^{24}}{\prod_{i<j}(1-t^2 e^{\pm v_{ij}})(1-t^3 u^{\pm\frac{1}{2}}e^{\pm v_{ij}})}\left[\chi_{\mathbf{20}}^{SU(2)} + \sum_{n=1}^{18}\chi_{\mathbf{n}}^{SU(2)}g_n(v_i, u)\right], \tag{2.57}$$

where $SU(2)$ is still diag$[SU(2)_r \times SU(2)_R]$, and $g_n(v_i, u)$'s are given by

$$g_{18} = \chi_7^{G_2} + 1, \qquad g_{17} = \chi_2^{SU(2)_l}(\chi_7^{G_2}+1), \qquad g_{16} = \chi_7^{G_2} + \chi_{27}^{G_2} + 1, \qquad g_{15} = \chi_2^{SU(2)_l}(3\chi_7^{G_2}+1),$$

$$g_{14} = \chi_3^{SU(2)_l}(\chi_7^{G_2}+1) + 2\chi_7^{G_2} + \chi_{27}^{G_2} + 1, \qquad g_{13} = \chi_2^{SU(2)_l}(\chi_7^{G_2}+\chi_{14}^{G_2}+\chi_{27}^{G_2}-\chi_{64}^{G_2}+2),$$

$$g_{12} = \chi_3^{SU(2)_l}(\chi_7^{G_2}+\chi_{14}^{G_2}-\chi_{64}^{G_2}+2) + 2\chi_7^{G_2} + 2\chi_{14}^{G_2} - 2\chi_{64}^{G_2} + 2$$

$$g_{11} = \chi_4^{SU(2)_l} + \chi_2^{SU(2)_l}(2\chi_7^{G_2}-\chi_{64}^{G_2}-\chi_{189}^{G_2}+1)$$

$$g_{10} = \chi_3^{SU(2)_l}(\chi_7^{G_2}-\chi_{14}^{G_2}-\chi_{77}^{G_2}) + 3\chi_7^{G_2} - \chi_{14}^{G_2} - \chi_{64}^{G_2} - 2\chi_{77}^{G_2} + \chi_{182}^{G_2} - \chi_{189}^{G_2} + 1$$

$$g_9 = \chi_4^{SU(2)_l}(\chi_7^{G_2}-\chi_{14}^{G_2}) + \chi_2^{SU(2)_l}(3\chi_7^{G_2}-\chi_{14}^{G_2}-\chi_{64}^{G_2}-3\chi_{77}^{G_2}+\chi_{182}^{G_2}+1)$$

$$g_8 = \chi_3^{SU(2)_l}(\chi_{77}^{G_2}-\chi_{14}^{G_2}) + 2\chi_7^{G_2} - \chi_{64}^{G_2} - \chi_{77}^{G_2} + \chi_{182}^{G_2} - \chi_{189}^{G_2} + \chi_{378}^{G_2} + 1$$

$$g_7 = \chi_4^{SU(2)_l}(\chi_{77}^{G_2} - \chi_7^{G_2}) + \chi_2^{SU(2)_l}(2\chi_7^{G_2} - \chi_{64}^{G_2} + 2\chi_{182}^{G_2} - \chi_{286}^{G_2} + \chi_{448}^{G_2} + 1)$$

$$g_6 = \chi_3^{SU(2)_l}(\chi_{77}^{G_2} + \chi_{182}^{G_2} - \chi_{64}^{G_2} + \chi_{189}^{G_2} + 1) + \chi_7^{G_2} + \chi_{14}^{G_2} + \chi_{27}^{G_2} - \chi_{64}^{G_2} + \chi_{182}^{G_2} - \chi_{286}^{G_2} + \chi_{378}^{G_2} + \chi_{448}^{G_2} + 1$$

$$g_5 = \chi_4^{SU(2)_l}(\chi_{77}^{G_2} - 2\chi_7^{G_2} - \chi_{14}^{G_2} - 1)$$
$$\quad + \chi_2^{SU(2)_l}(-\chi_7^{G_2} + 2\chi_{14}^{G_2} + \chi_{27}^{G_2} - 2\chi_{64}^{G_2} + 2\chi_{77}^{G_2} + \chi_{182}^{G_2} + \chi_{189}^{G_2} - \chi_{286}^{G_2} + \chi_{378}^{G_2} + 2) \quad \text{(continued)}$$

$$g_4 = -\chi_5^{SU(2)_l}\chi_7^{G_2} + \chi_3^{SU(2)_l}(2\chi_{77}^{G_2} - \chi_7^{G_2} + \chi_{14}^{G_2} - \chi_{27}^{G_2} - 2\chi_{64}^{G_2} + \chi_{182}^{G_2} - \chi_{286}^{G_2} + 1)$$
$$\quad + 2\chi_{14}^{G_2} + \chi_{27}^{G_2} - \chi_{64}^{G_2} + \chi_{77}^{G_2} + \chi_{182}^{G_2} - \chi_{273}^{G_2} - 2\chi_{286}^{G_2} + \chi_{448}^{G_2} + 1$$

$$g_3 = -\chi_4^{SU(2)_l}(\chi_7^{G_2} + \chi_{27}^{G_2} + \chi_{64}^{G_2}) + \chi_2^{SU(2)_l}(\chi_7^{G_2} - \chi_{14}^{G_2} + \chi_{182}^{G_2} - \chi_{189}^{G_2} - \chi_{286}^{G_2} - \chi_{729}^{G_2})$$

$$g_2 = -\chi_5^{SU(2)_l}(\chi_7^{G_2} + \chi_{14}^{G_2} + 1) + \chi_3^{SU(2)_l}(\chi_{64}^{G_2} - 4\chi_{14}^{G_2} - 2\chi_{77}^{G_2} + \chi_{182}^{G_2} - \chi_{189}^{G_2} - \chi_{448}^{G_2} - 2)$$
$$\quad + 2\chi_7^{G_2} - 2\chi_{14}^{G_2} + 2\chi_{64}^{G_2} - 3\chi_{77}^{G_2} - \chi_{273}^{G_2} - \chi_{729}^{G_2} - 1$$

$$g_1 = \chi_4^{SU(2)_l}(2\chi_7^{G_2} - 2\chi_{14}^{G_2} - \chi_{27}^{G_2} + \chi_{64}^{G_2} - 2\chi_{77}^{G_2} - 1)$$
$$\quad + \chi_2^{SU(2)_l}(2\chi_7^{G_2} - 3\chi_{14}^{G_2} + 2\chi_{64}^{G_2} - 4\chi_{77}^{G_2} + \chi_{182}^{G_2} - \chi_{273}^{G_2} - \chi_{448}^{G_2} - 1). \tag{2.58}$$

As the numerator is manifestly arranged into G_2 characters, it shows enhanced G_2 Weyl symmetry. The denominator is also invariant under the extra generator $v_i \to -v_i$ of D_6, being invariant under G_2 Weyl symmetry. One can also check the agreement with the known G_2 partition function at $k = 2$. For the simplicity of comparison, let us turn off all $v_i = 0$ and $\epsilon_- = 0$. Then, (2.57) becomes

$$\left(2\sinh\frac{\epsilon_{1,2}}{2}\right)Z_2 = \frac{t^7}{(1-t)^{14}(1+t)^8(1+t+t^2)^7}[1 + t + 10t^2 + 31t^3 + 75t^4 + 180t^5 + 385t^6$$
$$+ 637t^7 + 975t^8 + 1360t^9 + 1614t^{10} + 1666t^{11} + 1614t^{12} + \cdots + t^{22}], \tag{2.59}$$

where the omitted terms $\cdots$ can be restored by the $t \to t^{-1}$ Weyl symmetry of $SU(2)$ (i.e., the coefficients of t^p and t^{22-p} are same on the numerator). The overall t^7 factor is like a zero point energy factor and is needed to have this Weyl symmetry. Apart from this factor, (2.59) agrees with Eq. (9.5) of [46] after correcting a typo there, as noted in [45].

At $k = 3$, we only show the simplified form of (2.53) at $v_i = 0$, $\epsilon_- = 0$, which is

$$\left(2\sinh\frac{\epsilon_{1,2}}{2}\right)Z_3 = \frac{t^{11}}{(1-t)^{22}(1+t)^{14}(1+t^2)^7(1+t+t^2)^9}[1 + t + 11t^2 + 34t^3 + 124t^4 + 352t^5$$
$$+ 1055t^6 + 2657t^7 + 6584t^8 + 14635t^9 + 31194t^{10} + 61229t^{11} + 114367t^{12}$$
$$+ 198932t^{13} + 329172t^{14} + 511194t^{15} + 755093t^{16} + 1051845t^{17} + 1394817t^{18}$$
$$+ 1749632t^{19} + 2091341t^{20} + 2368619t^{21} + 2557449t^{22} + 2619060t^{23}$$
$$+ 2557449t^{24} + \cdots + t^{46}], \tag{2.60}$$

where $\cdots$ can again be restored by noting that coefficients of t^p and t^{46-p} are same on the numerator. Apart from the overall t^{11} factor which guarantees Weyl symmetry, this again agrees with Eq. (4.16) of [45]. Although we did comparisons till $k = 3$, one can in principle continue to test for higher k's whether our (2.53) agrees with the results of [45].

Now, as for the indices at $n_7 \geq 1$, these observables have not been computed or studied in the literature, to the best of our knowledge. Here we simply note that, making expansions of the indices in $t = e^{-\epsilon_+}$, one observes that the coefficients are characters of $G_2 \times Sp(n_7)$. At least, at $k = 1$, this does not need independent calculations, since

we already illustrated the symmetry enhancement of $SO(7) \times Sp(n_8)$ in the previous subsection. Also, whenever we provide concrete tests of some $SO(7)$ results in Secs. III and IV, this implies similar tests of the G_2 results at $n_7 = n_8 - 1$ by Higgsing.

At $n_7 = 1$, 6D SCFT exists with G_2 gauge group. This can be obtained from 6D $SO(7)$ theory at $n_8 = 2$ by Higgsing. Our 2D gauge theories on G_2 instantons can also be uplifted to 2D gauge theories. As in the previous subsection, this gauge theory is free of $U(k)$ gauge anomaly. The 2D anomaly of $G_2 \times Sp(n_7) \times SU(2)_R \times SU(2)_r \times SU(2)_l$ global symmetries, computed from

anomaly inflow, is also compatible with the $SU(3) \times U(n_7) \times U(1)_J \times SU(2)_l$ anomalies of our 2D gauge theories. To see this, one first restricts $F_{SO(7)} \to F_{G_2}$ which leaves $\mathrm{Tr}(F^2)$ invariant, $\mathrm{tr}_4(F^2_{Sp(2)}) \to \mathrm{tr}_2(F^2_{Sp(1)}) + \mathrm{tr}_2(F^2_{Sp(1)'})$, and note that $c_2(R) = \frac{1}{4}\mathrm{Tr}(F^2_R) = \frac{1}{2}\mathrm{tr}_{\mathrm{fund}}(F^2_R)$ [44]. Since we lock $Sp(1)'$ and $SU(2)_R$ during Higgsing, one identifies $F_{Sp(1)'} = F_R$. Then, both anomaly 4-forms (2.41), (2.45) reduce to

$$
I_4 = -\frac{3}{2}k^2\chi(T_4)
$$
$$
- 3k\left[\frac{1}{4}\mathrm{Tr}(F^2_{G_2}) + \frac{4}{3}c_2(R) + \frac{p_1(T)}{12} - \frac{1}{6}\mathrm{tr}_2(F^2_{Sp(1)})\right],
$$
$$
(2.61)
$$

with restrictions to UV symmetry understood for gauge theory anomalies. So the inflow anomaly and 2D gauge theory anomaly continue to agree with each other.

The elliptic genera for the strings can be computed similarly. One takes the formulas (2.52) or (2.53), and replace $2\sinh\frac{z}{2} \to \frac{i\theta_1(\tau|\frac{z}{2\pi i})}{\eta(\tau)} \equiv \theta(z)$ for all $2\sinh$ functions. The G_2 symmetry of this elliptic genus at $k = 1$ is systematically discussed in [19].

At $n_7 = 1$, one has a pair $\Psi, \tilde{\Psi}$ of Fermi multiplets. One can again investigate the effect of bulk Higgsing $G_2 \to SU(3)$. In the bulk, one decomposes $\mathbf{7} \to \mathbf{3} + \bar{\mathbf{3}} + \mathbf{1}$, where scalar in $\mathbf{1}$ assumes VEV and breaks G_2 into $SU(3)$. The other hypermultiplet fields are eaten up by vector multiplets for the broken symmetry. The constant VEV of the bulk scalar $\equiv Q$ in $\mathbf{1}$ will behave as a background field in 1D/2D ADHM-like models. With foresight on the $SU(3)$ instantons studied in [4], we propose that the coupling of the background bulk field Q to the G_2 ADHM-like gauge theory is given by

$$
J_\Psi \sim Q\phi, \qquad J_{\tilde{\Psi}} \sim Q\epsilon^{ijk}q_i\phi_j q_k^\dagger, \qquad (2.62)
$$

where $\phi \equiv \phi_4$. The $\mathcal{N} = (0, 1)$ superpotential $J_{\tilde{\Psi}}$ is compatible with symmetries, but at this stage it may not be obvious why we should turn it on in this way. Ψ and the chiral multiplet ϕ become massive due to J_Ψ and decouple at low energy. However, $\tilde{\Psi}$ does not decouple at low energy, since it does not acquire mass. In fact, the remaining system

(including $\tilde{\Psi}$, which was called ζ in [4]) with the above cubic superpotential was studied in [4], which showed various nontrivial physics of the $SU(3)$ instanton strings. In 1D, this provides a novel alternative ADHM-like description for $SU(3)$ instanton particles. In 2D, this is (by now) the uniquely known $SU(3)$ ADHM construction of instanton strings without matters. All models presented so far in this paper, for $SO(7)$ and G_2 instantons, were initially constructed by guessing the un-Higgsing procedures from $SU(3)$. See [4] for further discussions on the last $SU(3)$ model.

III. EXCEPTIONAL INSTANTONS FROM D-BRANES

A. Brane setup and quantum mechanics

In this section, we test some indices of the previous section, using 5-brane webs for the 5D $\mathcal{N} = 1$ gauge theories with $SO(N)$ gauge groups and matters in spinor representations [47]. A type IIB 5-brane web on x^5, x^6 plane consists of (p, q) 5-branes stretched along lines with slope q/p: e.g., D5-branes $(1,0)$ along x^5 and NS5-branes $(0,1)$ along x^6 directions. They occupy $x^0, ..., x^4$ directions for the 5D QFT. $SO(N)$ gauge theories are realized by 5-brane webs with orientifold 5-planes. An NS5-brane crossing the O5-plane bends to a suitable $(p, 1)$-brane and changes the types of O5 across NS5. An $SO(2N)$ theory is engineered by suspending N D5-branes between two NS5-branes, also with an $O5^-$, as shown in Fig. 1(a). $SO(2N + 1)$ theory is realized by N D5-branes and an $\widetilde{O5}^-$-plane, which is an $O5^-$ with a half D5. See Fig. 1(b). Dashed-dotted line is a monodromy cut to have (p, q) 5-branes at right angles with properly quantized charges [47]. In these constructions, instanton particles are D1-branes stretched between two NS5-branes, as shown in Fig. 2. In this setting, a 5D hypermultiplet in the spinor representation is introduced as follows [47]. One introduces another NS5-brane as shown in Fig. 3. D1'-branes suspended between $NS5_1$ and $NS5_2$ are the particles obtained by quantizing the hypermultiplet in the $SO(N)$ spinor representation. (See [47] for the chirality of the $SO(2N)$ spinor.) The mass of this field is proportional to the distance between $NS5_1$ and $NS5_2$. To introduce two hypermultiplets in the spinor representation, one puts another NS5-brane on the right side, as shown in Fig. 4. Note that for $SO(N)$
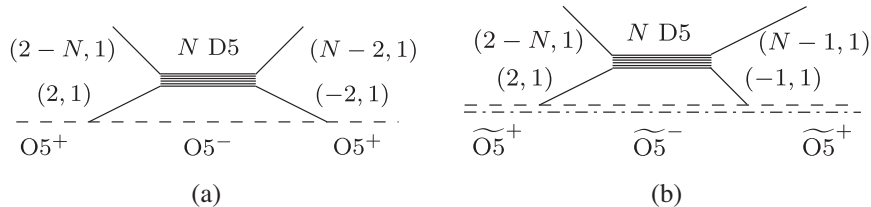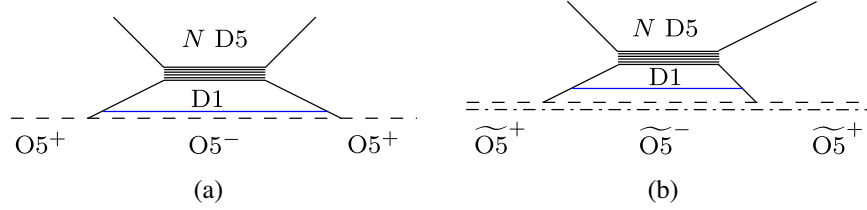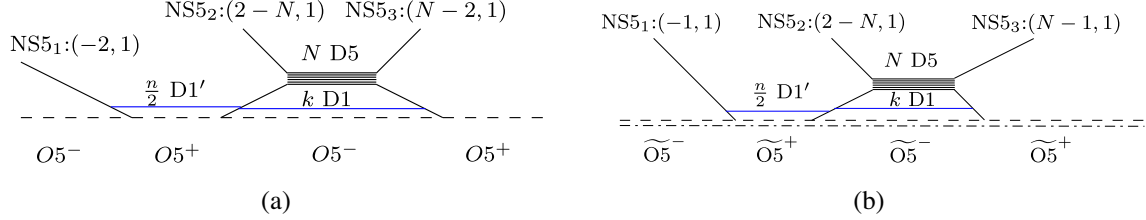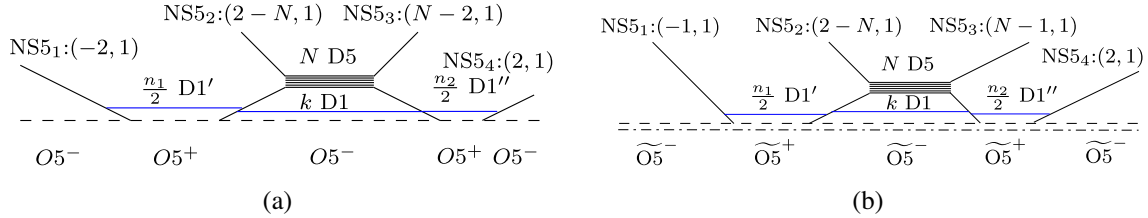

FIG. 1. Brane realizations of (a) $SO(2N)$ and (b) $SO(2N + 1)$ gauge theories.

FIG. 2. Instantons of (a) $SO(2N)$ and (b) $SO(2N+1)$ theories.

FIG. 3. Hypermultiplet in the spinor representation of (a) $SO(2N)$ and (b) $SO(2N+1)$.

FIG. 4. Two hypermultipets in the spinor representations of (a) $SO(2N)$ and (b) $SO(2N+1)$.

gauge theory with $N \le 6$, NS5$_1$- and NS5$_2$-branes do not intersect. For $N = 7, 8$, NS5$_1$ and NS5$_2$ are parallel to each other. In the last cases, there are extra continua of D1′ branes, orthogonally suspended between these parallel NS5-branes, which can escape to infinity and do not belong to 5D QFT. In Sec. III B, we discuss this extra sector in more detail. When $N \ge 9$, NS5$_1$ and NS5$_2$ meet at a certain point. In this case, we do not know how to use this setting to study the 5D QFT. So, in the rest of this paper, we focus on $SO(N)$ QFTs with $N \le 8$.

We discuss the quantum mechanical gauge theory, with given numbers of $SO(N)$ instantons k and hypermultiplet particles n_a. Their Witten indices will be used to test some results of Sec. II. In Sec. II, we did not fix the numbers of hypermultiplet particles, but instead had chemical potentials m_a for $Sp(n_8)$. Expanding the indices of Sec. II in e^{-m_a}, the coefficients will be the indices with fixed k, n_a, studied in this section.

We start from the case with one hypermultiplet, and consider the quantum mechanics of the D1 and D1′ branes. We first explain the symmetries. There is $SO(4) \sim SU(2)_l \times SU(2)_r$ rotating $x^1, \ldots, x^4$ and $SO(3) \sim SU(2)_R$ rotating x^7, x^8, x^9. The quantum mechanics preserves four real SUSY $\bar{Q}^{\dot{\alpha}A}$, where $\dot{\alpha}$ and A are doublet indices of
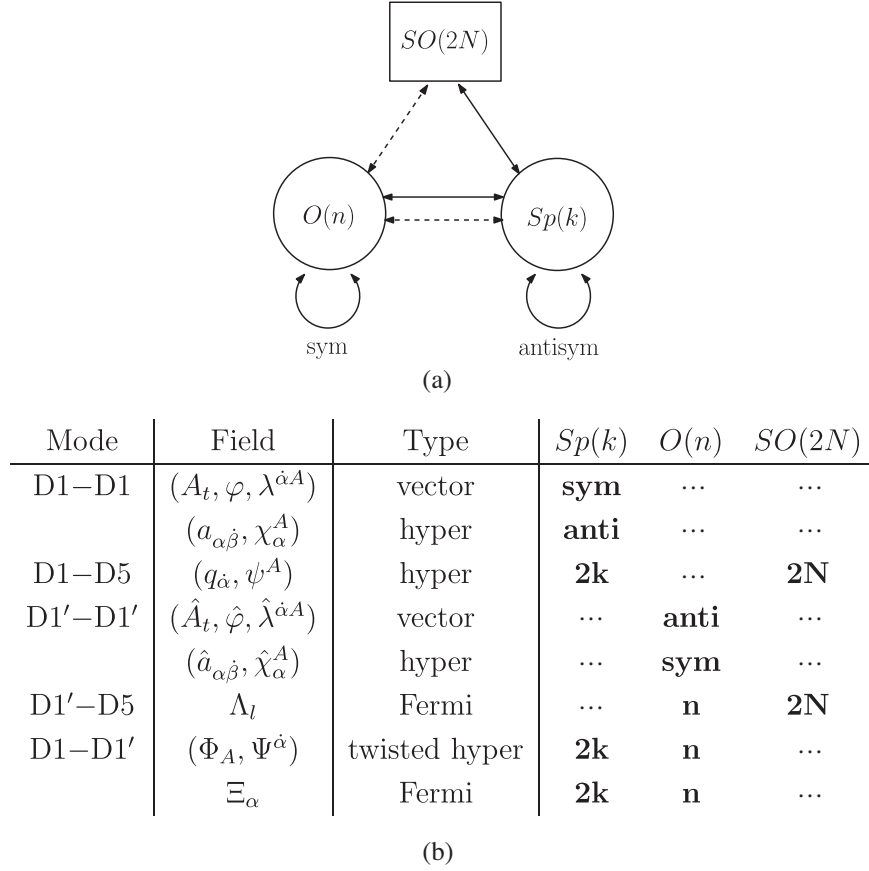
$SU(2)_r$ and $SU(2)_R$. It can be regarded as the 1D reduction of 2D $\mathcal{N} = (0, 4)$ SUSY. There are symmetries associated with D-branes and orientifolds. For r D1's and N D5's on various O5-planes, the symmetries are given as follows:

Branes	$O5^+$	$O5^-$	$\widetilde{O5}^+$	$\widetilde{O5}^-$
N D5	$Sp(N)$	$SO(2N)$	$Sp(N)$	$SO(2N+1)$
r D1	$O(2r)$	$Sp(r)$	$O(2r)$	$Sp(r)$

Here r is a half-integer $r = n/2$ for $O5^+$, $\widetilde{O5}^+$. So, D1 and D1′ in Fig. 3 have $Sp(k) \times O(n)$ gauge symmetry, while D5's induce $SO(2N)$ or $SO(2N+1)$ global symmetry.

The quantum mechanical "fields" are derived from open strings. They are shown in Figs. 5 and 6 for $SO(2N)$ and $SO(2N+1)$. The formal "$SO(1)$" in Fig. 6(a) comes from the half D5-brane on $\widetilde{O5}^-$, on the left side of NS5$_1$ in Fig. 3. The Lagrangian of this system preserving $\mathcal{N} = (0, 4)$ supersymmetry can be written down in a canonical manner. We focus on the bosonic part here. Along the strategy of [24], we first construct the Lagrangian in $\mathcal{N} = (0, 2)$ formalism, specifying the two possible types of superpotentials E and J for each Fermi multiplet [25]. Our $(0, 4)$ multiplets decompose to $(0,2)$ multiplets as follows:

FIG. 5. (a) 1D quiver and (b) matters for $SO(2N)$ (bold/dashed lines for hyper/Fermi).

$$\text{Vector}(A_t, \varphi, \lambda^{\dot\alpha A}) \rightarrow \text{vector } V(A_t, \varphi, \lambda^{\dot12}, \lambda^{\dot21}) + \text{Fermi } \lambda(\lambda^{\dot11}, \lambda^{\dot22})$$

$$\text{Vector}(\hat A_t, \hat\varphi, \hat\lambda^{\dot\alpha A}) \rightarrow \text{vector } \hat V(\hat A_t, \hat\varphi, \hat\lambda^{\dot12}, \hat\lambda^{\dot21}) + \text{Fermi } \hat\lambda(\hat\lambda^{\dot11}, \hat\lambda^{\dot22})$$

$$\text{Hyper}(a_{\alpha\dot\beta}, \chi_\alpha^A) \rightarrow \text{chiral } B(a_{c\dot1}, \chi_c^2) + \text{chiral } \tilde B^\dagger(a_{c\dot2}, \chi_c^1)$$

$$\text{Hyper}(\hat a_{\alpha\dot\beta}, \hat\chi_\alpha^A) \rightarrow \text{chiral } C(\varphi_{c\dot1}, \xi_c^2) + \text{chiral } \tilde C^\dagger(\varphi_{c\dot2}, \xi_c^1)$$

$$\text{Hyper}(q_{\dot\alpha}, \psi^A) \rightarrow \text{chiral } q(q_{\dot1}, \psi^2) + \text{chiral } \tilde q^\dagger(q_{\dot2}, \psi^1)$$

$$\text{Twisted hyper}(\Phi_A, \Psi^{\dot\alpha}) \rightarrow \text{chiral } \Phi(\Phi_1, \Psi^2) + \text{chiral } \tilde\Phi^\dagger(\Phi_2, \Psi^1)$$

$$\text{Fermi}(\Lambda_l), (\Lambda), (\Xi_\alpha) \rightarrow \text{Fermi}(\Lambda_l), (\Lambda), (\Xi_\alpha). \tag{3.1}$$
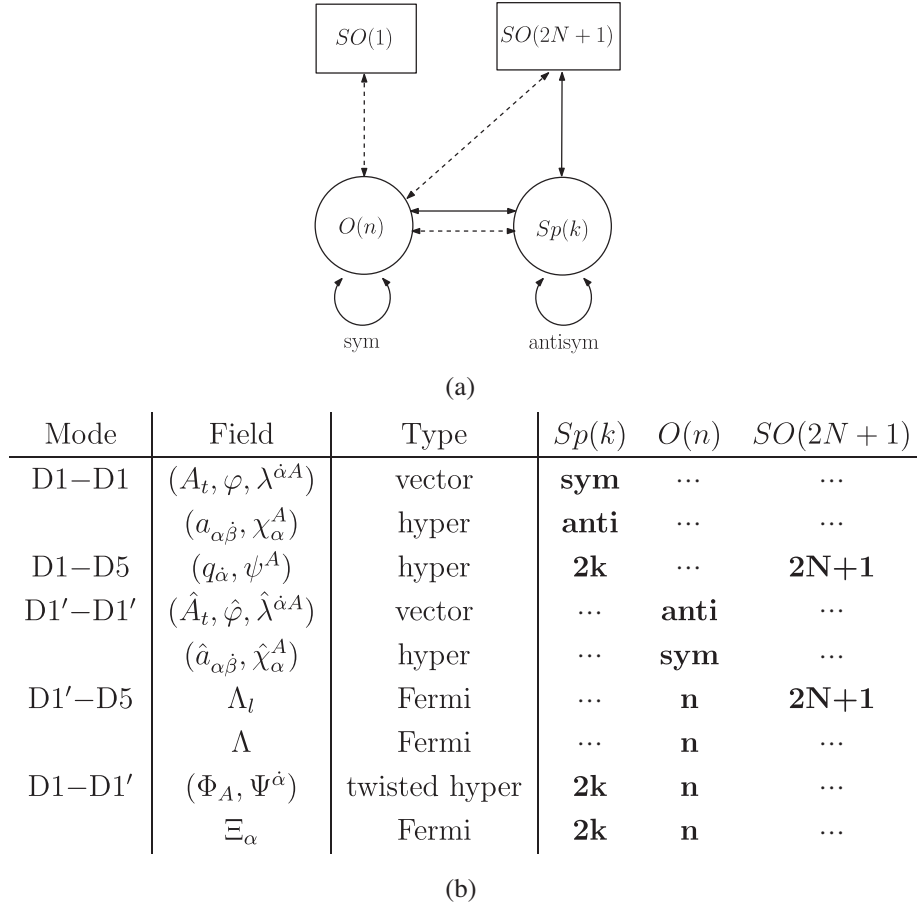
The scalars in rank 2 symmetric or antisymmetric representations are real. It decomposes to two (0,2) chiral multiplets whose scalars are complexified as $a_{c\dot\beta} = a_{1\dot\beta} + ia_{2\dot\beta}$ and likewise $\hat a_{c\dot\beta}$.

In (0,2) theories, one can turn on two types of holomorphic "superpotentials" for each Fermi multiplet Ψ, J_Ψ, and E_Ψ. The (0,2) supersymmetry demands the superpotentials to satisfy

$$\sum_{\nu \in \text{Fermi}} E_\nu J_\nu = 0. \tag{3.2}$$

We first consider the $SO(2N)$ theory, in which case E and J for Fermi multiplets are given by

$$J_\lambda = \sqrt2(q\tilde q + [B, \tilde B]) \qquad E_\lambda = -\sqrt2\tilde\Phi\Phi$$

$$J_{\hat\lambda} = \sqrt2[C, \tilde C] \qquad E_{\hat\lambda} = \sqrt2\Phi\tilde\Phi$$

$$J_{\Xi_1} = \sqrt2(\tilde\Phi\tilde C - \tilde B\tilde\Phi) \qquad E_{\Xi_1} = \sqrt2(C\Phi - \Phi B)$$

$$J_{\Xi_2} = -\sqrt2(\tilde\Phi C - B\tilde\Phi) \qquad E_{\Xi_2} = \sqrt2(\tilde C\Phi - \Phi\tilde B)$$

$$J_{\Lambda_l} = \sqrt2\tilde q\tilde\Phi \qquad E_{\Lambda_l} = \sqrt2\Phi q. \tag{3.3}$$

FIG. 6.   (a) 1D quiver and (b) matters for $SO(2N+1)$.

The first two lines, for (0,4) gauginos of $Sp(k) \times O(n)$, are required by demanding (0,4) SUSY enhancement [24]. Namely, gaugino fields' J and E acquire contributions only from hypermultiplets and twisted hypermultiplets, respectively. But with the first two lines only, (3.2) is not met. The next three lines are fixed (up to sign choices) by demanding (3.2) to hold, as illustrated in [24] in different models. D-terms are given by

$$D_{Sp(k)} = qq^\dagger - \tilde{q}^\dagger\tilde{q} + [B, B^\dagger] - [\tilde{B}^\dagger, \tilde{B}] - \Phi^\dagger\Phi + \tilde{\Phi}\tilde{\Phi}^\dagger$$

$$D_{O(n)} = [C, C^\dagger] - [\tilde{C}^\dagger, \tilde{C}] + \Phi\Phi^\dagger - \tilde{\Phi}^\dagger\tilde{\Phi}. \qquad (3.4)$$

With these superpotentials and D-terms, the bosonic potential energy is given by [24,25]

$$V = \sum_{G\in\text{gauge}} \frac{1}{2} D_G^2 + \sum_{\nu\in\text{Fermi}} (|E_\nu|^2 + |J_\nu|^2). \qquad (3.5)$$

One can show that (3.5) exhibits enhanced $SO(4) = SU(2)_r \times SU(2)_R$ R-symmetry,

$$V = \frac{1}{2}(q_{\dot\alpha}(\sigma^m)^{\dot\alpha}{}_{\dot\beta}q^{\dagger\dot\beta} + (\sigma^m)^{\dot\alpha}{}_{\dot\beta}[a_{\alpha\dot\alpha}, a^{\dagger\alpha\dot\beta}])^2$$

$$+ \frac{1}{2}((\sigma^m)^{\dot\alpha}{}_{\dot\beta}[\hat{a}_{\alpha\dot\alpha}, \hat{a}^{\dagger\alpha\dot\beta}])^2$$
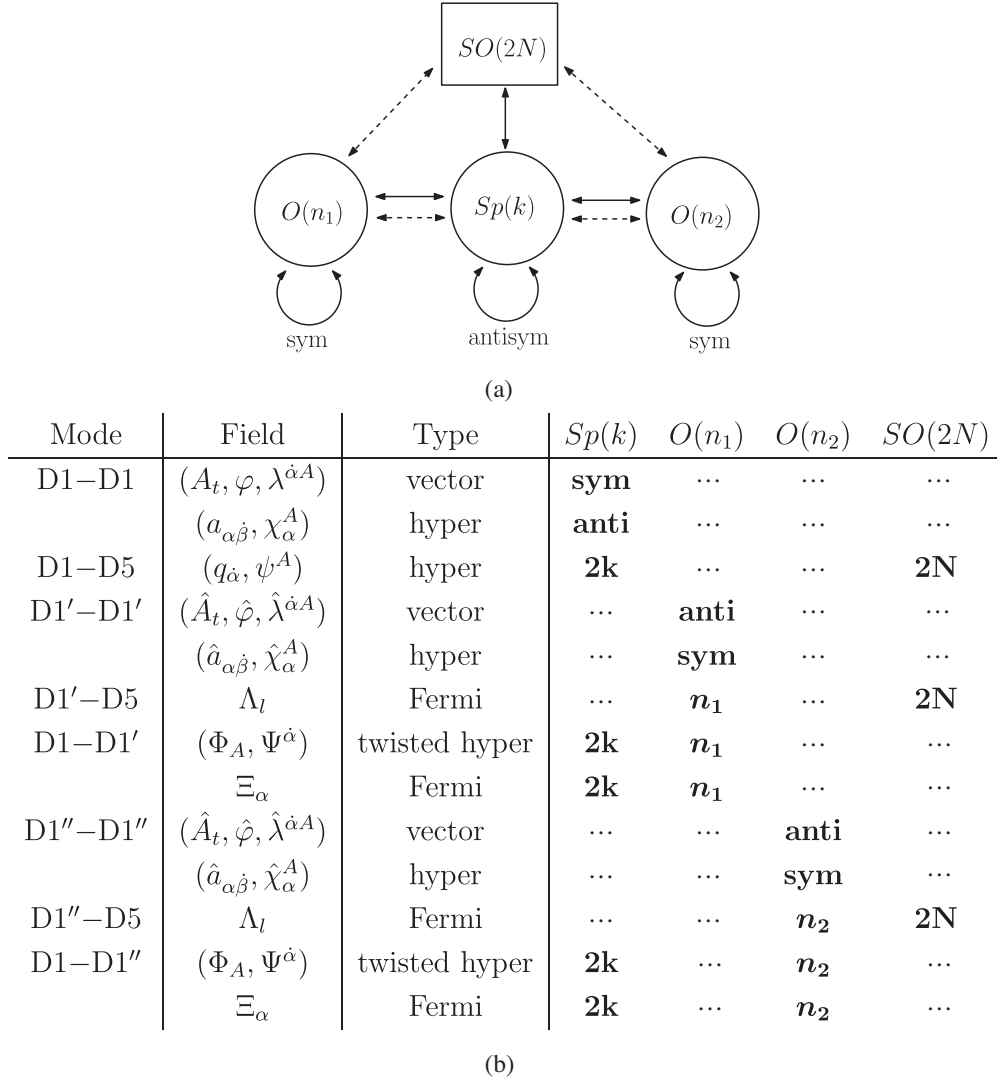
$$+ \frac{1}{2}(\Phi_A(\sigma^m)^A{}_B\Phi^{\dagger B})^2 + \frac{1}{2}(\Phi^{\dagger A}(\bar{\sigma}^m)_A{}^B\Phi_B)^2 + |\Phi_A q_{\dot\alpha}|^2$$

$$+ |\hat{a}_{\alpha\dot\beta}\Phi_A - \Phi_A a_{\alpha\dot\beta}|^2 + |\Phi^{\dagger A}\hat{a}_{\alpha\dot\beta} - a_{\alpha\dot\beta}\Phi^{\dagger A}|^2. \qquad (3.6)$$

Since $SO(4)$ is the $\mathcal{N} = (0,4)$ R-symmetry, this is a strong indication that the classical action indeed has (0,4) SUSY. We content ourselves with this observation, rather than checking (0,4) SUSY of the full action. The fields in the last expression satisfy the pseudoreality condition of $Sp(k)$, $\tilde{q}^T = \Lambda q$, $\tilde{\Phi}^T = \Phi(\Lambda^{-1})^T$, where Λ is the $Sp(k)$ skew-symmetric matrix.

One can repeat the analysis for the $SO(2N+1)$ quiver. One point to note here is that there is no superpotential for the Fermi multiplet Λ. So, despite the presence of $2N+2$ $O(n)$ fundamental Fermi multiplets Λ_l, Λ, their flavor symmetry is $SO(2N+1)$, as we expect from 5D bulk.

When there are two 5D hypermultiplets in the spinor representation of $SO(N)$, we can consider a sector with n_1 and n_2 particles and k instantons. The 1D quivers and fields are shown in Figs. 7 and 8. The Lagrangians can be

(a)

Mode	Field	Type	$Sp(k)$	$O(n_1)$	$O(n_2)$	$SO(2N)$
D1−D1	$(A_t, \varphi, \lambda^{\dot\alpha A})$	vector	**sym**	$\cdots$	$\cdots$	$\cdots$
	$(a_{\alpha\dot\beta}, \chi_\alpha^A)$	hyper	**anti**	$\cdots$	$\cdots$	$\cdots$
D1−D5	$(q_{\dot\alpha}, \psi^A)$	hyper	**2k**	$\cdots$	$\cdots$	**2N**
D1′−D1′	$(\hat A_t, \hat\varphi, \hat\lambda^{\dot\alpha A})$	vector	$\cdots$	**anti**	$\cdots$	$\cdots$
	$(\hat a_{\alpha\dot\beta}, \hat\chi_\alpha^A)$	hyper	$\cdots$	**sym**	$\cdots$	$\cdots$
D1′−D5	Λ_l	Fermi	$\cdots$	$\boldsymbol{n_1}$	$\cdots$	**2N**
D1−D1′	$(\Phi_A, \Psi^{\dot\alpha})$	twisted hyper	**2k**	$\boldsymbol{n_1}$	$\cdots$	$\cdots$
	Ξ_α	Fermi	**2k**	$\boldsymbol{n_1}$	$\cdots$	$\cdots$
D1″−D1″	$(\hat A_t, \hat\varphi, \hat\lambda^{\dot\alpha A})$	vector	$\cdots$	$\cdots$	**anti**	$\cdots$
	$(\hat a_{\alpha\dot\beta}, \hat\chi_\alpha^A)$	hyper	$\cdots$	$\cdots$	**sym**	$\cdots$
D1″−D5	Λ_l	Fermi	$\cdots$	$\cdots$	$\boldsymbol{n_2}$	**2N**
D1−D1″	$(\Phi_A, \Psi^{\dot\alpha})$	twisted hyper	**2k**	$\cdots$	$\boldsymbol{n_2}$	$\cdots$
	Ξ_α	Fermi	**2k**	$\cdots$	$\boldsymbol{n_2}$	$\cdots$

(b)

FIG. 7. The 1D quiver (a) and matters (b) for 5D $SO(2N)$ theory with two hypermultiplets.

constructed by following the completely same procedures, which we do not present here.

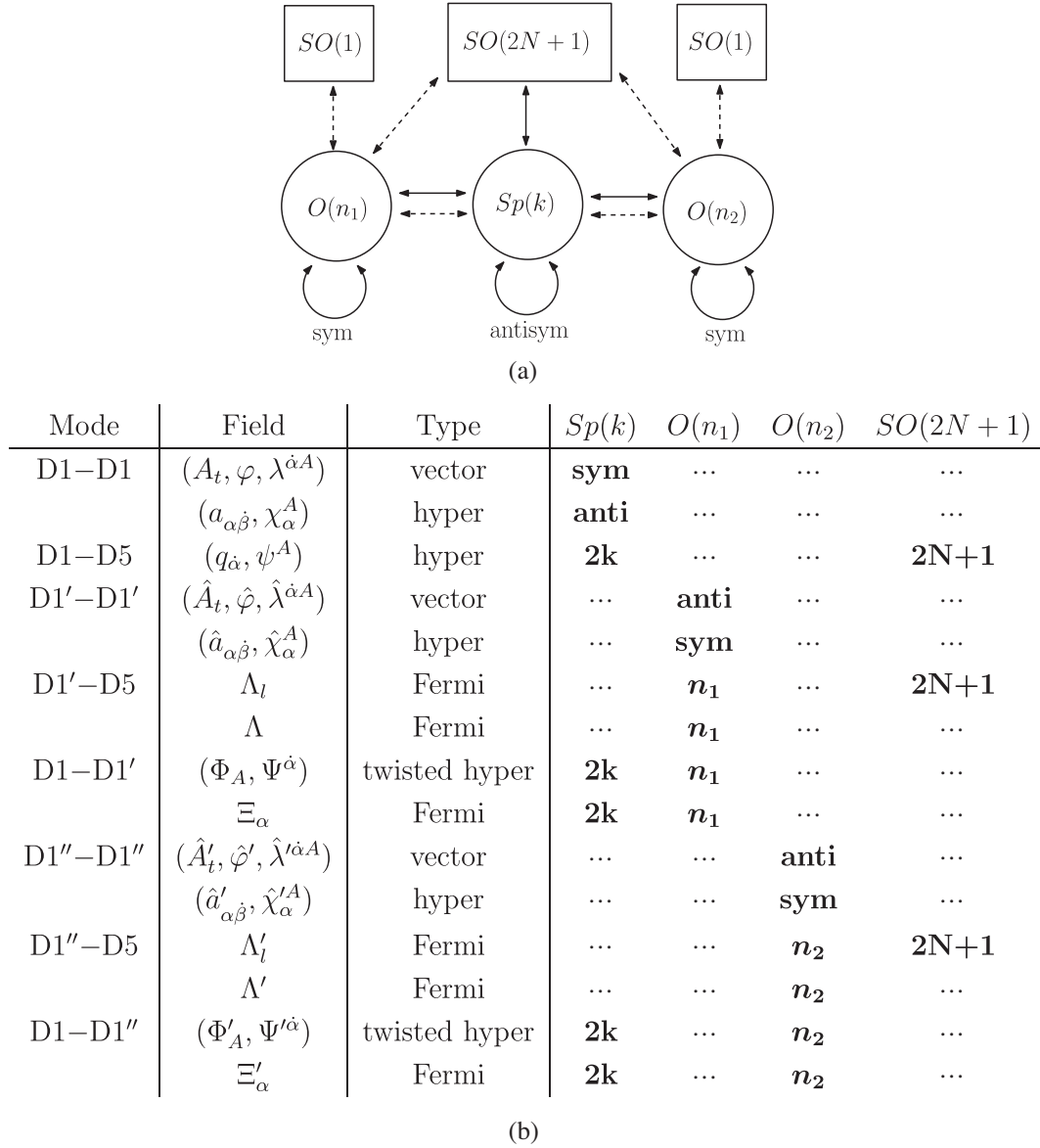### B. The instanton partition functions

We shall compute the Witten indices of the quantum mechanics presented in the previous subsection. They count BPS states preserving $Q = -\bar Q^{1\dot2}$ and $Q^\dagger = \bar Q^{2\dot1}$, and is defined by

$$Z_{QM} = \mathrm{Tr}[(-1)^F e^{-\beta\{Q,Q^\dagger\}} e^{-2\epsilon_+(J_r+J_R)} e^{-2\epsilon_- J_l} e^{-v_i q_i} e^{-z \cdot F}].$$

(3.7)

J_l, J_r, and J_R are Cartans of $SO(4) = SU(2)_l \times SU(2)_r$ and $SU(2)_R$, respectively, while q_i are the $SO(N)$ electric charges. F, z denote other charges and their chemical potentials.

We compute (3.7) using the contour integral formula of [11,22,27]. The zero modes in the path integral appear as the contour integral variables. They are the eigenvalues of the scalar φ and A_τ in the vector multiplet. For $O(n)$, the flat connections on S^1 have two disconnected sectors $O(n)_\pm$. $U = e^{R\phi} \equiv e^{R(\varphi+iA_\tau)}$, where R is the radius of the temporal circle, is given by

$$U_{O(2n)}^+ = \mathrm{diag}(e^{i\phi_1\sigma_2}, e^{i\phi_2\sigma_2}, \ldots, e^{i\phi_n\sigma_2}), \qquad U_{O(2n)}^- = \mathrm{diag}(e^{i\phi_1\sigma_2}, e^{i\phi_2\sigma_2}, \ldots, e^{i\phi_{n-1}\sigma_2}, \sigma_3)$$

$$U_{O(2n+1)}^+ = \mathrm{diag}(e^{i\phi_1\sigma_2}, e^{i\phi_2\sigma_2}, \ldots, e^{i\phi_n\sigma_2}, 1), \qquad U_{O(2n+1)}^- = \mathrm{diag}(e^{i\phi_1\sigma_2}, e^{i\phi_2\sigma_2}, \ldots, e^{i\phi_n\sigma_2}, -1)$$

$$U_{Sp(k)} = \mathrm{diag}(e^{i\phi_1\sigma_2}, e^{i\phi_2\sigma_2}, \ldots, e^{i\phi_k\sigma_2}).$$

(3.8)

Mode	Field	Type	$Sp(k)$	$O(n_1)$	$O(n_2)$	$SO(2N+1)$
D1−D1	$(A_t, \varphi, \lambda^{\dot\alpha A})$	vector	**sym**	$\cdots$	$\cdots$	$\cdots$
	$(a_{\alpha\dot\beta}, \chi_\alpha^A)$	hyper	**anti**	$\cdots$	$\cdots$	$\cdots$
D1−D5	$(q_{\dot\alpha}, \psi^A)$	hyper	**2k**	$\cdots$	$\cdots$	**2N+1**
D1′−D1′	$(\hat A_t, \hat\varphi, \hat\lambda^{\dot\alpha A})$	vector	$\cdots$	**anti**	$\cdots$	$\cdots$
	$(\hat a_{\alpha\dot\beta}, \hat\chi_\alpha^A)$	hyper	$\cdots$	**sym**	$\cdots$	$\cdots$
D1′−D5	Λ_l	Fermi	$\cdots$	$\boldsymbol{n_1}$	$\cdots$	**2N+1**
	Λ	Fermi	$\cdots$	$\boldsymbol{n_1}$	$\cdots$	$\cdots$
D1−D1′	$(\Phi_A, \Psi^{\dot\alpha})$	twisted hyper	**2k**	$\boldsymbol{n_1}$	$\cdots$	$\cdots$
	Ξ_α	Fermi	**2k**	$\boldsymbol{n_1}$	$\cdots$	$\cdots$
D1″−D1″	$(\hat A_t', \hat\varphi', \hat\lambda'^{\dot\alpha A})$	vector	$\cdots$	$\cdots$	**anti**	$\cdots$
	$(\hat a'_{\alpha\dot\beta}, \hat\chi'^A_\alpha)$	hyper	$\cdots$	$\cdots$	**sym**	$\cdots$
D1″−D5	Λ_l'	Fermi	$\cdots$	$\cdots$	$\boldsymbol{n_2}$	**2N+1**
	Λ'	Fermi	$\cdots$	$\cdots$	$\boldsymbol{n_2}$	$\cdots$
D1−D1″	$(\Phi'_A, \Psi'^{\dot\alpha})$	twisted hyper	**2k**	$\cdots$	$\boldsymbol{n_2}$	$\cdots$
	Ξ'_α	Fermi	**2k**	$\cdots$	$\boldsymbol{n_2}$	$\cdots$

(b)

FIG. 8.   The 1D quiver (a) and matters (b) for 5D $SO(2N+1)$ theory with two hypermultiplets.

σ_i are Pauli matrices, "diag" mean block-diagonal matrices, and $\det(U^\pm) = \pm 1$. The integrand acquires contributions from various multiplets. A chiral multiplet Φ and a Fermi multiplet Ψ contribute as

$$Z_\Phi = \prod_{\rho \in R_\Phi} \frac{1}{2\sinh(\frac{\rho(\phi)+2J\epsilon_+ + Fz}{2})},$$

$$Z_\Psi = \prod_{\rho \in R_\Psi} 2\sinh\left(\frac{\rho(\phi)+2J\epsilon_+ + Fz}{2}\right), \quad (3.9)$$

respectively. ρ runs over the weights of $Sp(k)$, $O(n)$ in the representation R_Φ, R_Ψ, and J are defined by $J = J_r + J_R$. F collectively denotes the remaining charges. A (0,2) vector multiplet V contributes similarly as $Z_V = \prod_{\alpha \in \text{root}} 2\sinh\frac{\alpha(\phi)}{2}$, where we used the formula for

a Fermi multiplet at $J = 0$, $F = 0$. Collecting all, the Witten index is given by

$$Z = \frac{1}{|W|} \oint \frac{d\phi}{2\pi i} Z_{\text{one-loop}}, \quad Z_{\text{one-loop}} \equiv \prod_V Z_V \prod_\Phi Z_\Phi \prod_\Psi Z_\Psi.$$
$$(3.10)$$

The $O(n)$ holonomy has two discrete sectors. The Witten index is given by [48]

$$Z = \frac{Z^+ + Z^-}{2}. \quad (3.11)$$

The Weyl factors $|W|$ of $O(2n)_\pm$, $O(2n+1)_\pm$, $Sp(k)$ are given by [48]

$$|W_{O(2n)_+}| = \frac{1}{2^{n-1}n!}, \qquad |W_{O(2n)_-}| = \frac{1}{2^{n-1}(n-1)!}, \qquad |W_{O(2n+1)_+}| = |W_{O(2n+1)_-}| = \frac{1}{2^n n!}, \qquad |W_{Sp(k)}| = \frac{1}{2^k k!}.$$
(3.12)

For $SO(N)$ with odd N, one can show that $Z_{\text{one-loop}} = 0$ in $O(2n)_-$ and $O(2n+1)_+$ sectors, since the fermionic zero modes from Λ [in table Fig. 6(b)] provide factors of 0's.

Let us call $Z_{k,n}$ the index of the $Sp(k) \times O(n)$ quiver. Being a multiparticle index, it acquires contribution from n hypermultiplet particles either bound or unbound to k instantons. Also, as we shall explain in more detail below, $Z_{k,n}$ for $n \geq 2$ also contains a spurious contribution from particles not belonging to the 5D QFT. To explain these structures clearly, we first discuss the indices $Z_{0,n}$ before considering the instanton partition functions at $k \neq 0$. At $n = 1$, $k = 0$, the $O(1)$ indices do not contain integrals. The results are given by

$$Z_{0,1}^{SO(2N)} = \frac{1}{2} \left(\frac{\prod_{l=1}^{N} 2 \sinh \frac{v_l}{2}}{2 \sinh \frac{\epsilon_1}{2} \cdot 2 \sinh \frac{\epsilon_2}{2}} + \frac{\prod_{l=1}^{N} 2 \cosh \frac{v_l}{2}}{2 \sinh \frac{\epsilon_1}{2} \cdot 2 \sinh \frac{\epsilon_2}{2}} \right)$$

$$Z_{0,1}^{SO(2N+1)} = \frac{\prod_{l=1}^{N} 2 \cosh \frac{v_l}{2}}{2 \sinh \frac{\epsilon_1}{2} \cdot 2 \sinh \frac{\epsilon_2}{2}}.$$
(3.13)

The overall factors $(2 \sinh \frac{\epsilon_1}{2} \cdot 2 \sinh \frac{\epsilon_2}{2})^{-1}$ in (3.13) come from the center-of-mass motion on $\mathbb{R}^4$. The remaining factor is the character of the $SO(2N)$ chiral spinor $\frac{\prod_{l=1}^{N} 2 \sinh \frac{v_l}{2} + \prod_{l=1}^{N} 2 \cosh \frac{v_l}{2}}{2}$ and that of $SO(2N+1)$ spinor $\prod_{l=1}^{N} 2 \cosh \frac{v_l}{2}$, respectively. They are the perturbative partition functions of matters in $SO(N)$ in spinor representations. Next, $Z_{0,2}$ is given by

$$Z_{0,2}^{SO(2N)} = \frac{1}{2} \left[\oint \frac{d\chi}{2\pi i} \frac{2 \sinh \epsilon_+ \cdot \prod_{l=1}^{N} 2 \sinh(\frac{v_l \pm \chi}{2})}{2 \sinh(\frac{\epsilon_{1,2}}{2}) \cdot 2 \sinh(\frac{\epsilon_{1,2} \pm 2\chi}{2})} \right.$$

$$\left. + \frac{2 \cosh \epsilon_+ \cdot \prod_{l=1}^{N} 2 \sinh v_l}{2 \cosh \frac{\epsilon_{1,2}}{2} \cdot (2 \sinh \frac{\epsilon_{1,2}}{2})^2} \right]$$

$$Z_{0,2}^{SO(2N+1)} = \frac{1}{2} \oint \frac{d\chi}{2\pi i}$$

$$\times \frac{2 \sinh \epsilon_+ \cdot \prod_{l=1}^{N} 2 \sinh(\frac{v_l \pm \chi}{2}) \cdot 2 \sinh(\pm \frac{\chi}{2})}{2 \sinh(\frac{\epsilon_{1,2}}{2}) \cdot 2 \sinh(\frac{\epsilon_{1,2} \pm 2\chi}{2})}.$$
(3.14)

For $SO(2N+1)$ and the first term of $SO(2N)$ index, one should evaluate JK-Res. With the choice $\eta > 0$, one keeps the residues at $\chi = -\frac{\epsilon_{1,2}}{2}$ and $\chi = -\frac{\epsilon_{1,2}}{2} + \pi i$.[6] For $N \leq 6$, one obtains

$$Z_{0,2}^{SO(N)} = \frac{Z_{0,1}^{SO(N)}(\epsilon_\pm, v_l)^2 + Z_{0,1}^{SO(N)}(2\epsilon_\pm, 2v_l)}{2}, \quad (3.15)$$

while for $N = 7, 8$, one obtains

$$Z_{0,2}^{SO(N)} = \frac{Z_{0,1}^{SO(N)}(\epsilon_\pm, v_l)^2 + Z_{0,1}^{SO(N)}(2\epsilon_\pm, 2v_l)}{2} - \frac{1}{2} \cdot \frac{2 \cosh \epsilon_+}{2 \sinh \frac{\epsilon_{1,2}}{2}}.$$
(3.16)

Equation (3.15) and the first term of (3.16) are the indices of two noninteracting identical particles, whose single particle index is given by $Z_{0,1}^{SO(N)}$. There are no bound states formed by these perturbative hypermultiplet particles, as expected. The second term of (3.16) requires more explanations, which we now turn to.

The second term of (3.16) comes from extra states in the brane system that do not belong to the 5D QFT. In particular, the fractional coefficient in the fugacity expansion implies that it comes from a sector which has a continuum unlifted by our massive deformations. In fact, following the arguments presented between (2.28) and (2.29), one finds that the linear one-loop potential from (3.14) vanishes for $N = 7, 8$, implying continua. Physically, this comes from a D1'-brane moving away from 5D QFT, suspended between two parallel 5-branes as in Fig. 9. Although we are not aware of fully logical arguments, it has been empirically observed that the last term $-\frac{1}{2} \frac{2 \cosh \epsilon_+}{2 \sinh \frac{\epsilon_{1,2}}{2}}$ is the contribution from the escaping particle for strings suspended between parallel 5-branes; e.g., see Eq. (3.62) of [22]. See also [49–51] for related results. The suspended string of Fig. 9 carries the same spacetime and R-symmetry quantum numbers as a 5D vector multiplet particles, since the configuration of Fig. 9 is locally dual to a fundamental string suspended between two D5-branes (a 5D vector W-boson). Indeed, the chemical potential dependence $\sim \frac{2 \cosh \epsilon_+}{2 \sinh \frac{\epsilon_{1,2}}{2}}$ is precisely that of a 5D W-boson and its superpartners. Such extra states start to appear at $n \geq 2$, since at $n = 1$, one only has fractional D1' stuck to O5.
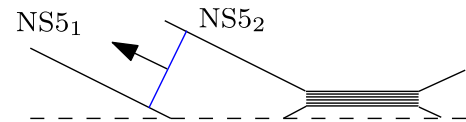

FIG. 9. D1'-brane escaping the 5D QFT.

[6]For $O(n)$ and $Sp(k)$ gauge theories, the choice of η does not affect the results due to Weyl symmetry [22].

Collecting all, we expect that the partition function at $k = 0$ is given by

$$\sum_{n=0}^{\infty} e^{-nm} Z_{0,n}^{SO(N)} = Z_{\text{pert}} \equiv \text{PE}[e^{-m} Z_{0,1}^{SO(N)}] \qquad (3.17)$$

for $N \leq 6$, while for $N = 7, 8$ we expect that it is given by

$$\sum_{n=0}^{\infty} e^{-nm} Z_{0,n}^{SO(N)} = Z_{\text{pert}} Z_{\text{extra}}$$

$$= \text{PE}[e^{-m} Z_{0,1}^{SO(N)}] \, \text{PE}\left[-\frac{1}{2} e^{-2m} \frac{2 \cosh \epsilon_+}{2 \sinh \frac{\epsilon_{1,2}}{2}} \right]. \qquad (3.18)$$

Here, $Z_{0,0} \equiv 1$ by definition, and $PE[f(x, y, \cdots)] \equiv \exp\left[\sum_{n=1}^{\infty} \frac{1}{n} f(nx, ny, \cdots)\right]$ is the multi-particle index for the single particle index f.

The full partition function would factorize as

$$\sum_{k,n=0}^{\infty} q^k e^{-nm} Z_{k,n}^{SO(N)}$$

$$= Z_{\text{inst}}(q, \epsilon_{1,2}, m) Z_{\text{pert}}(\epsilon_{1,2}, m) Z_{\text{extra}}(\epsilon_{1,2}, m). \qquad (3.19)$$

Expanding $Z_{\text{inst}}(q) = \sum_{k=0}^{\infty} Z_k q^k$ where $Z_0 \equiv 1$, (3.19) implies at given q^k order that

$$\sum_{n=0}^{\infty} e^{-nm} Z_{k,n} = Z_k Z_{\text{pert}} Z_{\text{extra}}. \qquad (3.20)$$

When there are two 5D hypermultiplets as in Fig. 4, the full partition function is

$$Z^{(2)} = \sum_{k,n_1,n_2=0}^{\infty} q^k e^{-n_1 m_1 - n_2 m_2} Z_{k_1, n_1, n_2}, \qquad (3.21)$$

where Z_{k,n_1,n_2} is the index for k D1, n_1 D1′, and n_2 D1″. $m_{1,2}$ are the $Sp(2)$ flavor chemical potentials. The contributions from perturbative and extra degrees of freedom in this case are

$$Z_{\text{pert}}^{(2)}(\epsilon_{1,2}, m_{1,2}) = Z_{\text{pert}}(\epsilon_{1,2}, m_1) Z_{\text{pert}}(\epsilon_{1,2}, m_2)$$

$$Z_{\text{extra}}^{(2)}(\epsilon_{1,2}, m_{1,2}) = Z_{\text{extra}}(\epsilon_{1,2}, m_1) Z_{\text{extra}}(\epsilon_{1,2}, m_2), \qquad (3.22)$$

where Z_{pert} and Z_{extra} take the same forms as in (3.18).

Although our methods apply well to both $SO(8)$ and $SO(7)$, we only study the cases with $SO(7)$ in this paper. We start from the case with one hypermultiplet field. From the field contents of Fig. 6, $Z_{\text{one-loop}}$ for k instantons and $2n(= \text{even})$ hypermultiplet particles is given by

$$[Z_{\text{one-loop}}]_{k,2n}^{SO(7)} = \frac{1}{2^k k!} \frac{(2 \sinh \epsilon_+)^k \cdot \prod_{i=1}^{k} 2 \sinh(\epsilon_+ \pm \phi_i) 2 \sinh(\pm \phi_i) \cdot \prod_{i>j} 2 \sinh(\frac{2\epsilon_+ \pm \phi_i \pm \phi_j}{2}) 2 \sinh(\frac{\pm \phi_i \pm \phi_j}{2})}{(2 \sinh(\frac{\epsilon_{1,2}}{2}))^k \cdot \prod_{i>j} 2 \sinh(\frac{\epsilon_{1,2} \pm \phi_i \pm \phi_j}{2}) \cdot \prod_{i=1}^{k} \prod_{l=1}^{3} 2 \sinh(\frac{\epsilon_+ \pm \phi_i \pm v_l}{2}) \cdot \prod_{i=1}^{k} 2 \sinh(\frac{\epsilon_+ \pm \phi_i}{2})}$$

$$\cdot \frac{1}{2^n n!} \frac{(2 \sinh \epsilon_+)^n \cdot \prod_{I>J} 2 \sinh(\frac{2\epsilon_+ \pm \chi_I \pm \chi_J}{2}) \cdot \prod_{I>J} 2 \sinh(\frac{\pm \chi_I \pm \chi_J}{2})}{(2 \sinh(\frac{\epsilon_{1,2}}{2}))^n \cdot \prod_{I=1}^{n} 2 \sinh(\frac{\epsilon_{1,2} \pm 2\chi_I}{2}) \cdot \prod_{I>J} 2 \sinh(\frac{\epsilon_{1,2} \pm \chi_I \pm \chi_J}{2})}$$

$$\cdot \prod_{I=1}^{n} \prod_{l=1}^{3} 2 \sinh\left(\frac{\pm \chi_I + v_l}{2}\right) \cdot \prod_{I=1}^{n} 2 \sinh\left(\frac{\chi_I}{2}\right) \cdot \frac{\prod_{i=1}^{k} \prod_{I=1}^{n} 2 \sinh(\frac{\epsilon_- \pm \phi_i \pm \chi_I}{2})}{\prod_{i=1}^{k} \prod_{I=1}^{n} 2 \sinh(\frac{-\epsilon_+ \pm \phi_i \pm \chi_I}{2})}, \qquad (3.23)$$

while $Z_{\text{one-loop}}$ for k instantons and $2n + 1$ hypermultiplet particles is given by

$$[Z_{\text{one-loop}}]_{k,2n+1}^{SO(7)} = \frac{1}{2^k k!} \frac{(2 \sinh \epsilon_+)^k \cdot \prod_{i=1}^{k} 2 \sinh(\epsilon_+ \pm \phi_i) 2 \sinh(\pm \phi_i) \cdot \prod_{i>j} 2 \sinh(\frac{2\epsilon_+ \pm \phi_i \pm \phi_j}{2}) 2 \sinh(\frac{\pm \phi_i \pm \phi_j}{2})}{(2 \sinh(\frac{\epsilon_{1,2}}{2}))^k \cdot \prod_{i>j} 2 \sinh(\frac{\epsilon_{1,2} \pm \phi_i \pm \phi_j}{2}) \cdot \prod_{i=1}^{k} \prod_{l=1}^{3} 2 \sinh(\frac{\epsilon_+ \pm \phi_i \pm v_l}{2}) \cdot \prod_{i=1}^{k} 2 \sinh(\frac{\epsilon_+ \pm \phi_i}{2})}$$

$$\cdot \frac{1}{2^n n!} \frac{(2 \sinh \epsilon_+)^n \cdot \prod_{I>J} 2 \sinh(\frac{2\epsilon_+ \pm \chi_I \pm \chi_J}{2}) \cdot \prod_{I>J} 2 \sinh(\frac{\pm \chi_I \pm \chi_J}{2})}{(2 \sinh(\frac{\epsilon_{1,2}}{2}))^{n+1} \cdot \prod_{I=1}^{n} 2 \sinh(\frac{\epsilon_{1,2} \pm 2\chi_I}{2}) \cdot \prod_{I>J} 2 \sinh(\frac{\epsilon_{1,2} \pm \chi_I \pm \chi_J}{2}) \prod_{I=1}^{n} 2 \cosh(\frac{\epsilon_{1,2} \pm \chi_I}{2})}$$

$$\cdot \prod_{I=1}^{n} \prod_{l=1}^{3} 2 \sinh\left(\frac{\pm \chi_I + v_l}{2}\right) \cdot \prod_{I=1}^{n} 2 \sinh\left(\frac{\chi_I}{2}\right) \cdot \prod_{I=1}^{n} 2 \cosh\left(\frac{2\epsilon_+ \pm \chi_I}{2}\right) \cdot \prod_{I=1}^{n} 2 \cosh\left(\frac{\chi_I}{2}\right) \prod_{l=1}^{3} 2 \cosh\left(\frac{v_l}{2}\right)$$

$$\cdot \frac{\prod_{i=1}^{k} \prod_{I=1}^{n} 2 \sinh(\frac{\epsilon_- \pm \phi_i \pm \chi_I}{2}) \cdot \prod_{i=1}^{k} 2 \cosh(\frac{\epsilon_- \pm \phi_i}{2})}{\prod_{i=1}^{k} \prod_{I=1}^{n} 2 \sinh(\frac{-\epsilon_+ \pm \phi_i \pm \chi_I}{2}) \cdot \prod_{i=1}^{k} 2 \cosh(\frac{-\epsilon_+ \pm \phi_i}{2})}. \qquad (3.24)$$

$i, j = 1, \ldots, k$ are $Sp(k)$ indices, $I, J = 1, \ldots, n$ are $O(2n)$ or $O(2n+1)$ indices, and $l = 1, 2, 3$ are $SO(7)$ indices. Equations (3.23) and (3.24) are computed on either $O(n)_+$ or $O(n)_-$ sector, where χ_I are eigenvalues of $\log U^{\pm}$ given by (3.8).

The partition function at $k = 1$, $n = 0$ is given by

$$Z_{1,0}^{SO(7)} = \oint \frac{d\phi}{2\pi i} \frac{1}{2} \cdot \frac{2\sinh\epsilon_+ \cdot 2\sinh(\epsilon_+ \pm \phi) \cdot 2\sinh(\pm\phi)}{2\sinh(\frac{\epsilon_{1,2}}{2}) \cdot \prod_{l=1}^3 2\sinh(\frac{\epsilon_+ \pm \phi \pm v_l}{2}) \cdot 2\sinh(\frac{\epsilon_+ \pm \phi}{2})}. \tag{3.25}$$

Poles chosen at $\eta > 0$ are $\phi = -\epsilon_+$, $\phi = -\epsilon_+ \pm v_l$, but the residue from $\phi = -\epsilon_+$ vanishes. Collecting the residues, one obtains

$$Z_{1,0}^{SO(7)} = \frac{t}{(1-tu)(1-t/u)} \prod_{i<j} \frac{t^4}{(1-t^2 b_i^\pm b_j^\pm)} (\chi_9^{SU(2)} + \chi_7^{SU(2)}(\chi_7^{SO(7)} + 1)$$

$$+ \chi_5^{SU(2)}(-\chi_{35}^{SO(7)} + \chi_7^{SO(7)} + 1) + \chi_3^{SU(2)}(-\chi_{35}^{SO(7)} + \chi_{27} + 1) + \chi_{105}^{SO(7)} - \chi_{21}^{SO(7)} + \chi_7^{SO(7)})$$

$$= \frac{t}{(1-tu)(1-t/u)} \sum_{p=0}^\infty \chi_{(0,p,0)}(v_l) t^{2p+4}, \tag{3.26}$$

where $t = e^{-\epsilon_+}$ and $u = e^{-\epsilon_-}$. Here $\chi_{\mathbf{R}}$ is the character of $SO(7)$ representation **R**. This is simply the well-known one-instanton partition function of $SO(7)$ gauge theory. E.g., see [52] for the above character expansion form.

Next, consider the sector at $k = 1$, $n = 1$. $Z_{1,1}^{SO(7)}$ is given by

$$Z_{1,1}^{SO(7)} = \oint \frac{d\phi}{2\pi i} [Z_{\text{one-loop}}]_{1,0}^{SO(7)} \frac{\prod_{l=1}^3 2\cosh(\frac{v_l}{2})}{2\sinh(\frac{\epsilon_{1,2}}{2})} \cdot \frac{2\cosh(\frac{\epsilon_- \pm \phi}{2})}{2\cosh(\frac{-\epsilon_+ \pm \phi}{2})}. \tag{3.27}$$

Poles chosen at $\eta > 0$ with nonzero residues are at $\phi = -\epsilon_+ \pm v_l$. As we explained around (3.20), $Z_{1,1}^{SO(7)}$ has contributions from Z_{pert} at $n = 1$. Let us call the proper contribution to the instanton partition function $\hat{Z}_{k,n}^{SO(7)}$. From (3.20), one obtains

$$\hat{Z}_{1,1}^{SO(7)} = Z_{1,1}^{SO(7)} - Z_{1,0}^{SO(7)} Z_{0,1}^{SO(7)}. \tag{3.28}$$

Hat denotes the instanton partition function at level (k, n), while $Z_{k,n}$ is simply the Witten index of our $Sp(k) \times O(n)$ quantum mechanics. From this formula, one obtains

$$\hat{Z}_{1,1}^{SO(7)} = \frac{t}{(1-tu^{\pm 1})} \prod_{i<j} \frac{t^4}{(1-t^2 b_i^\pm b_j^\pm)} (-\chi_8^{SU(2)} \chi_8^{SO(7)} - \chi_6^{SU(2)} \chi_8^{SU(2)} + \chi_4^{SU(2)} \chi_{112}^{SO(7)} - \chi_2^{SU(2)} \chi_{168}^{SO(7)})$$

$$= -\frac{t}{(1-tu^{\pm 1})} \sum_{p=0}^\infty \chi_{(0,p,1)} t^{2p+5}, \tag{3.29}$$

where $\sum_{p=0}^\infty \chi_{(0,p,1)} t^{2p+5} = \chi_8(v_l) + \chi_{112}(v_l) t^2 + \chi_{720}(v_l) t^4 + \cdots$. Then consider the sector at $k = 1$, $n = 2$. $Z_{1,2}^{SO(7)}$ is given by the $Sp(1) \times O(2)$ contour integral,

$$Z_{1,2}^{SO(7)} = \oint \frac{d\phi d\chi}{(2\pi i)^2} [Z_{\text{one-loop}}]_{1,0}^{SO(7)} \cdot \frac{1}{2} \cdot \frac{2\sinh\epsilon_+ \cdot \prod_{l=1}^3 2\sinh(\frac{\pm\chi + v_l}{2}) \cdot 2\sinh(\frac{\pm\chi}{2})}{2\sinh(\frac{\epsilon_{1,2}}{2}) \cdot 2\sinh(\frac{\epsilon_{1,2} \pm 2\chi}{2})} \cdot \frac{2\sinh(\frac{\epsilon_- \pm \phi \pm \chi}{2})}{2\sinh(\frac{-\epsilon_+ \pm \phi \pm \chi}{2})}. \tag{3.30}$$

Taking $\eta = (1, 1 + \epsilon)$ for small positive ϵ [22], the poles at $(\phi, \chi) = (-\epsilon_+ \pm v_l, -\frac{\epsilon_{1,2}}{2}[+\pi i])$, $(-\epsilon_+ \pm v_l, \pm v_l)$, $(\epsilon_+ \pm v_l, \mp v_l)$, $(0[+\pi i], \epsilon_+ + [\pi i])$, $(\frac{\epsilon_{1,2}}{2}[+\pi i], -\frac{\epsilon_{2,1}}{2}[+\pi i])$, $(\frac{3\epsilon_+ \pm \epsilon_-}{2}, -\frac{\epsilon_{1,2}}{2}[+\pi i])$ are chosen. $[+\pi i]$ means that there are two cases with and without $+\pi i$ addition. Subtracting the contribution from $Z_{\text{pert}} Z_{\text{extra}}$ in (3.20), the instanton partition function $\hat{Z}_{1,2}^{SO(7)}$ at this order is given by $\hat{Z}_{1,2} = Z_{1,2} - \hat{Z}_{1,1} Z_{0,1} - Z_{1,0} Z_{0,2}$. One finds after computations that

$$\hat{Z}_{1,2}^{SO(7)} = Z_{1,0}^{SO(7)}. \tag{3.31}$$

For $n \geq 3$, we find $\hat{Z}_{1,n} = 0$. We checked this exactly for $n = 3$. For $n = 4$, to save time, we plugged in random numbers in the chemical potentials and checked that $\hat{Z}_{1,4}^{SO(7)}$ is very small. (Below, we present an argument for this phenomenon.)

Collecting all the computations at $n = 0, 1, 2$, one obtains

$$
\begin{aligned}
Z_{k=1} &= e^m [Z_{1,0} + e^{-m} \hat{Z}_{1,1} + e^{-2m} \hat{Z}_{1,2}] \\
&= \frac{t}{(1 - tu^{\pm 1})} \prod_{i < j} \frac{t^4}{(1 - t^2 b_i^{\pm} b_j^{\pm})} [-\chi_8^{SU(2)} \chi_8^{SO(7)} - \chi_6^{SU(2)} \chi_8^{SO(7)} + \chi_4^{SU(2)} \chi_{112}^{SO(7)} - \chi_2^{SU(2)} \chi_{168}^{SO(7)} \\
&\quad + (\chi_9^{SU(2)} + \chi_7^{SU(2)})(\chi_7^{SO(7)} + 1) + \chi_5^{SU(2)}(-\chi_{35}^{SO(7)} + \chi_7^{SO(7)} + 1) \\
&\quad + \chi_3^{SU(2)}(-\chi_{35}^{SO(7)} + \chi_{27} + 1) + \chi_{105}^{SO(7)} - \chi_{21}^{SO(7)} + \chi_7^{SO(7)})(e^m + e^{-m})].
\end{aligned}
\tag{3.32}
$$

Here we multiplied an overall factor e^m, like the "'zero point energy'" factor, to have the expected Weyl symmetry $m \to -m$ of the $Sp(1)$ flavor symmetry. Noting that $e^m + e^{-m} = \chi_2^{Sp(1)}$, (3.32) completely agrees with (2.30), supporting our ADHM-like proposals of section II at $n_8 = 1$.

Here we discuss more about the maximal value of n with $\hat{Z}_{k,n}^{SO(7)} \neq 0$, at given k. Note that

$$
Z_{\text{inst}}(q, \epsilon_{1,2}, v, m) = e^{-\epsilon_0} \sum_{k=0}^{\infty} \sum_{n=0}^{\infty} q^k e^{-nm} \hat{Z}_{k,n}^{SO(7)}(\epsilon_{1,2}, v),
\tag{3.33}
$$

refining the previous definition by the zero point energylike factor. Note that m is the flavor chemical potential for the 5D hypermultiplet. Since a hypermultiplet only adds fermion zero modes on the instanton moduli space, the rotation parameter m acts only on these fermions. So, unlike the chemical potentials v_i, $\epsilon_{1,2}$ which act on noncompact zero modes, the coefficient Z_k of Z_{inst} at given q^k order should not have any poles in m. Since Z_k admits

fugacity expansions, this implies that Z_k is a finite polynomial in e^m and e^{-m}. So the sum over n should truncate to $0 \leq n \leq n_{\max}$ for some finite $n_{\max}$, also with a suitable m-dependent ϵ_0 to ensure the Weyl symmetry of $Sp(1)$. One can also naturally infer the value of $n_{\max}$. To see this, note that a 5D hypermultiplet in the spinor representation induces $kD(\mathbf{8}) = 2kT(\mathbf{8}) = 2k$ complex fermion zero modes on the moduli space, where we used $2T = 2^{N-2}$ for $SO(2N + 1)$ spinor representation. Quantizing them into $2k$ pairs of fermionic harmonic oscillators, each oscillator raises/lowers the particle number n by 1. This means that the charge difference between the lowest and highest states is $2k$, implying $n_{\max} = 2k$. Then $Sp(1)$ Weyl symmetry implies $n \to -n$ symmetry, demanding $\epsilon_0 = -km$ and $\hat{Z}_{k,2k-n} = \hat{Z}_{k,n}$. These completely agree with our empirical findings around (3.31). Below, we shall proceed with these properties assumed.

One can study the case with $k = 2$ in the same manner. We computed it at $v_l = \epsilon_- = 0$ due to computational complications. We simply report the following results:

$$
\begin{aligned}
Z_{2,0}^{SO(7)} &= \frac{t^{10}}{(1 - t)^{20}(1 + t)^{10}(1 + t + t^2)^9}(1 + t + 15t^2 + 48t^3 + 152t^4 + 446t^5 + 1126t^6 + 2374t^7 \\
&\quad + 4674t^8 + 8184t^9 + 12680t^{10} + 17816t^{11} + 22957t^{12} + 26449t^{13} + 27622t^{14} + \cdots + t^{28}) \\
\hat{Z}_{2,1}^{SO(7)} &= -\frac{8t^{11}}{(1 - t)^{20}(1 + t)^{10}(1 + t + t^2)^9}(1 + 3t + 17t^2 + 62t^3 + 183t^4 + 477t^5 + 1109t^6 + 2206t^7 \\
&\quad + 3921t^8 + 6285t^9 + 9004t^{10} + 11543t^{11} + 13459t^{12} + 14194t^{13} + \cdots + t^{26}) \\
\hat{Z}_{2,2}^{SO(7)} &= \frac{t^{10}}{(1 - t)^{20}(1 + t)^{10}(1 + t + t^2)^9}(1 + 3t + 45t^2 + 176t^3 + 647t^4 + 2087t^5 + 5560t^6 + 12639t^7 \\
&\quad + 25923t^8 + 46880t^9 + 74843t^{10} + 107589t^{11} + 139877t^{12} + 162758t^{13} + 170752t^{14} + \cdots + t^{28}).
\end{aligned}
\tag{3.34}
$$

Here, the omitted terms in $\cdots$ can be restored from the fact that coefficients of t^p and t^{28-p} are same in the numerator of $Z_{2,0}$ and also from similar reflection symmetries in $\hat{Z}_{2,1}$, $\hat{Z}_{2,2}$. Assuming $\hat{Z}_{k,n} = 0$ for $n > 4$ and $\hat{Z}_{2,n} = \hat{Z}_{2,4-n}$, as discussed in the previous paragraph, one can compute the full

two instanton partition function for $SO(7)$ gauge theory at $n_8 = 1$,

$$
Z_{k=2} = e^{2m} \sum_{n=0}^{4} e^{-nm} \hat{Z}_{k=2,n}.
\tag{3.35}
$$

We have checked that this completely agrees with our index of Sec. II.

Next, we consider the instanton quantum mechanics of 5D $SO(7)$ gauge theory with two hypermultiplets. From Fig. 8, the contour integrand $Z_{\text{one-loop}}$ of k instantons with n_1 and n_2 hypermultiplet particles is given by

$$[Z_{\text{one-loop}}]_{k,n_1,n_2}^{SO(7)}(\phi_i, \chi_I, \chi'_{I'})$$

$$= \frac{[Z_{\text{one-loop}}]_{k,n_1}^{SO(7)}(\phi_i, \chi_I) \cdot [Z_{\text{one-loop}}]_{k,n_2}^{SO(7)}(\phi_i, \chi'_{I'})}{[Z_{\text{one-loop}}]_{k,0}^{SO(7)}(\phi_i)},$$

$$(3.36)$$

where $[Z_{\text{one-loop}}]_{k,n}^{SO(7)}$ is given by (3.23) and (3.24). Here $i = 1, ..., k$ is the $Sp(k)$ index, $I = 1, ..., n_1$ and $I' = 1, ..., n_2$ are $O(n_1)$ and $O(n_2)$ indices, respectively. We summarize the results of our calculations as follows:

$$Z_{1,0,0}^{SO(7)} = \hat{Z}_{1,0,2}^{SO(7)} = \hat{Z}_{1,2,0}^{SO(7)} = Z_{1,0}^{SO(7)}$$

$$\hat{Z}_{1,1,0}^{SO(7)} = \hat{Z}_{1,0,1}^{SO(7)} = \hat{Z}_{1,1,2}^{SO(7)} = \hat{Z}_{1,2,1}^{SO(7)} = \hat{Z}_{1,1}^{SO(7)}$$

$$\hat{Z}_{1,1,1}^{SO(7)} = \frac{t}{(1-tu^{\pm 1})} \prod_{i<j} \frac{t^4}{(1-t^2 b_i^\pm b_j^\pm)}$$

$$\times [\chi_9^{SU(2)} + \chi_7^{SU(2)}(\chi_{35}^{SO(7)} + \chi_7^{SO(7)} + 1)$$

$$+ \chi_5^{SU(2)}(-\chi_{105}^{SO(7)} + 1) + \chi_3^{SU(2)}(-\chi_{168'}^{SO(7)} + \chi_{77}^{SO(7)}$$

$$- \chi_{21}^{SO(7)}) + \chi_{330}^{SO(7)} + \chi_{189}^{SO(7)} + \chi_{27}^{SO(7)}], \quad (3.37)$$

where $Z_{1,0}^{SO(7)}$ and $Z_{1,1}^{SO(7)}$ are given by (3.26), (3.29). With the data shown in (3.37), one can compute $Z_{k=1}$ for the $SO(7)$ at $n_8 = 2$, using the fermion zero mode structures and $Sp(2)$ Weyl symmetry, extending the discussions for $n_8 = 1$ in the paragraph containing (3.33). Namely, at k instanton sector, there are $2k$ fermion zero modes which rotate in m_1 and m_2, respectively. This means that $(n_1)_{\max} = (n_2)_{\max} = 2k$, with zero point energy factor $e^{-\varepsilon_0} = e^{k(m_1+m_2)}$ from Weyl symmetry. Weyl symmetry also requires $\hat{Z}_{k,n_1,n_2} = \hat{Z}_{k,2k-n_1,n_2} = \hat{Z}_{k,n_1,2k-n_2}$. (Our calculus on the second line of (3.37), relating $\hat{Z}_{1,1,2}$, $\hat{Z}_{1,2,1}$ to other coefficients, partially reconfirms this general argument.) With these structures and (3.37), one finds

$$Z_1 = e^{m_1+m_2}[Z_{1,0}^{SO(7)} + (e^{-m_1} + e^{-m_2})\hat{Z}_{1,1}^{SO(7)}$$

$$+ (e^{-2m_1} + e^{-2m_2})Z_{1,0}^{SO(7)} + e^{-m_1-m_2}\hat{Z}_{1,1,1}^{SO(7)}$$

$$+ (e^{-2m_1-m_2} + e^{-m_1-2m_2})\hat{Z}_{1,1}^{SO(7)} + e^{-2m_1-2m_2}Z_{1,0}^{SO(7)}]$$

$$= \chi_4^{Sp(2)}\hat{Z}_{1,1}^{SO(7)} + \chi_5^{Sp(2)}Z_{1,0}^{SO(7)} + (\hat{Z}_{1,1,1}^{SO(7)} - Z_{1,0}^{SO(7)}),$$

$$(3.38)$$

where $\chi_4^{Sp(2)} = \sum_\pm (e^{\pm m_1} + e^{\pm m_2})$, $\chi_5^{Sp(2)} = 1 + \sum_{\pm,\pm} e^{\pm m_1 \pm m_2}$. This completely agrees with (2.31).

As explained in Sec. II, one can Higgs the $SO(7)$ gauge theory with a matter hypermultiplet in **8**, to pure G_2 Yang-Mills theory by giving VEV to the hypermultiplet. In the index, this amounts to setting $m_{n_8} = \epsilon_+$, $v_4 = 0$. See Sec. II B. Since we have provided concrete tests of $SO(7)$ instanton partition functions of Sec. II using our D-brane-based methods, Higgsing both sides do not yield any further significant information or tests. Namely, calculations in this section at $n_8 = 1$, 2 already tested our G_2 instanton calculus of Sec. II at $n_7 = 0$, 1. Therefore, we shall not repeat the analysis of Higgsings to G_2 in our D-brane-based formalism.

IV. STRINGS OF NON-HIGGSABLE 6D SCFTS

In this section, we study the strings of non-Higgsable 6D SCFTs containing G_2 theories or $SO(7)$ theories with matters in **8**. In particular, we shall construct the 2D gauge theories for the strings of 6D atomic SCFTs with two- and three-dimensional tensor branches [10].

We first briefly review the "atomic classification" [5,6,10] of 6D $\mathcal{N} = (1,0)$ SCFTs. This is based on F-theory engineering of 6D SCFTs, on elliptic Calabi-Yau threefold (CY$_3$). Elliptic CY$_3$ admits a T^2 fibration over a 4D base $\mathcal{B}$, which is noncompact and singular. The singular point on $\mathcal{B}$ hosts 6D degrees of freedom which decouple from 10D bulk at low energy. In 6D QFT, resolving this singularity corresponds to going to the tensor branch. Namely, there is a 6D supermultiplet called tensor multiplet, consisting of a self-dual 2-form potential $B_{\mu\nu}$ (whose field strength $H = dB + \cdots$ satisfies $H = \star_6 H$), a real scalar Φ, and fermions. Giving VEV to Φ, one goes into the tensor branch. Geometrically, the singularity of $\mathcal{B}$ is resolved into a collection of intersecting 2-cycles $\mathbb{P}^1$. Associated with the i'th $\mathbb{P}^1$, there is a tensor multiplet B^i, Φ^i, and sometimes a non-Abelian vector multiplet A^i with simple gauge group G_i. The VEV of Φ^i is proportional to the volume of the i'th $\mathbb{P}^1$. Depending on how the 2-cycles intersect, the vector multiplets form a sort of quiver possibly with charged hypermultiplet matters. Geometrically, the vector and hypermultiplets are determined by how the T^2 fiber degenerates on $\mathcal{B}$. Equivalently, they depend on the 7-branes wrapping $\mathcal{B}$. With a given resolution of the singularity on $\mathcal{B}$, there are families of theories related to others by Higgsings. The classification of [5,6,10] proceeds by first identifying possible non-Higgsable theories and then considering possible "un-Higgsings."

Non-Higgsable theories are constructed by first taking a finite set of "quiver nodes" and connecting them with certain rules. Technically, the nodes are connected by suitably gauging the E-string theory and identifying them with the gauge groups of the quiver nodes. See [5] for the detailed rules. Roughly speaking, the possible quiver nodes are given in Tables III and IV. More precisely, the SCFTs at

TABLE III.   Symmetries/matters of SCFTs with rank 1 tensor branches.

n	1	2	3	4	5	6	7	8	12
Gauge symmetry	$\cdots$	$\cdots$	$SU(3)$	$SO(8)$	F_4	E_6	E_7	E_7	E_8
Global symmetry	E_8	$SO(5)_R$	$\cdots$		$\cdots$	$\cdots$	$\cdots$	$\cdots$	$\cdots$
Matter			$\cdots$		$\cdots$	$\cdots$	$\cdots$	$\frac{1}{2}\mathbf{56}$	$\cdots$	$\cdots$

$n = 1$ and $n = 2$ play different roles: see [5,6] for the precise ways of using the SCFTs in Tables III and IV. The SCFTs in Table III are called "minimal SCFTs" in [14]. Here, the numbers on the first rows denote the negative of the self-intersection numbers of $\mathbb{P}^1$. Thus, in Table IV, there are two or three 2-cycles (tensor multiplets).

We are interested in the self-dual strings, which are charged under $B_{\mu\nu}^i$ with equal electric and magnetic charges. If a node has gauge symmetry, the string is identified as an instanton string soliton. See, e.g., [4] and references therein for a review. In this section, we are interested in the strings of the SCFTs given in Table IV. Since they involve G_2 gauge group with matters in $\mathbf{7}$ or $SO(7)$ gauge group with matters in $\mathbf{8}$, the gauge theories on these strings will be constructed using our gauge theories of Sec. II as ingredients.

A. 2,3,2: $SU(2) \times SO(7) \times SU(2)$ gauge group

Since this QFT has three factors of simple gauge groups, one can assign three topological numbers k_1, k_2, k_3 for the instanton strings in $SU(2)_1$, $SO(7)$, $SU(2)_2$. To construct the 2D quiver for these strings, we proceed in steps. We first consider the case in which two of the three gauge symmetries are ungauged in 6D, when only one of k_1, k_2, k_3 is nonzero. They are instanton strings of either $SU(2)$ or $SO(7)$ gauge theory with certain matters. After identifying three ADHM(-like) gauge theories, we then consider the case with all k_1, k_2, k_3 nonzero and form a quiver of the three ADHM(-like) theories.

We first consider the case with $k_1 = k_3 = 0$, when $SU(2)_1 \times SU(2)_2$ is ungauged. Then $SU(2)^2 \sim Sp(1)^2$ becomes a flavor symmetry rotating the hypermultiplets, which in the strict ungauging limit enlarges to $Sp(2)$. This is because the matters in $\frac{1}{2}(\mathbf{2},\mathbf{8},\mathbf{1}) + \frac{1}{2}(\mathbf{1},\mathbf{8},\mathbf{2})$ will arrange into $\frac{1}{2}(\mathbf{8},\mathbf{4})$ of $SO(7) \times Sp(2)$ in the ungauging limit. This theory was discussed in Sec. II A, the 6D $SO(7)$ theory at $n_8 = 2$. So as the ADHM-like description, we take this

theory with $U(k_2)$ gauge symmetry and reduced $SU(4) \times U(2) \subset SO(7) \times Sp(2)$ global symmetry. Note that in Sec. II, our 2D gauge theory can have $U(4)$ global symmetry rotating four Fermi multiplets, but it reduced to $U(2)$ after coupling to the 5D/6D background fields, especially the hypermultiplet scalar VEV. So, the relevant global symmetry of this model (as describing higher dimensional QFT's soliton) depends on the bulk information. Here, since we shall use this model for the strings of the non-Higgsable 2,3,2 SCFT, with $SU(2)^2$ gauged, one cannot turn on such a background hypermultiplet field. Instead, $SU(2)^2 \subset U(4)$ global symmetry will remain in 2D after 6D gauging. Four Fermi fields are divided into two pairs, and we can rotate them only within a pair.

We also consider the limit in which $SO(7) \times SU(2)_2$ is ungauged, and consider k_1 instanton strings in $SU(2)_1$. The matter $\frac{1}{2}(\mathbf{1},\mathbf{8},\mathbf{2})$ will not affect the ADHM construction since it is neutral in $SU(2)_1$. $\frac{1}{2}(\mathbf{2},\mathbf{8},\mathbf{1})$ will reduce to four fundamental hypermultiplets in $SU(2)$. Its ADHM construction is well known. The 2D (0,4) field contents are given as follows:

$$(A_\mu, \lambda_0, \lambda): \text{vector mutiplet in } (\mathbf{adj}, \mathbf{1})$$
$$q_{\dot\alpha} = (q, \tilde{q}^\dagger): \text{hypermultiplet in } (\mathbf{k}, \bar{\mathbf{2}})$$
$$a_{\alpha\dot\beta} \sim (a, \tilde{a}^\dagger): \text{hypermultiplet in } (\mathbf{adj}, \mathbf{1})$$
$$\Psi_a: \text{Fermi multiplet in } (\mathbf{k}, \mathbf{1}), \qquad (4.1)$$

where $a = 1, \dots, 4$. We showed the representations of $U(k_1) \times SU(2)$. As for the hypermultiplets, we have only shown the scalar components. $\alpha, \dot\alpha = 1, 2$ are the doublet indices for $SU(2)_l$ and $SU(2)_r$. Although $\bar{\mathbf{2}} \sim \mathbf{2}$ for $SU(2)$, we put bar since the ADHM construction classically has $U(2)$ symmetry as a default. This is the UV quiver description for the $SU(2)$ instanton string at $n_2 = 4$. This quiver classically has $U(k_1)$ gauge symmetry and $U(2) \times U(4)_F$ global symmetries. $U(k_1)$ is anomaly free [12]. The overall $U(1)_G \subset U(2)$ and $U(1)_F \subset U(4)_F$ has mixed anomaly with $U(1) \subset U(k_1)$, and only $G + F$ is free of mixed anomaly [12]. Moreover, considering all fields in this ADHM quiver, $G + F$ can be eaten up by $U(1) \subset U(k_1)$. This implies that $U(k_1)$ gauge-invariant observables will not see G, F. So, this system only has $SU(2) \times SU(4)_F$ symmetry [12]. In the IR, this enhances to $SU(2) \times SO(7)_F$. This is in contrast to the $SU(2)$ theory at $n_2 = 4$ in lower dimensions, in which case $U(4)_F$ enhances

TABLE IV.   Non-Higgsable atomic SCFTs with higher rank tensor branches.

Base	3,2	3,2,2	2,3,2
Gauge symmetry	$G_2 \times SU(2)$	$G_2 \times SU(2) \times \{\}$	$SU(2) \times SO(7) \times SU(2)$
Matter	$\frac{1}{2}(\mathbf{7}+\mathbf{1},\mathbf{2})$	$\frac{1}{2}(\mathbf{7}+\mathbf{1},\mathbf{2})$	$\frac{1}{2}(\mathbf{2},\mathbf{8},\mathbf{1}) + \frac{1}{2}(\mathbf{1},\mathbf{8},\mathbf{2})$

to $SO(8)$. The $SO(7)_F$ symmetry of this model was noticed in [6,53]. Replacing k_1 by k_3, one can also obtain the ADHM gauge theory when $SU(2)_1 \times SO(7)$ is ungauged in 6D.

Now when all k_1, k_2, k_3 are nonzero, one can form a quiver of the above three ADHM(-like) theories. We shall add more 2D matters to account for the zero modes coming from 6D hypermultiplets and introduce extra potentials. Between adjacent $SU(2)_1 \times SO(7)$ or $SO(7) \times SU(2)_2$ pair of nodes, one has bifundamental hypermultiplet in $\frac{1}{2}(\mathbf{8}, \mathbf{2})$. Since we seek for a 2D UV description seeing $SU(2) \times SU(4)$ subgroup only, this hypermultiplet is in $(\mathbf{2}, \bar{\mathbf{4}})$ bifundamental representation of the latter. Usually in D-brane models with bifundamental matters, the induced (0,4) matters on the $U(k_1) \times U(k_2)$ ADHM construction of instantons are as follows:

$$\Phi_A = (\Phi, \tilde{\Phi}^\dagger): \text{ twisted hypermultiplet in } (\mathbf{k}_1, \bar{\mathbf{k}}_2)$$

$$\Psi_\alpha = (\Psi_1, \Psi_2): \text{ two Fermi multiplet fields in } (\mathbf{k}_1, \bar{\mathbf{k}}_2)$$

$$\text{(4.2)}$$

and

Ψ_a: Fermi multiplets in $(\mathbf{k}_1, \bar{\mathbf{4}})$ of $U(k_1) \times SU(4)$

    $(a = 1, \ldots, 4)$

Ψ_i: Fermi multiplets in $(\bar{\mathbf{k}}_2, \mathbf{2})$ of $U(k_2) \times SU(2)$

    $(i = 1, 2)$.   (4.3)

See, e.g., [12,15] for the details. Although our construction is not guided by D-brane models, we advocate the same field contents as our natural ansatz. The fields Ψ_a with $a = 1, \ldots, 4$ are not new, but come from the last line of (4.1). This is natural because the 6D $SU(4) \subset SO(7)$ gauge symmetry is obtained by gauging the global symmetry in the setting of (4.1). Also, Ψ_i with $i = 1, 2$ can also be found in the ADHM-like quiver in Sec. II. Namely, in Sec. II, we had four Fermi multiplet fields in $\mathbf{k_2}$ representation of $U(k_2)$, at $n_\mathbf{8} = 2$. Ψ_i of (4.3) is obtained by taking two of these four. (The other two will be associated with the $SO(7) \times SU(2)_2$ pair.) The bifundamental fields in (4.2) are new and link the two ADHM(-like) gauge nodes. Similarly, between the second and third nodes, bifundamental fields of the form of (4.2), replacing $k_1 \to k_3$, are added. The remaining Fermi fields in the second and third nodes take the form of (4.3), with $k_1 \to k_3$. The flavor symmetry of these Fermi multiplets in an ADHM node is locked with the 6D gauge symmetry of the adjacent ADHM node. The resulting quiver is shown schematically in Fig. 10.

In the previous paragraph, and in Fig. 10, we locked some 6D flavor symmetries of an ADHM theory with 6D gauge symmetries of adjacent ADHM theories. This has to be justified by writing down the interactions which lock the symmetries as claimed. Now we explain such
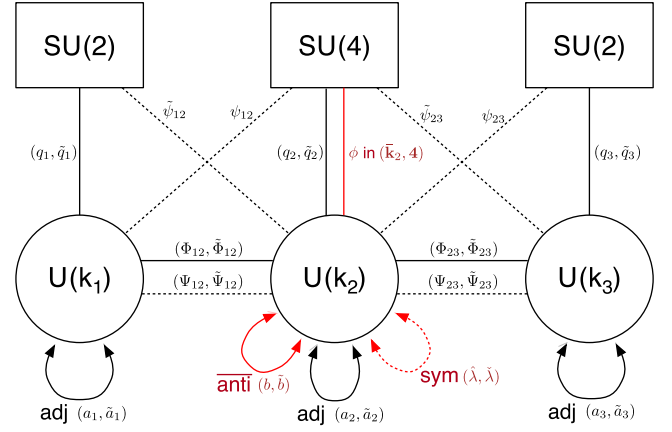

FIG. 10. 2D quiver for the strings of 6D 2,3,2 SCFT. Black lines are fields taking the form of $\mathcal{N} = (0, 4)$ multiplets, being either hypermultiplet/twisted hypermultiplet (bold line) or Fermi multiplet (dashed). Red lines are $\mathcal{N} = (0, 2)$ chiral(bold)/Fermi (dashed) multiplets. All the named (0,2) superfields are described in Table II and Eqs. (4.4) and (4.5).

superpotentials. In the (0,2) off-shell description [24] of (0,4) theories, one can introduce interactions by two kinds of superpotentials J_Ψ, E_Ψ given for each Fermi multiplet. There are some constraints on J_Ψ's and E_Ψ's to be met, either for (0,2) SUSY or for (0,4) enhancement of the classical action. These conditions are all mentioned in Sec. III, when we discussed models with manifest (0,4) SUSY. In our current ADHM-like models, some part of the matters and interactions inevitably break manifest (0,4) SUSY. However, most of the fields still take the form of (0,4) multiplets, so that we find it is convenient to turn on classical interactions in two steps. We first turn on manifestly (0,4) supersymmetric classical interactions for the fields shown in Fig. 10 with black lines/nodes. Then we rephrase these interactions in $\mathcal{N} = (0, 1)$ language, after which we turn on further (0,1) interactions for the fields shown as red lines in Fig. 10. We find that securing the partial (0,4) SUSY structure plays important roles for the correct physics, e.g., yielding the right multiparticle structures of the elliptic genus, etc.

In (0,4) gauge theories, one has two types of hypermultiplets: hypermultiplet whose scalars form a doublet of $SU(2)_r$ and twisted hypermultiplet whose scalars form a doublet of $SU(2)_R$. These two multiplets contribute differently to the J, E superpotentials for the fermions in the (0,4) vector multiplet. Namely, in the (0,2) formalism of [24], a (0,4) vector multiplet decomposes into a (0,2) vector multiplet A_μ, λ_0 and an adjoint Fermi multiplet λ (plus auxiliary field). A hypermultiplet field $(\Phi_{\dot{\alpha}})_\mathbf{R} = (\Phi, \tilde{\Phi}^\dagger)_\mathbf{R}$ in the representation $\mathbf{R}$ of the gauge group contributes $J_{\lambda^a} = \Phi_\mathbf{R}[T_\mathbf{R}^a]\tilde{\Phi}_\mathbf{R}$. A twisted hypermultiplet $(\Phi_A)_\mathbf{R} = (\Phi, \tilde{\Phi}^\dagger)_\mathbf{R}$ contributes to $E_{\lambda^a} = \Phi_\mathbf{R}[T_\mathbf{R}^a]\tilde{\Phi}_\mathbf{R}$. This is the requirement of (0,4) supersymmetry. (In our

normalization of Sec. III, one has $\sqrt{2}$ factors multiplied.) However, from the (0,2) SUSY, they should satisfy $\sum_\Psi J_\Psi E_\Psi = 0$. To meet this condition, one has to turn on extra potentials for the Fermi multiplets shown as black lines in Fig. 10. This is in complete parallel with the results shown in Sec. III. Let us name the fields in Fig. 10 with black lines/nodes as follows. The ADHM fields within an ADHM node are named as follows:

$$\text{Node 1}: q_1, \tilde{q}_1 \in (\mathbf{k}_1, \bar{\mathbf{2}}_1) + (\bar{\mathbf{k}}_1, \mathbf{2}_1), \quad a, \tilde{a} \in \mathbf{adj}_1$$
$$\text{Node 2}: q_2, \tilde{q}_2 \in (\mathbf{k}_2, \bar{\mathbf{4}}) + (\bar{\mathbf{k}}_2, \mathbf{4}), \quad a, \tilde{a} \in \mathbf{adj}_2$$
$$\text{Node 3}: q_3, \tilde{q}_3 \in (\mathbf{k}_3, \bar{\mathbf{2}}_3) + (\bar{\mathbf{k}}_3, \mathbf{2}_3), \quad a, \tilde{a} \in \mathbf{adj}_3,$$

$$(4.4)$$

while the fields linking the adjacent nodes are named as

$$\text{Link 1–2}: \Phi_{12}, \tilde{\Phi}_{12} \in (\mathbf{k}_1, \bar{\mathbf{k}}_2) + (\bar{\mathbf{k}}_1, \mathbf{k}_2), \qquad \Psi_{12}, \tilde{\Psi}_{12} \in (\mathbf{k}_1, \bar{\mathbf{k}}_2) + (\bar{\mathbf{k}}_1, \mathbf{k}_2)$$
$$\psi_{12}, \tilde{\psi}_{12} \in (\mathbf{k}_1, \bar{\mathbf{4}}) + (\bar{\mathbf{k}}_2, \mathbf{2}_1)$$
$$\text{Link 2–3}: \Phi_{23}, \tilde{\Phi}_{23} \in (\mathbf{k}_2, \bar{\mathbf{k}}_3) + (\bar{\mathbf{k}}_2, \mathbf{k}_3), \qquad \Psi_{23}, \tilde{\Psi}_{23} \in (\mathbf{k}_2, \bar{\mathbf{k}}_3) + (\bar{\mathbf{k}}_2, \mathbf{k}_3)$$
$$\psi_{23}, \tilde{\psi}_{23} \in (\mathbf{k}_2, \bar{\mathbf{2}}_3) + (\bar{\mathbf{k}}_3, \mathbf{4}).$$

$$(4.5)$$

Here, notations like $\mathbf{2}_1$, $\mathbf{2}_3$ mean representations of $SU(2)$ on the first (leftmost) and the third (rightmost) nodes, respectively. Then, using the results of [54], Eqs. (3.3) and (3.4), we find the following superpotentials after mapping our fields with those in Table 4 of [54]:

$$\text{Nodes}: J_{\lambda_i} = \sqrt{2}(q_i \tilde{q}_i + [a_i, \tilde{a}_i]) \quad (\text{for } i = 1, 2, 3), \qquad E_{\lambda_1} = \sqrt{2}\Phi_{12}\tilde{\Phi}_{12},$$
$$E_{\lambda_2} = \sqrt{2}(\Phi_{23}\tilde{\Phi}_{23} - \tilde{\Phi}_{12}\Phi_{12}), \qquad E_{\lambda_3} = -\sqrt{2}\tilde{\Phi}_{23}\Phi_{23}$$
$$\text{Links}: E_{\Psi_{i-1,i}} = \sqrt{2}(\Phi_{i-1,i}a_i - a_{i-1}\Phi_{i-1,i}), \qquad J_{\Psi_{i-1,i}} = \sqrt{2}(\tilde{a}_i\tilde{\Phi}_{i-1,i} - \tilde{\Phi}_{i-1,i}\tilde{a}_{i-1}),$$
$$E_{\tilde{\Psi}_{i-1,i}} = \sqrt{2}(\tilde{a}_{i-1}\Phi_{i-1,i} - \Phi_{i-1,i}\tilde{a}_i), \qquad J_{\tilde{\Psi}_{i-1,i}} = \sqrt{2}(a_i\tilde{\Phi}_{i-1,i} - \tilde{\Phi}_{i-1,i}a_{i-1}),$$
$$E_{\psi_{i-1,1}} = \sqrt{2}\Phi_{i-1,i}q_i, \qquad J_{\psi_{i-1,i}} = \sqrt{2}\tilde{q}_i\tilde{\Phi}_{i-1,i}$$
$$E_{\tilde{\psi}_{i-1,1}} = \sqrt{2}\tilde{q}_{i-1}\Phi_{i-1,i}, \qquad J_{\tilde{\psi}_{i-1,i}} = -\sqrt{2}\tilde{\Phi}_{i-1,i}q_{i-1} \quad (\text{for } i = 2, 3).$$

$$(4.6)$$

(We correct overall normalization of [54] by $\sqrt{2}$ factors.) These are part of the interactions, and we shall add more interactions later preserving less SUSY. Only with the interactions shown above, one can check the (0,4) SUSY of the classical action, for instance, in the bosonic potential [24,54]. The rearrangement of the potential energy with $SU(2)_r \times SU(2)_R$ symmetry can be made similar to Eq. (3.6) of [54]. In particular, the flavor symmetries which rotate Fermi multiplets are locked by these interactions as shown in Fig. 10.

We now proceed to write down all the interactions preserving only (0,1) symmetry, for the red fields associated with the middle "3" node. This will basically be the same as the interactions explained in Sec. II A, for $SO(7)$ instanton strings at $n_8 \neq 0$. However, before doing that, we should rephrase the previous (0,4) interactions in the (0,1) superfield language. In (0,2) superfield, one has a pair of complex superspace coordinates $\theta, \bar{\theta}$. E_Ψ appears as the top component $\sim \theta\bar{\theta}E_\Psi(\Phi)$ of the Fermi multiplet [25]. On the other hand, J_Ψ appears as a term in the Lagrangian, of the form $\int d\theta \Psi J_\Psi + \text{H.c.}$ However, since (0,1) supersymmetry only has one real superspace coordinate θ, there is no separate notion of E_Ψ. There can be superpotentials

$\int d\theta(\Psi J_\Psi^{(0,1)} - \text{H.c.})$, where $J_\Psi^{(0,1)}$ can be any nonholomorphic function of the scalars. To realize J_Ψ and E_Ψ in the previous paragraph, one writes

$$\sum_\Psi \int d\theta[\Psi(J_\Psi(\Phi) + \bar{E}_\Psi(\bar{\Phi})) - \text{H.c.}]. \quad (4.7)$$

One finds the correct bosonic potential $\sum_\Psi |J_\Psi + \bar{E}_\Psi|^2 = \sum_\Psi(|J_\Psi|^2 + |E_\Psi|^2)$, using $\sum_\Psi J_\Psi E_\Psi = 0$ of (4.6). The Yukawa couplings associated with J_Ψ and $E_\Psi \sim \sum_\Psi \Psi(\frac{\partial J_\Psi}{\partial \phi^i}\psi^i + \frac{\partial \bar{E}}{\partial \phi_i}\psi_i)$ are also correctly reproduced. Now with (4.6) rewritten as $J_\Psi^{(0,1)} = J_\Psi + \bar{E}_\Psi$, we add further interactions for $\hat{\lambda}$, $\check{\lambda}$ on the middle node, as given by (2.7).

With these potentials, one can show that the moduli space is that of each ADHM-like quiver, at $\Phi_{i-1,i} = 0$, $\tilde{\Phi}_{i-1,i} = 0$. In particular, no extra branch is formed by $\Phi_{i-1,i}, \tilde{\Phi}_{i-1,i}$.

One can compute the 2D anomalies from our gauge theory and compare with the result known from anomaly inflow. The 6D one-loop anomaly 8-form in the tensor branch is given by

$$I_{\text{one-loop}} = -\frac{3}{32}[\text{Tr}(F^2_{SO(7)})]^2 - \frac{1}{16}[\text{Tr}(F^2_{SU(2)_1})]^2 - \frac{1}{16}[\text{Tr}(F^2_{SU(2)_2})]^2$$
$$+ \frac{1}{16}\text{Tr}(F^2_{SO(7)})[\text{Tr}(F^2_{SU(2)_1}) + \text{Tr}(F^2_{SU(2)_2})] - \frac{1}{16}p_1(T)\text{Tr}(F^2_{SO(7)})$$
$$- \frac{1}{4}c_2(R)[5\text{Tr}(F^2_{SO(7)}) + 2\text{Tr}(F^2_{SU(2)_1}) + 2\text{Tr}(F^2_{SU(2)_2})] + \cdots. \tag{4.8}$$

We only showed the terms containing $SU(2)_1 \times SO(7) \times SU(2)_2$ gauge fields. This can be written as $I_{\text{one-loop}} = -\frac{1}{2}\Omega^{ij}I_iI_j + \cdots$, with $i, j = 1, 2, 3$, where

$$\Omega^{ij} = \begin{pmatrix} 2 & -1 & 0 \\ -1 & 3 & -1 \\ 0 & -1 & 2 \end{pmatrix}, \qquad I_i = \begin{pmatrix} \frac{1}{4}\text{Tr}(F^2_{SU(2)_1}) + \frac{11}{4}c_2(R) + \frac{1}{16}p_1(T) \\ \frac{1}{4}\text{Tr}(F^2_{SO(7)}) + \frac{7}{2}c_2(R) + \frac{1}{8}p_1(T) \\ \frac{1}{4}\text{Tr}(F^2_{SU(2)_2}) + \frac{11}{4}c_2(R) + \frac{1}{16}p_1(T) \end{pmatrix}. \tag{4.9}$$

Using (2.40), one finds the following anomaly 4-form I_4:

$$I_4 = \left(k_1k_2 + k_2k_3 - k_1^2 - \frac{3}{2}k_2^2 - k_3^2\right)\chi(T_4) + k_2(I_1 + I_3 - 3I_2) + k_1(I_2 - 2I_1) + k_3(I_2 - 2I_3) \tag{4.10}$$

on the instanton strings with string numbers $k_i = (k_1, k_2, k_3)$.

We now compute the anomaly from our gauge theory. We first compute the anomalies of three ADHM quivers $I_4^{(i)}$ ($i = 1$, 2, 3), restricting them according to the symmetry locking rules. We then compute the anomalies I_4^{bif} of matters $\Phi_{i-1,i}, \tilde{\Phi}_{i-1,i}$. The net anomaly is $I_4 = \sum_{i=1}^3 I_4^{(i)} + I_4^{\text{bif}}$. Using (2.41), one first finds

$$I_4^{(2)} = -\frac{3}{2}k_2^2\chi(T_4) - k_2\left[\frac{3}{4}\text{Tr}(F^2_{SO(7)}) + 5c_2(R) + \frac{p_1(T)}{4} - \frac{1}{4}(\text{Tr}(F^2_{SU(2)_1}) + \text{Tr}(F^2_{SU(2)_2}))\right], \tag{4.11}$$

where we replaced $\text{tr}_4(F^2_{Sp(2)}) \to \text{tr}_2(F^2_{SU(2)_1}) + \text{tr}_2(F^2_{SU(2)_2}) = \frac{1}{2}[\text{Tr}(F^2_{SU(2)_1}) + \text{Tr}(F^2_{SU(2)_2})]$. As in Sec. II A, $F_{SO(7)}$ is restricted to $SU(4)$ in our UV gauge theory, and fields in $c_2(R)$, $c_2(r)$ are also restricted to F_J. $I_4^{(1)}$ and $I_4^{(3)}$ can be computed from the known anomaly polynomial for the instanton strings of 6D $SU(2)$ theory at $n_2 = 4$. The result is Eq. (5.19) of [4] at $N = 2$, with k replaced by k_1 or k_3,

$$I_4^{(1)} = -k_1^2\chi(T_4) - \frac{k_1}{2}\text{Tr}(F^2_{SU(2)_1}) + \frac{k_1}{4}\text{Tr}(F^2_{SO(7)}) - 2k_1c_2(R), \qquad I_4^{(3)} = (k_1, SU(2)_1 \to k_3, SU(2)_2). \tag{4.12}$$

Here we replaced $F = SU(4)$ of [4] by $SO(7)$, assuming symmetry enhancement. Finally, I_4^{bif} is also computed in [4], Eq. (3.58), which for our model is

$$I_4^{\text{bif}} = (k_1k_2 + k_2k_3)\chi(T_4). \tag{4.13}$$

One finds that $I_4 = \sum_{i=1}^3 I_4^{(i)} + I_4^{\text{bif}}$ agrees with (4.10), providing a check of our gauge theory.

The elliptic genus of this gauge theory is given by (note again the definition $\theta(z) \equiv \frac{i\theta_1(\tau|\frac{z}{2\pi i})}{\eta(\tau)}$)

$$Z_{k_1,k_2,k_3} = \oint \prod_{I_1=1}^{k_1} \frac{\prod_{i=1}^4 \theta(v_i - u_{I_1})}{\theta(\epsilon_+ \pm u_{I_1} \pm v)} \cdot \frac{\prod_{I_1 \neq J_1}\theta(u_{I_1J_1})\prod_{I_1,J_1}\theta(2\epsilon_+ + u_{I_1J_1})}{\prod_{I_1,J_1=1}^{k_1}\theta(\epsilon_{1,2} + u_{I_1J_1})} \cdot (1 \to 3, \nu \to \tilde{\nu})$$

$$\cdot \prod_{I_2=1}^{k_2} \frac{\theta(v \pm u_{I_2})\theta(\tilde{v} \pm u_{I_2})}{\prod_{i=1}^4 \theta(\epsilon_+ \pm (u_{I_2} - v_i))\theta(\epsilon_+ - u_{I_2} - v_i)} \cdot \frac{\prod_{I_2 \neq J_2}\theta(u_{I_2J_2})\prod_{I_2,J_2}\theta(2\epsilon_+ + u_{I_2J_2})}{\prod_{I_2,J_2=1}^{k_2}\theta(\epsilon_{1,2} + u_{I_2J_2})}$$

$$\cdot \frac{\prod_{I_2 \leq J_2}\theta(u_{I_2} + u_{J_2})\theta(u_{I_2} + u_{J_2} - 2\epsilon_+)}{\prod_{I_2 < J_2}\theta(\epsilon_{1,2} - u_{I_2} - u_{J_2})}$$

$$\cdot \prod_{I_1=1}^{k_1}\prod_{I_2=1}^{k_2} \frac{\theta(\epsilon_- \pm (u_{I_1} - u_{I_2}))}{\theta(-\epsilon_+ \pm (u_{I_1} - u_{I_2}))} \cdot \prod_{I_2=1}^{k_2}\prod_{I_3=1}^{k_3} \frac{\theta(\epsilon_- \pm (u_{I_2} - u_{I_3}))}{\theta(-\epsilon_+ \pm (u_{I_2} - u_{I_3}))}. \tag{4.14}$$

v_i (with $\sum_i v_i = 0$) is the $SU(4) \subset SO(7)$ chemical potential, $\pm\nu$ and $\pm\tilde\nu$ are the chemical potentials for 6D $SU(2)^2$. The contour integral is given with suitable weight [30], including the $U(k_1) \times U(k_2) \times U(k_3)$ Weyl factor. The contour integral is again given by the JK-residues [30]. We again choose $\eta_1 = (1, ..., 1)$, $\eta_2 = (1, ..., 1)$, $\eta_3 = (1, ..., 1)$. Then, similar to the residue choices made in Sec. II, one can show that the residues are labeled by three sets of colored Young diagrams, $(Y_1^{(1)}, Y_2^{(1)})$ with k_1 boxes for u_{I_1}, $(Y_1^{(2)}, ..., Y_4^{(2)})$ with k_2 boxes for u_{I_2}, and

$(Y_1^{(3)}, Y_2^{(3)})$ with k_3 boxes for u_{I_3}. The residues all come from the poles at

$$
\begin{aligned}
u_{I_1}&: \epsilon_+ + u_{I_1} \pm \nu = 0, && \epsilon_{1,2} + u_{I_1 J_1} = 0 \\
u_{I_2}&: \epsilon_+ + u_{I_2} - v_i = 0, && \epsilon_{1,2} + u_{I_2 J_2} = 0 \\
u_{I_3}&: \epsilon_+ + u_{I_3} \pm \tilde\nu = 0, && \epsilon_{1,2} + u_{I_3 J_3} = 0,
\end{aligned}
\tag{4.15}
$$

coming from the first, second, and third lines of (4.14), respectively. The residue sum is given by

$$
\begin{aligned}
Z_{k_1,k_2,k_3} = \sum_{\substack{Y_{(1,2,3)} \\ |Y_{(a)}|=k_a}} \prod_{i=1}^{2} & \left(\prod_{s_1 \in Y_{(1)i}} \frac{\prod_{l=1}^{4} \theta(v_l - \phi(s_1))}{\prod_{j=1}^{2} \theta(E_{ij}(s_1))\theta(E_{ij}(s_1) - 2\epsilon_+)} \right) \times \prod_{i=1}^{2}(1 \to 3) \\
\times \prod_{i=1}^{4} & \left(\prod_{s_2 \in Y_{(2)i}} \frac{\theta(2\phi(s_2))\theta(2\phi(s_2) - 2\epsilon_+) \cdot \theta(v \pm \phi(s_2))\theta(\tilde v \pm \phi(s_2))}{\prod_{j=1}^{4} \theta(E_{ij}(s_2))\theta(E_{ij}(s_2) - 2\epsilon_+)\theta(\epsilon_+ - \phi(s_2) - v_j)} \right. \\
\times \prod_{s_2 \in Y_{(2)i}} & \prod_{j \geq i} \prod_{\substack{\tilde s_2 \in Y_{(2)j} \\ s_2 < \tilde s_2}} \frac{\theta(\phi(s_2) + \phi(\tilde s_2))\theta(\phi(s_2) + \phi(\tilde s_2) - 2\epsilon_+)}{\theta(\epsilon_{1,2} - \phi(s_2) - \phi(\tilde s_2))} \\
\times \prod_{j=1}^{2} & \prod_{s_1 \in Y_{(1)j}} \frac{\theta(-\epsilon_- \pm (\phi(s_1) - \phi(s_2)))}{\theta(-\epsilon_+ \pm (\phi(s_1) - \phi(s_2)))} \times \left. \prod_{j=1}^{2} \prod_{s_3 \in Y_{(3)j}} \frac{\theta(-\epsilon_- \pm (\phi(s_2) - \phi(s_3)))}{\theta(-\epsilon_+ \pm (\phi(s_2) - \phi(s_3)))} \right),
\end{aligned}
\tag{4.16}
$$

where s_a (for $a = 1, 2, 3$) labels the k_a boxes in the a'th colored Young diagram, and $(v_{(1)})_{1,2} = \pm\nu$, $(v_{(3)})_{1,2} = \pm\tilde\nu$. $\phi(s_a)$ and $E_{ij}(s_a)$ are defined as

$$
E_{ij}(s_a) = v_{(a)i} - v_{(a)j} - \epsilon_1 h_i(s_a) + \epsilon_2(v_j(s_a) + 1),
\tag{4.17}
$$

$$
\phi(s_a) = v_{(a)i} - \epsilon_+ - (n_a - 1)\epsilon_1 - (m_a - 1)\epsilon_2
\tag{4.18}
$$

for $s_a = (m_a, n_a) \in Y_i^{(a)}$.

It is important to note that $\Phi_{i-1,i}, \tilde\Phi_{i-1,i}$ do not provide extra JK-Res, for the following reason. For instance, suppose that we take the "pole" from $\theta(-\epsilon_+ + u_{I_1} - u_{I_2})^{-1}$ on the fourth line, at $-\epsilon_+ + u_{I_1} - u_{I_2} = 0$ to determine u_{I_1}, with u_{I_2} determined from (4.15). Suppose that u_{I_2} is determined by $\epsilon_+ + u_{I_2} - v_i = 0$. Then on the first line of (4.14), a Fermi multiplet contribution $\theta(v_i - u_{I_1})$ vanishes at the pole, because $u_{I_1} - v_i = (-\epsilon_+ + u_{I_1} - u_{I_2}) + (\epsilon_+ + u_{I_2} - v_i) = 0$. On the other hand, suppose that u_{I_2} is determined by one of $\epsilon_{1,2} + u_{I_2} - u_{J_2} = 0$, with u_{J_2} determined by other equations. Then, from $\Psi_{12}, \tilde\Psi_{12}$'s contributions $\theta(\epsilon_- \pm (u_{I_1} - u_{J_2}))$ on the fourth line, one again finds that one of the two θ factors vanishes at the pole location. Therefore, one finds that the residue vanishes due to the vanishing determinant from certain

Fermi multiplet. This idea turns out to hold most generally, so that one can show that the fourth line of (4.14) never provides a pole with nonzero JK-residue. Based on these observations, one can make a recursive proof of this statement, similar to that made for the 5D $\mathcal{N} = 1^*$ instanton partition function in [22]. Note that the symmetry locking provided by the (0,4) potentials (4.6) played crucial roles for the vanishing of these residues.

B. Tests from 5D descriptions

In this subsection, we test the elliptic genera of Sec. IV A, using a recently proposed 5D description for the 6D 2,3,2 SCFT compactified on S^1 [16]. The description is available when the elliptic CY_3 in F-theory admits an orbifold description of the form $[\mathcal{B} \times T^2]/\Gamma$ with a discrete group Γ. One can dualize F-theory to M-theory on same CY_3. The small S^1 limit (together with suitably scaling other massive parameters) on the F-theory side corresponds to the large T^2 limit on the M-theory dual. There may be fixed points of Γ on T^2, as it decompactifies into $\mathbb{R}^2$. Near each fixed point, there exists an interacting 5D SCFTs. So, in this 5D limit, one obtains factors of decoupled 5D SCFTs. The 6D Kaluza-Klein (KK) momentum degrees of freedom can be restored by locking certain global symmetries of these 5D SCFTs and gauging it, so that the instanton quantum number of this 5D gauge theory provides the 6D KK momentum. See [16,55–57] for the details.
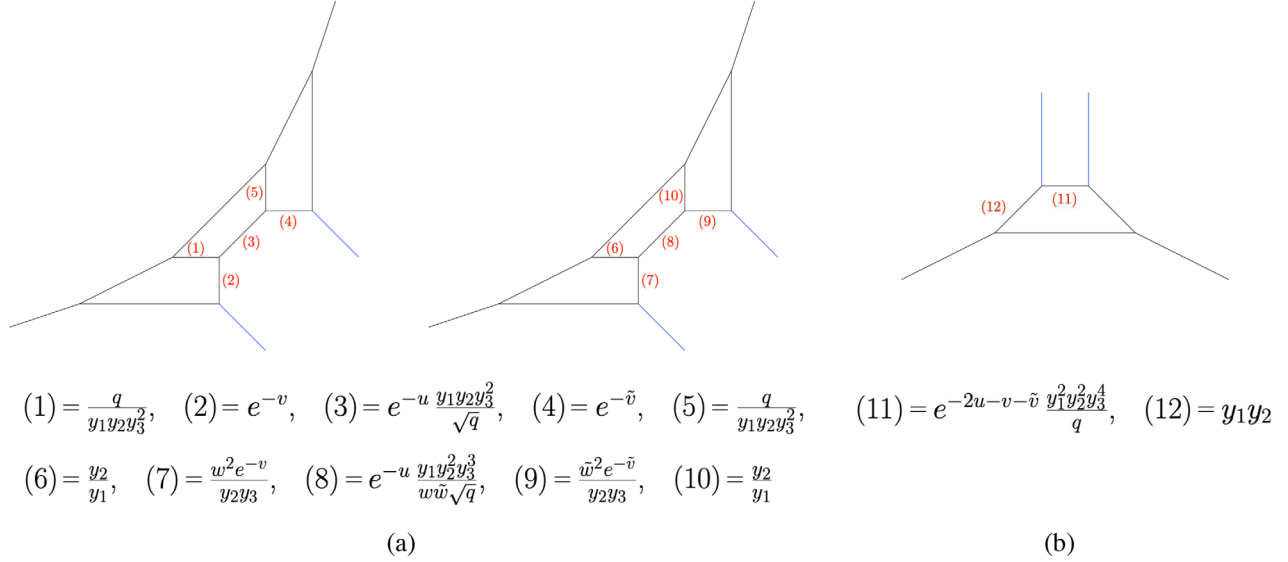
$$(1) = \frac{q}{y_1 y_2 y_3^2}, \quad (2) = e^{-v}, \quad (3) = e^{-u}\frac{y_1 y_2 y_3^2}{\sqrt{q}}, \quad (4) = e^{-\tilde{v}}, \quad (5) = \frac{q}{y_1 y_2 y_3^2}, \quad (11) = e^{-2u-v-\tilde{v}}\frac{y_1^2 y_2^2 y_3^4}{q}, \quad (12) = y_1 y_2$$

$$(6) = \frac{y_2}{y_1}, \quad (7) = \frac{w^2 e^{-v}}{y_2 y_3}, \quad (8) = e^{-u}\frac{y_1 y_2^2 y_3^3}{w\hat{w}\sqrt{q}}, \quad (9) = \frac{\tilde{w}^2 e^{-\tilde{v}}}{y_2 y_3}, \quad (10) = \frac{y_2}{y_1}$$

(a)   (b)

FIG. 11. The 5-brane webs for the 6D 2,3,2 SCFT in a 5D limit. (1)–(12) are the Kähler parameters in terms of our fugacities. $v, u, \tilde{v}$ are tensor VEVs for $SU(2)_1 \times SO(7) \times SU(2)_2$.

If a 6D SCFT admits a 6D gauge theory description, an obvious 5D limit is given by the 5D gauge theory with same gauge group. This is obtained by a scaling limit with 6D tensor multiplet scalar VEV, $v = \langle \Phi \rangle \to \infty$. Namely, $v = g_{6D}^{-2}$ and $Rv = g_{5D}^{-2}$ are the 6D and 5D inverse gauge couplings, respectively, where R is the circle radius. If one takes $R \to 0$, $v \to \infty$ with g_{5D}^{-2} kept fixed, one often gets a 5D SCFT with a relevant deformation made by $g_{5D}^{-2} \neq 0$ [57]. The 5D factorization limit described in the previous paragraph takes different scaling limit of massive parameters when taking $R \to 0$. The latter 5D limit scales other massive parameters like the holonomies of gauge fields on S^1. From the viewpoint of former 5D limit, the latter 5D limit keeps a different slice of 5D states, which contains states with nonzero KK momenta from the former viewpoint. For our 2,3,2 SCFT, the new 5D limit consists of three 5D SCFTs. The three 5D SCFTs admit IIB 5-brane web engineerings, given by Fig. 11 [16]. Each factor in Fig. 11(a) is a non-Lagrangian theory, in that it does not admit a relevant deformation to 5D Yang-Mills theory. (Figure 11(a) is related to that in [16] by a flop transition.) To have states with general KK momenta, one locks the three $SU(2)_g$ flavor symmetries associated with gauge symmetries on the blue-colored parallel 5-branes of Fig. 11 and gauge it. The relations between 6D parameters and the Kähler parameters of 5-brane web are shown below Fig. 11, which will be (empirically) justified. Reference [16] also discusses the gauging of $SU(2)_g$ in the brane web context as trivalent gluing, with some prescriptions for computations. But here we shall only discuss computations in the factorization limit.

We want to test our elliptic genera (4.14) and (4.16) using this 5D description. The test will be made in the 5D factorization limit in which $SU(2)_g$ is ungauged, as in

Fig. 11 with semi-infinite blue lines. In some sectors with special values of k_1, k_2, k_3, the BPS spectrum of the brane configuration is well known, so our elliptic genera in these sectors will be tested against known results. More generically, we shall do topological vertex calculus. Technically, identifying the parameters of 6D gauge theory (and our elliptic genus) and those in the 5-brane web is not straightforward. The relations between the two sets of parameters are often determined empirically in the literature. We follow the strategy of [16] which studied the 5D description of 6D gauge theories. [16] used the guidance from 6D affine gauge symmetry structure to partly determine the relations between 5D/Dd parameters, and then empirically fixed the rest. In our problem, we shall use the affine $SO(7)$ symmetry to partly determine the relation and then focus on well-known subsectors to fix the rest.

We first determine the parameter relation that can be inferred from $SO(7)$ group theory. To this end, we focus on the part of web diagrams of Fig. 11 associated with the Kähler parameters $(1) = (5), (6) = (10), (12)$ and the blue 5-branes. Considering how the associated four faces are connected to others (after $SU(2)_g$ gauging), it is natural to conceive that the four Kähler parameters are fugacities for the affine $SO(7)$ symmetry. This is somewhat similar to the identifications of 6D $SU(3)$, $SO(8)$, $E_{6,7,8}$ fugacities in [16], using their affine Dynkin diagrams. For $SO(7)$, the affine Dynkin diagram is given by Fig. 12, where e_1, e_2, e_3 are orthonormal vectors. We call the fugacities corresponding to the simple roots as $(t_1, t_2, t_3, t_4) \leftrightarrow (\alpha_1, \alpha_0, \alpha_3, \alpha_2)$. From the expressions of the roots in Fig. 12, one obtains

$$t_1 = \frac{z_1^2}{z_2^2}, \qquad t_2 = \frac{q}{z_1^2 z_2^2}, \qquad t_3 = z_3^2, \qquad t_4 = \frac{z_2^2}{z_3^2}, \qquad (4.19)$$

FIG. 12.   Affine Dynkin diagram of $SO(7)$.

where we used the fact that the KK momentum fugacity $q \equiv e^{2\pi i \tau}$ is associated with α_0 in the affine Lie algebra. The root relation $\alpha_1 + 2\alpha_2 + 2\alpha_3 + \alpha_0 = 0$ is reflected in the above parametrization as $t_1 t_2 t_3^2 t_4^2 = q$. z_1, z_2, z_3 are the fugacities of $SO(7)$ rotating three orthogonal 2-planes. More precisely, the characters of **7** and **8** are given in these parameters by

$$\chi_{\mathbf{8}} = z_1 z_2 z_3 + \frac{z_1 z_2}{z_3} + \frac{z_2 z_3}{z_1} + \frac{z_3 z_1}{z_2}$$
$$+ \text{(inverse of all four terms)}$$
$$\chi_{\mathbf{7}} = 1 + z_1^2 + z_2^2 + z_3^2 + \text{(inverse of all three terms)}.$$
$$(4.20)$$

The $SU(4)$ fugacity basis $y_i = e^{-v_i}$ ($i = 1, 2, 3$) that we have been using is related to $z_{1,2,3}$ by $z_1^2 = y_2 y_3$, $z_2^2 = y_3 y_1$, $z_3^2 = y_1 y_2$, so that the characters are given by

$$\chi_{\mathbf{8}} = y_1 + y_2 + y_3 + \frac{1}{y_1 y_2 y_3} + \text{(inverse of all four terms)}$$
$$\chi_{\mathbf{7}} = 1 + y_1 y_2 + y_2 y_3 + y_3 y_1 + \text{(inverse of all three terms)}.$$
$$(4.21)$$

$t_{1,2,3,4}$ are given in terms of $y_{1,2,3}$, q by

$$t_1 = \frac{y_2}{y_1} = (6) = (10), \qquad t_2 = \frac{q}{y_1 y_2 y_3^2} = (1) = (5),$$
$$t_3 = y_1 y_2 = (12), \qquad t_4 = \frac{y_3}{y_2}. \qquad (4.22)$$

t_4 is roughly the Kähler parameter for the blue line in Fig. 11, which is sent to zero in the factorization limit, with

$t_{1,2,3}$ fixed. This limit requires $q \sim y_3^2 \to 0$ with fixed y_1, y_2. To fully specify this 5D limit, we still have to specify the scaling of other parameters in $q \to 0$. The remaining parameters are two $SU(2)$ inverse gauge couplings (or tensor VEVs) which we call e^{-v}, $e^{-\tilde{v}}$ in this subsection, two $SU(2)$ fugacities $w, \tilde{w}$ (related to $\nu, \tilde{\nu}$ of Sec. IV A by $w = e^{-\nu}$, $\tilde{w} = e^{-\tilde{\nu}}$), $SO(7)$ inverse gauge coupling e^{-u}. All the scaling rules except that of e^{-u} will be determined below by considering an $SU(2)$ subsector. The scaling of e^{-u} will then be determined next by considering the $SO(7)$ subsector, at which stage we shall already make some tests of our elliptic genera. Then we consider more general sectors for further tests.

$SU(2)$ subsector: We first study the limit in which $SO(7)$ is ungauged, or equivalently, when $k_2 = 0$. The limit $u \to \infty$ should yield two 6D $SU(2)$ theories at $n_2 = 4$, decoupled to each other. So, in this limit, the brane web of Fig. 11 (with $SU(2)_g$ gauged) should factorize into two. The natural identification of $u \to \infty$ in the web is to take the distance between the parallel blue lines to infinity. [Assuming the identification of Kähler parameters in Fig. 11, the distance between two blue lines is proportional to $(11) = (2)(3)^2(4) = (7)(8)^2(9) \propto e^{-2u}$.] The string suspended between the two parallel blue lines is infinitely heavy in this limit. So the 5D description suggests that the 6D $SU(2)$ theory at $n_2 = 4$ is given by $U(1)_g(\subset SU(2)_g)$ gauging of three factors, where two of them take the form of Fig. 13(a) and one takes the form of Fig. 13(b). Upon a suitable $SL(2, \mathbb{Z})$ transformation, Fig. 13(a) is the standard 5-brane web for the 5D $\mathcal{N} = 1$ pure $SU(2)$ theory. Similarly, Fig. 13(b) describes the 5D "$SU(1)$ theory." The $SU(1)$ theory simply refers to the brane configuration of Fig. 13(b), not containing an interacting 5D SCFT. This sector will be void. So we shall take a suitable 5D scaling limit of the elliptic genera of 6D $SU(2)$ theory at $n_2 = 4$ and find the parameter map which exhibits two copies of 5D pure $SU(2)$ theories.

The 5D $SU(2)$ theory's BPS spectrum can be computed from its instanton partition function [3]. It contains two fugacities, Q for the instanton number, and W for the $SU(2)$ electric charge in the Coulomb branch. It also contains Omega deformation parameters $\epsilon_{1,2}$. Here, we only consider the unrefined single particle spectrum, defined as follows. The partition function $Z^{SU(2)}(Q, W, \epsilon_{1,2})$ is written
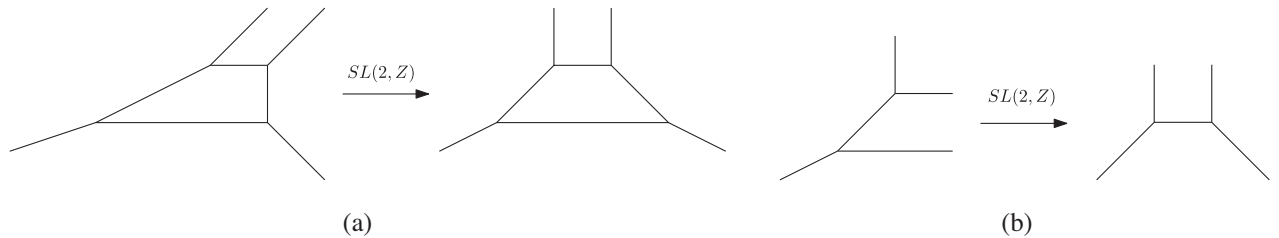

(a)   (b)

FIG. 13.   Ingredients of the 5D description of 6D $SU(2)$ theory at $n_2 = 4$.

TABLE V. BPS spectrum of 5D $\mathcal{N}=1$ pure $SU(2)$ theory.

$k\backslash n$	1	2	3	4	5	6	7
0	-2	0	0	0	0	0	0
1	-2	-4	-6	-8	-10	-12	-14
2	0	0	-6	-32	-110	-288	-644
3	0	0	0	-8	-110	-756	-3556
4	0	0	0	0	-10	-288	-3556

TABLE VII. $N_{2,p,m}$ in the limit.

$p\backslash m$	0	1	2	3	4	5
0	0	0	0	0	$-\frac{4}{y_1 y_2}$	0
1	0	0	$-\frac{4}{y_1 y_2}$	0	0	0
2	0	0	0	0	0	0
3	0	0	0	0	0	0

as $Z^{SU(2)} = \exp\left[\sum_{n=1}^{\infty} \frac{1}{n} f(Q^n, W^n, n\epsilon_{1,2})\right]$, where f is the single particle index. Then one considers the limit

$$\lim_{\epsilon_{1,2}\to 0}\left[\left(2\sinh\frac{\epsilon_{1,2}}{2}\right)f(Q,W,\epsilon_{1,2})\right]$$
$$\equiv f_{\rm rel}(Q,W) = \sum_{k=0}^{\infty}\sum_{n=0}^{\infty} Q^k W^{2n} N_{k,n}. \qquad (4.23)$$

The subscript "rel" denotes the relative degrees of freedom of the bound states, as we divided the contribution $\frac{1}{4\sinh\frac{\epsilon_1}{2}\sinh\frac{\epsilon_2}{2}}$ from the center-of-mass degrees of freedom. We list some known coefficients $N_{k,n}$ in Table V. The states at $k=0$, $n=1$ come from the perturbative partition function, from a massive 5D vector multiplet of W-boson. We would like to identify two copies of Table V, by taking a 5D scaling limit of the elliptic genus for the instanton strings of 6D $SU(2)$ theory at $n_2 = 4$. The elliptic genus can be obtained as a special case of (4.16) at $k_2 = k_3 = 0$.

After some trial-and-errors, we find it useful to expand the 6D index as

$$f_{\rm rel}(v,q,w,y_{1,2,3})$$
$$= \sum_{n=0}^{\infty} e^{-nv} f_n(q,w,y_{1,2,3})$$
$$= \sum_{n=0}^{\infty}\sum_{p=0}^{\infty}\sum_{m=0}^{\infty} e^{-nv}\left(\frac{q}{w^2 y_3}\right)^p \left(w y_3^{-\frac{1}{2}}\right)^m N_{n,p,m}(y_{1,2,3}),$$
$$\qquad (4.24)$$

where $f_{\rm rel}$ is defined in the completely same manner as (4.23). w is exponential of the $SU(2)$ Coulomb VEV and $y_i \equiv e^{-v_i}$. We take the scaling limit $q \sim y_3^2 \sim w^4 \to 0$, with v, y_1, y_2 fixed. Note that $q \sim y_3^2$ is compatible with the scaling rules we already found, based on affine $SO(7)$

structure. The nonzero terms in this limit are listed in Tables VI–IX for $n \leq 4$. All terms except $N_{1,0,1}$ are finite in this limit. The two terms in $N_{1,0,1} \sim y_3^{-\frac{1}{2}}$ are divergent in the scaling limit. This implies the following situation. Suppose that we reduce $q \sim y_3^2 \sim w^4$, maintaining their ratios finite. Reducing q physically means reducing the radius R of S^1. When $e^{-v} w y_3^{-1} = 1$ or $e^{-v} w (y_1 y_2 y_3)^{-1} = 1$, the two terms in $N_{1,0,1}$ become 1, respectively. This means that the two states labeled by these terms become massless, causing a phase transition. Each term contributes $+1$ to the index, implying that $N_{1,0,1}$ comes from two hypermultiplets. Massless hypermultiplets cause flop phase transitions. Since the hypermultiplet's central charge changes sign after the transition, one should get $e^v w^{-1} y_3 (1 + y_1 y_2)$ after the two phase transitions. As we further reduce $q \sim y_3^2 \sim w^4$ to zero after the phase transitions, these two terms vanish, and we are left with the remaining finite numbers in the tables. One can then show that the remaining numbers in the tables are two copies of Table V. Namely, one finds

$$f_{\rm rel} \to -2e^{-v}\left[1 + \frac{QW^2}{y_1 y_2}\right] - 4e^{-2v}\frac{QW^2}{y_1 y_2}$$
$$- 6e^{-3v}\left[\frac{QW^2}{y_1 y_2} + \left(\frac{QW^2}{y_1 y_2}\right)^2\right]$$
$$- e^{-4v}\left[8\frac{QW^2}{y_1 y_2} + 32\left(\frac{QW^2}{y_1 y_2}\right)^2 + 8\left(\frac{QW^2}{y_1 y_2}\right)^3\right] - \cdots$$
$$- 2\frac{W^2 e^{-v}}{y_2}\left[1 + \frac{y_2}{y_1}\right] - 4\left(\frac{W^2 e^{-v}}{y_2}\right)^2 \cdot \frac{y_2}{y_1}$$
$$- 6\left(\frac{W^2 e^{-v}}{y_2}\right)^3\left[\frac{y_2}{y_1} + \frac{y_2^2}{y_1^2}\right]$$
$$- \left(\frac{W^2 e^{-v}}{y_2}\right)^4\left[8\frac{y_2}{y_1} + 32\frac{y_2^2}{y_1^2} + 8\frac{y_2^3}{y_1^3}\right] - \cdots, \qquad (4.25)$$

TABLE VI. $N_{1,p,m}$ in the scaling limit.

$p\backslash m$	0	1	2	3
0	-2	$y_3^{-\frac{1}{2}}(1 + \frac{1}{y_1 y_2})$	$-2(\frac{1}{y_1} + \frac{1}{y_2})$	0
1	0	0	$-\frac{2}{y_1 y_2}$	0
2	0	0	0	0
3	0	0	0	0

TABLE VIII. $N_{3,p,m}$ in the limit.

$p\backslash m$	0	1	2	3	4	5	6
0	0	0	0	0	0	0	$-\frac{6}{y_1 y_2}\left(\frac{1}{y_1} + \frac{1}{y_2}\right)$
1	0	0	$-\frac{6}{y_1 y_2}$	0	0	0	0
2	0	0	0	0	$-\frac{6}{y_1^2 y_2}$	0	0
3	0	0	0	0	0	0	0

TABLE IX. $N_{4,p,m}$ in the limit.

$p \backslash m$	0	1	2	3	4	5	6	7	8
0	0	0	0	0	0	0	0	0	$-\frac{1}{y_1 y_2}\left(\frac{8}{y_1^2} + \frac{8}{y_2^2} + \frac{32}{y_1 y_2}\right)$
1	0	0	$-\frac{8}{y_1 y_2}$	0	0	0	0	0	0
2	0	0	0	0	$-\frac{32}{y_1^2 y_2^2}$	0	0	0	0
3	0	0	0	0	0	0	$-\frac{8}{y_1^3 y_2^3}$	0	0

where $\mathcal{Q} \equiv \frac{q}{w^2 y_3}$, $\mathcal{W} \equiv wy_3^{-\frac{1}{2}}$. The first two lines yield a 5D pure $SU(2)$ index, with the identification of Kähler parameters

$$Q_1 = \frac{\mathcal{Q}\mathcal{W}^2}{y_1 y_2} = \frac{q}{y_1 y_2 y_3^2} (\equiv t_2), \qquad W_1^2 = e^{-v}. \quad (4.26)$$

$$f_{\text{rel}} = -U\left[\frac{1 + Q_2}{W_2 \tilde{W}_2 (1 - Q_2)^2} + (2 \to 1)\right]$$

$$- 2U^2\left[\frac{3Q_2^2 + 4Q_2^3 + 3Q_2^4}{(W_2 \tilde{W}_2)^2 (1 - Q_2)^4 (1 - Q_2^2)^2} + (2 \to 1)\right]$$

$$- U^3\left[\frac{Q_2^3 (27 + 70Q_2 + 119Q_2^2 + 119Q_2^3 + 70Q_2^4 + 27Q_2^5)}{(W_2 \tilde{W}_2)^3 (1 - Q_2)^8 (1 - Q_2^3)^2} + (2 \to 1)\right] + \cdots, \quad (4.28)$$

where $U \equiv e^{-u - \frac{v + \tilde{v}}{2}} q^{-\frac{1}{2}} y_1 y_2 y_3^2$. So f_{rel} decomposes into two factors. To have such a factorization, one should scale $e^{-u} \to \infty$ so that $e^{-u} q^{-1/2} y_3^2 \sim e^{-u} q^{1/2}$ is finite, which guarantees that U is finite. Here, one can show that each factor takes the form of the instanton partition function for the 5D $\tilde{E}_1$ SCFT, upon identifying $U(Q_i^{1/2} W_i \tilde{W}_i)^{-1}$ as the instanton number fugacity and Q_i as the electric charge fugacity (Coulomb VEV), for $i = 1, 2$, respectively. To understand this from the brane web description, we take the 5D factorization limit $q \sim y_3^2 \to 0$, and also consider the limit $v, \tilde{v} \to \infty$ to realize the sector with $k_1 = k_3 = 0$. One finds that Fig. 11(b) decomposes into two $SU(1)$ theories in this limit since $(11) \to 0$, thus void. Each factor of Fig. 11(a) becomes the left side of Fig. 14, since $(2), (4), (7), (9) \to 0$. After an $SL(2, \mathbb{Z})$ transformation, it becomes the right side of Fig. 14. This is the standard brane configuration for the 5D $\tilde{E}_1$ theory [58]. It is the 5D

FIG. 14. Brane web for the 5D $\tilde{E}_1$ SCFT.

The last two lines yield another copy of 5D $SU(2)$ index, with parameters

$$Q_2 = \frac{y_2}{y_1} (\equiv t_1), \qquad W_2^2 = \frac{\mathcal{W}^2 e^{-v}}{y_2} = \frac{w^2 e^{-v}}{y_2 y_3}. \quad (4.27)$$

Note that the identifications of Q_1, Q_2 are consistent with our previous findings based on affine $SO(7)$ structure. This identifies the parameters (2), (7) of Fig. 11 and similarly (4), (9).

$SO(7)$ subsector: We now consider another subsector with $k_1 = k_3 = 0$, $k_2 \neq 0$. We start from the elliptic genus of the $SO(7)$ instanton strings at $n_8 = 2$, studied in Sec. II. In the 5D scaling limit, e.g., at $k_2 = 1$, we found the following exact factorization:

$U(2)$ theory at Chern-Simons level 1. From these studies, one can identify the Kähler parameters (3), (8) of Fig. 11. Note that in (4.28), the leading term at U^1 order is $\frac{U}{W_i \tilde{W}_i}$ (with $i = 1, 2$) for the two 5D $\tilde{E}_1$ factors. This is the Kähler parameter for the bottom horizontal line on the right side of Fig. 14, since the leading BPS states come from the strings stretched along this line. So one finds $(3) = \frac{U}{W_1 \tilde{W}_1} = e^{-u} \frac{y_1 y_2 y_3^2}{\sqrt{q}}$, $(8) = \frac{U}{W_2 \tilde{W}_2} = e^{-u} \frac{y_1 y_2^2 y_3^3}{w \tilde{w} \sqrt{q}}$, which were already shown in Fig. 11. Once we know (3) and (8), one can determine (11) from the gluing condition $(11) = (2)(3)^2(4) = (7)(8)^2(9)$, again already shown in Fig. 11. Thus, we fixed all Kähler parameters of Fig. 11 in terms of our 6D fugacities.

We have in fact made a nontrivial test of our elliptic genera of Sec. II, for the $SO(7)$ instanton strings at $n_8 = 2$, using the 5-brane web description, from (4.28). Although apparently we tested the elliptic genera in a 5D factorizing limit, this is different from the tests made in Sec. III. This is because the "5D limit" here scales other massive parameters and keeps a different slice of BPS states in its zero momentum sector. Indeed, using the original 6D variables, (4.28) is a nontrivial series in $Q_1 = \frac{q}{y_1 y_2 y_3^2} \sim q$, acquiring contributions from the 6D KK tower. So, this provides an independent nontrivial test of our results in Sec. II.

More general sectors: We shall continue to study the scaling limit of the elliptic genera for more general

winding sectors at $(k_1, k_2, k_3) = (1, 1, 0), (1, 2, 0),$ $(1, 1, 1), (1, 2, 1)$.

In the first three sectors, Fig. 11(b) factorizes to two "5D $SU(1)$" factors which are void, as these sectors are realized by $(4), (9), (11) \to 0$ for $(k_1, k_2, k_3) = (1, 1, 0),$ $(1, 2, 0)$ and $(11) \to 0$ for $(k_1, k_2, k_3) = (1, 1, 1)$. So, we

expect the factorization of the single particle index into two identical pieces, each representing a non-Lagrangian 5D SCFT engineered by Fig. 11(a) in a particular limit. In all cases, we find exact factorizations of $f_{\rm rel}$ into two functions of identical form as follows:

$$(1, 1, 0): f_{\rm rel} = e^{-v-u} \frac{y_1 y_2 y_3^2}{\sqrt{q}} \cdot \frac{(1 + q/y_1 y_2 y_3^2)^2}{(1 - q/y_1 y_2 y_3^2)^2} + e^{-v-u} \frac{w y_1 y_2 y_3^2}{\tilde{w} \sqrt{q}} \cdot \frac{(1 + y_2/y_1)^2}{(1 - y_2/y_1)^2}$$

$$(1, 2, 0): f_{\rm rel} = e^{-v-2u} \frac{y_1^2 y_2^2 y_3^4}{q} \cdot \frac{-10(q/y_1 y_2 y_3^2)^2(1 + q/y_1 y_2 y_3^2)}{(1 - q/y_1 y_2 y_3^2)^6}$$

$$+ e^{-v-2u} \frac{y_1^2 y_2^3 y_3^5}{\tilde{w}^2 q} \cdot \frac{-10(y_2/y_1)^2(1 + y_2/y_1)}{(1 - y_2/y_1)^6}$$

$$(1, 1, 1): f_{\rm rel} = e^{-v-u-\tilde{v}} \frac{y_1 y_2 y_3^2}{\sqrt{q}} \frac{(1 + q/y_1 y_2 y_3^2)^3}{(1 - q/y_1 y_2 y_3^2)^2} + e^{-v-u-\tilde{v}} \frac{w \tilde{w} y_1 y_3}{\sqrt{q}} \frac{(1 + y_2/y_1)^3}{(1 - y_2/y_1)^2}. \tag{4.29}$$

Each term is a product of the prefactor $(2)^{k_1}(3)^{k_2}(4)^{k_3}$ or $(7)^{k_1}(8)^{k_2}(9)^{k_3}$ and a function of Kähler parameter $(1) = (5)$ or $(6) = (10)$, respectively. To test these results, extracted from the elliptic genera in Sec. IV A, we shall independently do the topological vertex calculus for the 5D SCFT of Fig. 11(a).

The topological vertex [59] computes all genus topological string amplitudes, which is equivalent to the logarithm of the 5D Nekrasov partition function on Omega-deformed $\mathbf{R}^4 \times S^1$ [60]. Here we refer to [49,50] for its detailed description. We select an orientation of every edge in the 5-brane web. Each internal edge is associated with a Young diagram. We also assign an empty Young diagram to every external edge. The 5D partition function is given by a sum over all combinations of Young diagrams. The summand is a product of factors coming from every edge and vertex. We turn off $\epsilon_+ = 0$ to simplify the formulas. When all three edges are outgoing from a given vertex, the vertex factor is given by (where $u = e^{-\epsilon_-}$, $\|\mu\|^2 = \sum_i \mu_i^2$)
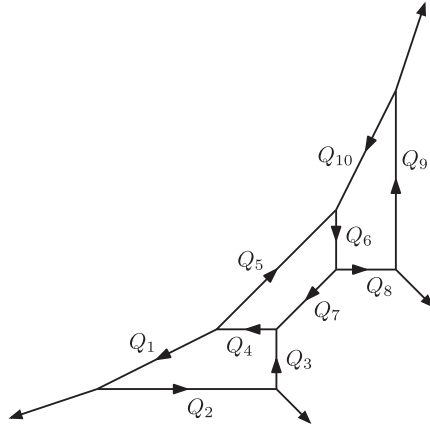
$$C_{\lambda\mu\nu}(u) = u^{\frac{\|\mu\|^2 + \|\nu\|^2 - \|\mu^t\|^2}{2}} \prod_{s \in \nu} (1 - u^{l_\nu(s) + a_\nu(s) + 1})^{-1}$$
$$\cdot \sum_\eta s_{\lambda^t/\eta}(u^{-\rho} u^{-\nu}) s_{\mu/\eta}(u^{-\rho} u^{-\nu^t}). \tag{4.30}$$

λ, μ, ν are Young diagrams associated to the edges. For an incoming edge, the assigned Young diagram should be transposed. The skew-Schur function $s_{\lambda/\eta}(\mathbf{x})$ depends on a possibly infinite vector $\mathbf{x}$, which in above is $u^{-\rho} u^{-\nu} \equiv (u^{\frac{1}{2}-\nu_1}, u^{\frac{3}{2}-\nu_2}, u^{\frac{5}{2}-\nu_3}, \cdots)$. The functions $l_\nu(s)$ and $a_\nu(s)$ are defined by $l_\nu(s) = \nu_i - j$ and $a_\nu(s) = \nu_j^t - i$, where i, j represent the horizontal and vertical positions of the box s from the upper-left corner of ν. It is known that $C_{\lambda\mu\nu}(u)$ is invariant under the cyclic permutation of λ, μ, ν using Schur function identities [59]. An internal edge glues a pair of vertices by multiplying the edge factor and summing over the assigned Young diagram. Denoting its Kähler parameter by Q, the edge factor is given by

$$= (-Q)^{|\nu|} f_\nu(u)^n \tag{4.31}$$

where $f_\nu(u) = (-1)^{|\nu|} u^{\frac{\|\nu^t\|^2 - \|\nu\|^2}{2}}$ and $n = \det(u_1, v_1)$. Applying these rules, one obtains the following partition function of 5D SCFT engineered from the brane web of Fig. 11(a)

$$\sum_{\nu_1,\cdots,\nu_{10}} \prod_{i=1}^{10}(-Q_i)^{|\nu_i|}$$
$$\times f_{\nu_1} f_{\nu_2}^3 f_{\nu_3} f_{\nu_4}^{-1} f_{\nu_5}^{-2} f_{\nu_6}^{-1} f_{\nu_8} f_{\nu_9}^3 f_{\nu_{10}}$$
$$\times C_{\nu_1^t \nu_2 \phi} C_{\nu_2^t \nu_3 \phi} C_{\nu_3^t \nu_4 \nu_7^t} C_{\nu_4^t \nu_1 \nu_5}$$
$$\times C_{\nu_5^t \nu_{10}^t \nu_6} C_{\nu_6^t \nu_8 \nu_7} C_{\nu_8^t \nu_9 \phi} C_{\nu_9^t \nu_{10} \phi} \qquad (4.32)$$

$Q_1, \ldots, Q_{10}$ are identified with the Kähler parameters in Fig. 11(a) as

$$Q_1 = Q_3 = \alpha, \quad Q_4 = Q_6 = \beta, \quad Q_7 = \gamma, \quad Q_8 = Q_{10} = \delta, \quad Q_2 = \alpha^2 \beta, \quad Q_5 = \beta \gamma, \quad Q_9 = \beta \delta^2, \quad (4.33)$$

where $(\alpha, \beta, \gamma, \delta) = (e^{-v}, \frac{q}{y_1 y_2 y_3^2}, e^{-u} \frac{y_1 y_2 y_3^2}{\sqrt{q}}, e^{-\tilde{v}})$ or $(\frac{w^2 e^{-v}}{y_2 y_3}, \frac{y_2}{y_1}, e^{-u} \frac{y_1 y_2^2 y_3^3}{w \tilde{w} \sqrt{q}}, \frac{\tilde{w}^2 e^{-\tilde{v}}}{y_2 y_3})$, respectively. To derive the single particle spectrum of (k_1, k_2, k_3) sector, we perform the sum (4.32) over Young diagrams until $|\nu_1| + 2|\nu_2| + |\nu_3| \leq k_1$, $|\nu_5| + |\nu_7| \leq k_2$, $|\nu_8| + 2|\nu_9| + |\nu_{10}| \leq k_3$ and take the Plethystic logarithm. To compare with (4.29), we further multiply $-(2 \sinh \frac{\epsilon_-}{2})^2$ on it and take the limit $\epsilon_- \to 0$. After these manipulations, one obtains

$$(1,1,0): f_{\text{top}} = \alpha\gamma \cdot (1 + 4\beta + 8\beta^2 + 12\beta^3 + 16\beta^4 + 20\beta^5 + \mathcal{O}(\beta^6))$$
$$(1,2,0): f_{\text{top}} = \alpha\gamma^2 \cdot (-10\beta^2 - 70\beta^3 - 270\beta^4 - 770\beta^5 + \mathcal{O}(\beta^6))$$
$$(1,1,1): f_{\text{top}} = \alpha\gamma\delta \cdot (1 + 5\beta + 12\beta^2 + 20\beta^3 + 28\beta^4 + 36\beta^5 + \mathcal{O}(\beta^6)). \qquad (4.34)$$

These agree with f_{rel} in (4.29), testing our elliptic genera in Sec. IV A.

We finally consider the (1,2,1) sector. f_{rel} in the factorization limit is given by

$$f_{\text{rel}} = e^{-v-2u-\tilde{v}} \frac{y_1^2 y_2^2 y_3^4}{q} \cdot \left[\frac{-2y_1 y_2}{(1-y_1 y_2)^2} + \left(\frac{-2k(k^4 + 4k^3 + 30k^2 + 4k + 1)}{(k-1)^6} \right) \Big|_{k=\frac{y_2}{y_1}} \right.$$
$$\left. + \left(\frac{-2k(k^4 + 4k^3 + 30k^2 + 4k + 1)}{(k-1)^6} \right) \Big|_{k=\frac{q}{y_1 y_2 y_3^2}} + (-2) \right]. \qquad (4.35)$$

The common prefactor $e^{-v-2u-\tilde{v}} y_1^2 y_2^2 y_3^4 / q$ is $(2)(3)^2(4) = (7)(8)^2(9) = (11)$. The first term agrees with the one instanton partition function of 5D pure $SU(2)$ gauge theory, if we identify $\sqrt{y_1 y_2}$ as the fugacity of the $SU(2)$ electric charge. It belongs to the 5D E_1 SCFT of Fig. 11(b). The next two terms take the same functional form, respecting the $\mathbb{Z}_2$ symmetry of the two factors. To test this function, we performed the topological vertex calculus for (4.32). We first sum over all Young diagrams with $|\nu_1| + 2|\nu_2| + |\nu_3| \leq 1$, $|\nu_5| + |\nu_7| \leq 2$, $|\nu_8| + 2|\nu_9| + |\nu_{10}| \leq 1$ and take the Plethystic logarithm. We then subtract the extra factor $\alpha\gamma^2 \delta (2 \sinh \frac{\epsilon_-}{2})^{-2}$ that arises because the strings can propagate along the parallel 5-branes [49,50]. Dividing out the center-of-mass factor $-(2 \sinh \frac{\epsilon_-}{2})^{-2}$ and turning off $\epsilon_- \to 0$, the topological string partition function becomes

$$(1,2,1): f_{\text{top}} = \alpha\gamma^2 \delta \cdot (-2\beta - 20\beta^2 - 150\beta^3 - 648\beta^4 - 2010\beta^5 + \mathcal{O}(\beta^6)). \qquad (4.36)$$

It agrees with the second and third terms of f_{rel} in (4.35). The final (-2) comes from the perturbative $SU(2)_g$ vector multiplet. Again, this result gives a nontrivial independent test of our elliptic genera in Sec. IV A.

C. 3,2 and 3,2,2: $G_2 \times SU(2)$ gauge group

We construct 2D quivers for the strings of other 6D SCFTs in IV. The tests we can provide about them are weak (e.g., anomalies). We keep the presentations rather brief.
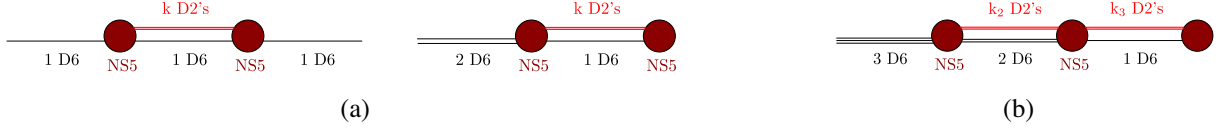
FIG. 15. Brane configurations for (a) 6D (2,0) SCFT of type A_1, (b) 6D 3,2,2 SCFT in the limit with ungauged G_2.

3,2,2 SCFT strings: The strategy is similar to that of Sec. IV A. We first consider the limits in which all except one gauge symmetry are ungauged in 6D and take three factors of ADHM(-like) quivers. We then combine these quivers by locking certain symmetries and introducing bifundamental matters of the form of (4.2). To be more precise, we have no 6D gauge group associated with the "2" node on the right. Although the notion of ungauging is absent for this node, we can still take the tensor VEV associated with this node to infinity. Whenever a node has a 6D gauge group, its inverse coupling is proportional to the tensor VEV $\langle \Phi \rangle$, so taking $\langle \Phi \rangle \to \infty$ ungauges the symmetry.

If one takes all tensor VEVs to infinity except the 3 node, one obtains the 6D G_2 theory at $n_7 = 1$. This is because the 6D matter in $\frac{1}{2}(\mathbf{7}, \mathbf{2})$ behaves like one full hypermultiplet in $\mathbf{7}$, while $\frac{1}{2}(\mathbf{1}, \mathbf{2})$ is neutral in G_2 and invisible in the gauge dynamics. So, with a G_2 theory at $n_7 = 1$, its k_1 G_2 instanton strings are described by the 2D $U(k_1)$ gauge theory explained in Sec. II B, with fields given by (2.49), (2.50), (2.51) at $n_7 = 1$. The ungauged $SU(2) \sim Sp(1)$ acts as the flavor symmetry of the 6D hypermultiplet. In the ADHM-like quiver at general n_7, one may have as big as $U(2n_7)$ flavor symmetry which rotates Fermi multiplets. But the coupling to bulk fields only allowed $U(n_7)$ part, which we further expected to enhance to $Sp(n_7)$. This is similar to the flavor symmetries of $SO(7)$ ADHM-like theory at $n_8 \neq 0$. In the current context, again like the 2,3,2 quiver, we should couple the system to different bulk fields. At $n_7 = 1$, one can classically have as big as $U(2n_7) \to U(2)$ flavor symmetry. We restrict it to $SU(2)$ which rotates $\Psi, \tilde{\Psi}^\dagger$ of (2.51) as a doublet. Also, as explained in Sec. II B, only $SU(3) \subset G_2$ is visible in this quiver. More formally, it will be convenient to regard the fields $q_i, \tilde{q}^i, \phi_i, \phi_4$ as transforming in $SU(3) \times SU(1) \subset SU(4)$.

When G_2 is ungauged and the tensor VEV for the right 2 node is sent to infinity, we have 6D $SU(2)$ theory at $n_2 = 4$. Its ADHM quiver is explained around (4.1). In this limit, G_2 is enhanced to $SO(7)$ flavor symmetry rotating the four hypermultiplets in $\mathbf{8}$ of $SO(7)$, but only $SU(4) \subset SO(7)$ is visible in the UV ADHM, as explained in Sec. IV A. $SO(7)$ will later be broken to G_2 by gauging. In our ADHM-like quiver, which only sees $SU(3) \subset G_2$, $SU(4)$ will be broken to $SU(3) \times SU(1)$, locked with the G_2 ADHM of the previous paragraph.

We finally ungauge $G_2 \times SU(2)$, leaving one tensor VEV for the right 2 node finite. One then obtains the 6D $\mathcal{N} = (2,0)$ SCFT of A_1 type, geometrically engineered on the $O(-2) \to \mathbb{P}^1$ base with no associated gauge group. Although the strings of this SCFT in the tensor branch lack the instanton string interpretation, one still knows the UV 2D gauge theory description [13]. For k strings, this is a $U(k)$ gauge theory. The 2D fields are given by

$$
\begin{aligned}
(A_\mu, \lambda_0, \lambda): &\ \text{vector mutiplet in } (\mathbf{adj}, 0) \\
q_{\dot\alpha} = (q, \tilde{q}^\dagger): &\ \text{hypermultiplet in } (\mathbf{k}, -1) \\
a_{\alpha\dot\beta} \sim (a, \tilde{a}^\dagger): &\ \text{hypermultiplet in } (\mathbf{adj}, 0) \\
\Psi_a: &\ \text{Fermi multiplet in } (\mathbf{k}, 0),
\end{aligned}
\tag{4.37}
$$

where $a = 1, 2$. We showed the representation and charge of the classical symmetry $U(k) \times U(1)$, where one should further restrict $U(1) \to SU(1)$ due to mixed anomaly. This formally takes the form of the ADHM instanton strings of "6D $SU(1)$ theory" with two charged quarks. The $SU(2)_F$ flavor symmetry which rotates Ψ_a is identified with the enlarged R-symmetry group of the 6D (2,0) theory. Namely, we expect that $SU(2)_R$ of 6D (1,0) SCFT enhances to $SO(5)_R$. In the tensor branch, this is broken to $SO(4) \sim SU(2)_R \times SU(2)_L$, where the latter $SU(2)_L$ is realized as $SU(2)_F$ in the 2D quiver. The 6D A_1 (2,0) theory and the above 2D gauge theory admit D-brane engineerings. Using D2-D6-NS5, one can use either of Fig. 15(a), in IIA or massive IIA string theory [61,62].

Before fully combining the three ADHM(-like) quivers, we note that the combination of two 2 nodes (with G_2 ungauged) is dictated by a D-brane setting. This is given by the brane configuration of Fig. 15(b) in the massive IIA theory. The 2D quiver is given by Fig. 16 at $k_1 = 0$. The quiver and the brane system only has manifest $SU(3) \times SU(2) \times U(1)$ symmetry, where the last $U(1)$ is a combination of three overall $U(1)$'s in $U(3) \times U(2) \times U(1)$

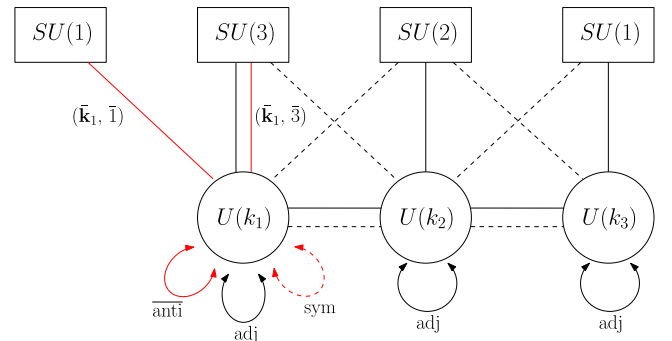

FIG. 16. 2D quiver for the strings of 6D 3,2,2 SCFT.

which survive the mixed anomaly cancellation with $U(k_2) \times U(k_3)$. More precisely, taking the overall $U(1)$ generators Q_i for $SU(i)$, $i = 1, 2, 3$, only $Q_1 + Q_2 + Q_3$ is free of the mixed anomaly. (This $U(1)$ is not shown in Fig. 16, as it will be irrelevant generally at $k_1, k_2, k_3 \neq 0$.) One can see that the 2D quiver exhibits $SU(3) \times U(1) \rightarrow SO(7)$ symmetry enhancement, say by studying the elliptic genera. This should be the case since one has 6D $SU(2)$ theory at $n_2 = 4$. Just to be sure, we tested the $SO(7)$ enhancement of the elliptic genus at $k_2 = k_3 = 1$.

Now we keep $k_1 \neq 0$, with G_2 gauged. In our UV gauged linear sigma model, we can only see $SU(3) \subset G_2$, which we lock with the $SU(3)$ symmetry of the quiver in the previous paragraph. The resulting $U(k_1) \times U(k_2) \times U(k_3)$ quiver is given by Fig. 16. The potentials can be written down in a similar manner as the 2,3,2 quiver of Sec. IV A. We skip the details here.

As a small test of our quiver, we compute the 2D anomalies. We first compute it from inflow. The Green-Schwarz part of the 6D anomaly 8-form is given by $I_{\mathrm{GS}} = \frac{1}{2} \Omega^{ij} I_i I_j$ with

$$I_i = \begin{pmatrix} \frac{1}{4} \mathrm{Tr}(F_{G_2}^2) + \alpha_1 c_2(R) + \alpha_2 p_1(T) \\ \frac{1}{4} \mathrm{Tr}(F_{SU(2)}^2) + \beta_1 c_2(R) + \beta_2 p_1(T) \\ \gamma_1 c_2(R) + \gamma_2 p_1(T) \end{pmatrix},$$

$$\Omega^{ij} = \begin{pmatrix} 3 & -1 & 0 \\ -1 & 2 & -1 \\ 0 & -1 & 2 \end{pmatrix}, \qquad (4.38)$$

where $(\alpha_1, \beta_1, \gamma_1) = (\frac{17}{7}, \frac{23}{7}, \frac{15}{7})$, $(\alpha_2, \beta_2, \gamma_2) = (\frac{3}{28}, \frac{1}{14}, \frac{1}{28})$. We explain how to get this result. Reference [44] uses two methods to compute I_{GS}. One is applicable when all nodes have gauge symmetries. In this case, one demands that I_{GS} cancels all terms in $I_{\mathrm{one\text{-}loop}}$ containing dynamical fields. This is the method we used so far in this paper. When some nodes do not have gauge symmetries, this method alone cannot completely determine I_{GS}. We use the following strategy to compute (4.38). Firstly, we compute the one-loop anomaly containing the dynamical $G_2 \times SU(2)$ gauge fields and demand that this part is completely canceled by I_1, I_2 part of I_{GS} [43]. Then one obtains I_i of the form (4.38), where the six coefficients $\alpha_{1,2}, \beta_{1,2}, \gamma_{1,2}$ are constrained only by the following four equations:

$$3\alpha_1 - \beta_1 = 4, \qquad 3\alpha_2 - \beta_2 = \frac{1}{4},$$
$$2\beta_1 - \alpha_1 - \gamma_1 = 2, \qquad 2\beta_2 - \alpha_2 - \gamma_2 = 0. \qquad (4.39)$$

To further constrain them, we consider the limit in which two tensor VEVs are sent to infinity so that $G_2 \times SU(2)$ are ungauged. In this limit, we can use the known expression for I_{GS} for the A_1 (2,0) theory in the tensor branch [43,44],

$$I_{\mathrm{GS}} = \frac{1}{2} \Omega \left(\frac{1}{2} (c_2(R) - c_2(L)) \right)^2, \qquad \Omega = 2, \qquad (4.40)$$

with enhanced $SU(2)_R \times SU(2)_L = SO(4) \subset SO(5)$ R-symmetry. After taking this limit, we can set $\frac{1}{4} \mathrm{Tr}(F_{SU(2)}^2) = c_2(L)$ by identifying the ungauged $SU(2)$ with $SU(2)_L$. To take this limit, consider the vector kinetic terms proportional to $\mathcal{L}_{\mathrm{v}} \sim \Omega^{ij} \Phi_i \mathrm{Tr}(F_j^2) \equiv \Phi^i \mathrm{Tr}(F_i^2)$. We keep $\Phi^3 = 2\Phi_3 - \Phi_2$ finite, while taking $\Phi^1 = 3\Phi_1 - \Phi_2$ and $\Phi^2 = 2\Phi_2 - \Phi_1 - \Phi_3$ to $+\infty$, to ungauge $G_2 \times SU(2)$. To properly do so, note that the kinetic terms for Φ_i are proportional to $\mathcal{L}_t \sim \Omega^{ij} \partial^\mu \Phi_i \partial_\mu \Phi_j$. This is diagonalized by taking, say, $\Phi_3 = a + \chi$, $\Phi_2 = 2a$, $\Phi_1 = b + \frac{2a}{3}$, since $\mathcal{L}_t \sim \frac{14}{3}(\partial a)^2 + 3(\partial b)^2 + 2(\partial \chi)^2$. So one holds the scalars a, b very large and fixed, unaffected by the dynamical χ and its superpartner. More precisely, a, b can be hold fixed, given by infinite constant plus a finite background function given by the background gauge fields. χ is a dynamical scalar associated with the right 2 node with normalization $\Omega = 2$. In this parametrization χ, a, b of tensor multiplet scalars, one can similarly show that the superpartners H_a, H_b of a, b can be consistently taken to be fixed background functions, unaffected by dynamical χ and its superpartner H_χ. Now, consider the equation of motion for H_χ. The coupling between B_χ and the dynamical/background vector fields is given by

$$\Omega^{ij} B_i \wedge I_j \rightarrow B_\chi \Omega^{3i} I_i = B_\chi \wedge (2I_3 - I_2). \qquad (4.41)$$

We used $\Omega^{ij} B_j = (\cdots, -B_\chi + \cdots, 2B_\chi)$, where $\cdots$ depend on B_a, B_b, so that it depends on B_χ as $\Omega^{i3} B_\chi$. From the equation of motion for B_χ, one obtains

$$d \star H_\chi = (\Omega^{33})^{-1} \Omega^{3i} I_i = I_3 - \frac{1}{2} I_2. \qquad (4.42)$$

By comparing this with (4.40), one obtains $I_3 - \frac{1}{2} I_2 = \frac{c_2(R) - c_2(L)}{2}$ with $c_2(L) = \frac{1}{4} \mathrm{Tr}(F_{SU(2)}^2)$. This leads to two more equations for $\alpha_{1,2}, \beta_{1,2}, \gamma_{1,2}$,

$$2\gamma_1 - \beta_1 = 1, \qquad 2\gamma_2 - \beta_2 = 0. \qquad (4.43)$$

The unique solution of (4.39), (4.43) is the one stated right below (4.38).[7]

---

[7] In fact, expanding the arguments of this paragraph, one can compute I_{GS} if one knows the Green-Schwarz anomalies of all individual rank 1 nodes before combining them. The general rule is as follows [44]. Suppose that $I_{\mathrm{GS}}^{(i)} = \frac{1}{2} \Omega^{ii} (I_i)_{\mathrm{single}}^2$ (no sum of i) when only i'th node is kept. Then defining $I^i \equiv (\Omega^{ii})^{-1} (I_i)_{\mathrm{single}}$ (no sum of i), one finds $I_{\mathrm{GS}} = \frac{1}{2} (\Omega^{-1})_{ij} I^i I^j$. I_i that we computed in (4.9) and (4.38) are given by $I_i = (\Omega^{-1})_{ij} I^j$.

This leads to the anomaly 4-form on the strings from inflow, (2.40), given by

$$I_4 = \left(k_1 k_2 + k_2 k_3 - \frac{3}{2} k_1^2 - k_2^2 - k_3^2 \right) \chi(T_4) + k_1 (I_2 - 3I_1)$$
$$+ k_2 (I_1 + I_3 - 2I_2) + k_3 (I_2 - 2I_3). \qquad (4.44)$$

This is computed from our 2D gauge theory as follows. We again decompose the anomaly into contributions $I_4^{(1)}$ from the G_2 ADHM-like quiver, $I_4^{(2)}$ from the middle 2 node (6D $SU(2)$ theory at $n_2 = 4$), $I_4^{(3)}$ from the right 2 node, and $I_4^{bif} = (k_1 k_2 + k_2 k_3)\chi(T_4)$. $I_4^{(1)}$ and $I_4^{(2)}$ are given by (2.61) and (4.12) replacing $F_{SO(7)} \rightarrow F_{G_2}$. $I_4^{(3)}$ is given by Eq. (5.21) of [4] at $N = 1$,

$$I_4^{(3)} = -\frac{k_3}{2} \mathrm{Tr}(F_{SU(1)}^2) + \frac{k_3}{4} \mathrm{Tr}(F_{SU(2)}^2) - k_3 c_2(R) - k^2 \chi(T_4),$$
$$(4.45)$$

where one should set $F_{SU(1)} = 0$. Adding $\sum_{i=1}^{3} I_4^{(i)} + I_4^{bif}$, one precisely reproduces (4.44).

3,2 SCFT strings: This SCFT can be obtained from the previous 3,2,2 SCFT by taking the tensor VEV of the right 2 node to infinity. The corresponding 2D quiver for its strings can be obtained from our previous quiver for the 3,2,2 model, by taking $k_3 = 0$. All the discussions made for the 3,2,2 string quivers apply here as well.

V. CONCLUSION AND REMARKS

In this paper, we first proposed 1D ADHM-like gauge theories for Yang-Mills instantons for 5D $SO(7)$ theories with $n_8 \leq 4$ matters in spinor representation and for G_2 theories with $n_7 \leq 3$ matters in **7**. At $n_8 = 2$ for $SO(7)$ and at $n_7 = 1$ for G_2, where anomaly-free 6D gauge theories exist, our gauge theories uplift to 2D for instanton strings. These ADHM strings can be used to construct the 2D quivers for the atomic non-Higgsable 6D SCFTs of Table IV. These gauge theories do not describe the symmetric phase physics of instantons, but we propose them to compute the Coulomb phase partition functions correctly. Although the world volumes of instantons host $\mathcal{N} = (0, 4)$ SUSY (or its 1D reduction), our gauge theories are made of $\mathcal{N} = (0, 2)$ supermultiplets, and some of their interactions only exhibit $\mathcal{N} = (0, 1)$ SUSY. We expect various symmetry enhancements in 1D/2D.

We tested our 1D/2D gauge theories by computing their Witten indices or elliptic genera using various other methods. First, for 5D G_2 theory without matters, $n_7 = 0$, we used the results of [45], which uses 3D Coulomb branch techniques. We tested our results for instanton numbers $k \leq 3$, but the comparisons can in principle be made for arbitrary high k's. In Sec. III, we

developed another D-brane-based method to study the instantons of 5D $SO(7)$ theories at $n_8 = 1$, 2 and related G_2 theories at $n_7 = 0$, 1. This method provides a much more elaborate computational procedure, which however does not require guesswork. We used this method to successfully test our results for $n_8 = 2$ at $k = 1$ and for $n_8 = 1$ at $k = 1$, 2. Finally, we used the 5-brane web description of [16] to test the $SO(7)$ instanton strings at $n_8 = 2$ and also the strings of the 6D 2,3,2 SCFT of Table IV. All the methods that we used to test our results exhibit manifest $(0,4)$ SUSY. So the agreements of our indices with these alternative calculus are indirect signals that our systems exhibit $(0,4)$ SUSY enhancement.

As we alluded to at the beginning of Sec. II, we have made similar trials to construct ADHM-like gauge theories with other gauge groups, e.g., some of them in Table I. For technical reasons, we focused on the E_7 case, using a formalism which only sees manifest $SU(8) \subset E_7$. We managed to build a model which exhibits the correct anomaly polynomial 4-form for E_7 instanton strings, which also "closely" (but not precisely) reproduces the one-instanton Hilbert series of the E_7 instanton particle. For instance, keeping $t = e^{-\epsilon_+}$ fugacity only and multiplying the center-of-mass factor $2 \sinh \frac{\epsilon_{1,2}}{2}$, the correct Hilbert series [46] and the index of our trial gauge theory are given as follows (up to 0-point energy factor):

$$\hat{Z}_{k=1}^{E_7} = 1 + 133t^2 + 7371t^4 + 238602t^6 + 5248750t^8$$
$$+ 85709988t^{10} + 1101296924t^{12}$$
$$+ 11604306012t^{14} + 103402141164t^{16}$$
$$+ 797856027500t^{18} + 5431803835220t^{20} + \cdots,$$
$$\hat{Z}_{k=1}^{trial} = 1 + 133t^2 + 7300t^4 + 234689t^6 + 5143821t^8$$
$$+ 83863116t^{10} + 1077066537t^{12}$$
$$+ 11349844981t^{14} + 101164274246t^{16}$$
$$+ 780860775912t^{18} + 5317874678676t^{20} + \cdots.$$
$$(5.1)$$

The coefficient of t^{2n} for the correct result $\hat{Z}_{k=1}^{E_7}$ is the n'th symmetric product of the E_7 adjoint representation **133**. The index $\hat{Z}_{k=1}^{trial}$ is close to $\hat{Z}_{k=1}^{E_7}$ at low orders in t (e.g., exact at t^2), but slightly deviates and converges to $\approx -1.928\%$ error asymptotically at large orders. We think this failure provides helpful lessons on our ADHM-like trials and possible subtle points (some stated at the beginning of Sec. II).

First of all, the gauge theory we constructed which yields $\hat{Z}_{k=1}^{trial}$ has two branches of moduli spaces. The first branch has the $SU(8)$ instanton moduli space as a subspace and has the right complex dimension $2kc_2(E_7) = 36k$ for E_7 instantons. The second branch meets the first one at a point, the small instanton singularity, and arises from the

extra matters we added to the $SU(8)$ ADHM. We find that the second branch cannot be eliminated (with given extra matters) by turning on $\mathcal{N} = (0, 1)$ potentials. We suspect that there may be a contribution to $\hat{Z}_{k=1}^{\mathrm{trial}}$ from the second branch, which spoils the results. Since we are doing a UV computation in which two branches are not separated, we do not know how/whether one can separate the contributions from two branches. Certainly, this may be one reason for the deviation. In case this is the dominant reason for the deviation, there should be large enough contributions from massless fermions on the second branch, as $\hat{Z}_{k=1}^{\mathrm{trial}}$ is always no greater than $\hat{Z}_{k=1}^{E_7}$.

Second, there is another reason why we suspect the deviation happens. To explain this, note that **133** at t^2 order is correctly reproduced in our trial gauge theory. From the branching rule **133** $\rightarrow$ **63** $\oplus$ **70**, two different contributions make this to happen. **63** is nothing but the t^2 order contribution from the $SU(8)$ ADHM fields. **70** comes from gauge-invariant operators of the $SU(8)$ ADHM fields and extra fields we added. The next order t^4 contains the irrep. **7371** of E_7, which is rank 2 symmetric product of **133**. We are missing some states in $\hat{Z}_{k=1}^{\mathrm{trial}}$, which is **70** $\oplus$ **1**, the rank 4 antisymmetric representation, and a singlet of $SU(8)$. If we blindly take the operators in our trial gauge theory which successfully reproduced **133**, and take rank 2 symmetric product of them, we find that the representation **70** $\oplus$ **1** is missing due to the compositeness of **70** that appeared at t^2 order. This is like the quarks of QCD accounting for the plethora of gauge-invariant mesons at low energy, with less microscopic degrees of freedom, while quarks manifest themselves at high energy. So it appears that we should add more extra fields to make up for these missing states. We have found several possible combinations of extra supermultiplets which one may add to the $SU(8)$ ADHM, satisfying very strong constraints of the correct 2D anomaly. But we have not managed yet to construct the model which exhibits the right Hilbert series of (5.1).

Finally, while restricting to $SU(8) \subset E_7$ subset of moduli space, we deleted one simple root so that we lost extra possibility of embedding $SU(2)$ single instanton. Note that the deleted root has same length as the roots kept in $SU(8)$, so that we might have lost extra small instanton saddle points residing in the deleted $SU(2)$. This may be related to the observations in the previous paragraph. In any case, if the basic idea of this paper is applicable to other exceptional instantons, we have many strong constraints which may eventually guide us to the correct ADHM-like models. We hope to come back to this problem in the future.

One important spirit of our construction is to take advantage of symmetry enhancements of gauge theories after RG flow. One is the enhancement of global symmetries from a classical group to an exceptional one. Another is the SUSY enhancement to $\mathcal{N} = (0, 4)$. Allowing less number of SUSY in UV provides more room to engineer the desired

system. Being in 1D or 2D, we can have as little as one Hermitian SUSY in UV, the minimal number which admits any computation relying on SUSY. Still the requirement of using gauge theories puts some constraints. However, we are not fully aware of whether we have overlooked the possibilities of subtler supermultiplets or more general interactions, even within gauge theory.

It may also be interesting to further study the physics of exceptional instanton strings from recent 4D $\mathcal{N} = 1$ gauge theory descriptions for $\mathcal{N} = 2$ SCFTs, by suitably reducing them to 2D [63,64]. Many aspects of these constructions are different from ours. For instance, different symmetries are manifest in UV, so it may be helpful to compare the two approaches.

Some of our 1D/2D gauge theories are not tested with their Witten indices and elliptic genera, simply because we have not thoroughly thought about alternative approaches. The recent engineering of 5D SCFTs (e.g., see [36,57]) will allow more geometric/brane realizations. We may be able to test our models relying on these developments, perhaps using topological vertices. Also, for studying 6D strings, one can use the topological string approach (e.g., see [14] and references therein) or the modular bootstrap like approach [17–19].

The strategy of this paper was just to write down UV models and test them empirically when data from alternative descriptions are available. It will be nice to have a more conceptual understandings of the ADHM-like models, either from string theory or by other means. Here we feel that, compared to the simple Young diagram sums for the indices and elliptic genera, the microscopic explanations in terms of $\mathcal{N} = (0, 1)$ UV gauge theories look less elegant, although practically useful and flexible. In particular, at least at the moment, it is hard for us to imagine a viable string theory engineering of our gauge theories. It is not clear to us whether we are making UV uplifts intrinsically beyond the territory of string theory, or whether there are nicer reformulations which may allow string theory embeddings.

Finally, it will be interesting to see if our ADHM-like gauge theories can be used to study other observables in the Coulomb branch. For instance, study of the Wilson loops or other defect operators will be interesting. See, e.g., [65–68] and references therein. As many of these constructions rely on D-brane settings, one should see if employing similar prescriptions without D-brane engineering will work (as we did for the partition function in this paper).

Note added.—Before posting this paper on arXiv, we were informed about a partly overlapping work [69], which computes the 5D G_2 Nekrasov partition function from the brane web construction.

APPENDIX: COMMENTS ON EXTRA INSTANTON MODULI

The basic idea of this paper is to apply the ADHM construction associated with a subgroup H of the gauge group G for describing the G instantons. Let us implement this idea to the case with $H = SU(4)$ and $G = SO(7)$, where the $SO(7)$ adjoint representation (**21**) comprises the $SU(4)$ adjoint (**15**) and antisymmetric (**6**) representations. We need to consider the additional moduli induced from the $SU(4)$ antisymmetric vector multiplet, on top of the standard ADHM moduli originated from the $SU(4)$ adjoint vector multiplet.

The k-instanton zero modes associated with 5D/6D $\mathcal{N} = 1$ supermultiplets are captured in their equivariant indices. We summarize some useful results here. First, for $SU(N)$ representations **N** and **N̄**, the hypermultiplet indices are

$$\text{Ind}^{\text{h}}(\mathbf{N}) = +\frac{\cosh\frac{m}{2}}{2\sinh\frac{\epsilon_1}{2}2\sinh\frac{\epsilon_2}{2}}\text{Ch}(\mathcal{E}),$$

$$\text{Ind}^{\text{h}}(\mathbf{\bar{N}}) = +\frac{\cosh\frac{m}{2}}{2\sinh\frac{\epsilon_1}{2}2\sinh\frac{\epsilon_2}{2}}\text{Ch}(\mathcal{E}^*), \qquad (A1)$$

where $\text{Ch}(\mathcal{V})$ denotes the Chern character of a vector bundle $\mathcal{V}$. $\mathcal{E}$ and $\mathcal{E}^*$ are the universal bundle and its complex conjugate, whose equivariant Chern characters are [3]

$$\text{Ch}(\mathcal{E}) = \chi_{\mathbf{4}}^{SU(4)}(v_{1,2,3,4}) - (e^{+\epsilon_+} + e^{-\epsilon_+} - e^{+\epsilon_-} - e^{-\epsilon_-})$$
$$\cdot \chi_{\mathbf{k}}^{U(k)}(\phi_{1,...,k}), \qquad (A2)$$

$$\text{Ch}(\mathcal{E}^*) = \chi_{\mathbf{\bar{4}}}^{SU(4)}(v_{1,2,3,4}) - (e^{+\epsilon_+} + e^{-\epsilon_+} - e^{+\epsilon_-} - e^{-\epsilon_-})$$
$$\cdot \chi_{\mathbf{\bar{k}}}^{U(k)}(\phi_{1,...,k}). \qquad (A3)$$

Second, for a general tensor product representation of **N** and **N̄**, it was suggested in [23] that the equivariant index

for a hypermultiplet can be computed by taking the tensor product of $\text{Ch}(\mathcal{E})$ and its complex conjugate $\text{Ch}(\mathcal{E}^*)$. For instance, the indices for $SU(N)$ adjoint and antisymmetric hypermultiplets are, respectively, written as [3,23]

$$\text{Ind}^{\text{h}}(\mathbf{adj}) = +\frac{\cosh\frac{m}{2}}{2\sinh\frac{\epsilon_1}{2}2\sinh\frac{\epsilon_2}{2}}\text{Ch}(\mathcal{E})\overline{\text{Ch}(\mathcal{E})}$$

$$\text{Ind}^{\text{h}}(\mathbf{anti}) = +\frac{\cosh\frac{m}{2}}{2\sinh\frac{\epsilon_1}{2}2\sinh\frac{\epsilon_2}{2}}\frac{\text{Ch}(\mathcal{E})^2 - \text{Ch}(\mathcal{E})|_{x\to2x}}{2},$$

$$(A4)$$

where $\text{Ch}(\mathcal{E})|_{x\to2x}$ means all chemical potentials appearing in $\text{Ch}(\mathcal{E})$ have to be doubled. Finally, the equivariant index for an adjoint vector multiplet is given by

$$\text{Ind}^{\text{v}}(\mathbf{adj}) = -\frac{\cosh\frac{\epsilon_+}{2}}{2\sinh\frac{\epsilon_1}{2}2\sinh\frac{\epsilon_2}{2}}\text{Ch}(\mathcal{E})\overline{\text{Ch}(\mathcal{E})}, \qquad (A5)$$

in which the overall negative sign reflects the opposite chirality of the gaugino with respect to hypermultiplet fermions.

Let us now extend the vector multiplet index (A5) to other representations as we do with hypermultiplets in (A4). Specifically, the index for an antisymmetric vector multiplet would be

$$\text{Ind}^{\text{v}}(\mathbf{anti}) = -\frac{\cosh\frac{\epsilon_+}{2}}{2\sinh\frac{\epsilon_1}{2}2\sinh\frac{\epsilon_2}{2}}\frac{\text{Ch}(\mathcal{E})^2 - \text{Ch}(\mathcal{E})|_{x\to2x}}{2}.$$

$$(A6)$$

Inserting (A2)–(A6), the equivariant index $\text{Ind}^{\text{v}}(\mathbf{anti})$ can be written as

$$\text{Ind}^{\text{v}}(\mathbf{anti}) = e^{+\epsilon_+}\cdot\chi_{\mathbf{\bar{k}}}^{U(k)}\chi_{\mathbf{\bar{4}}}^{SU(4)} + e^{+\epsilon_+}(e^{+\epsilon_-} + e^{-\epsilon_-})$$
$$\cdot\chi_{\mathbf{\overline{anti}}}^{U(k)} - e^{-\epsilon_+}(e^{+\epsilon_+} + e^{-\epsilon_+})\cdot\chi_{\mathbf{sym}}^{U(k)} \qquad (A7)$$

up to $U(k)$ independent terms that correspond to the 5D/6D perturbative zero modes. It consists of $k(k+3)$ bosonic terms and $k(k+1)$ fermionic terms, which we treat as our ansatz (2.6) for the UV resolution of $4k$ extra real bosonic zero modes of the instantons.

[1] M. F. Atiyah, N. J. Hitchin, V. G. Drinfeld, and Y. I. Manin, Phys. Lett. **65A**, 185 (1978).N. H. Christ, E. J. Weinberg, and N. K. Stanton, Phys. Rev. D **18**, 2013 (1978).

[2] N. Seiberg and E. Witten, Nucl. Phys. **B426**, 19 (1994); **B430**, 485 (1994).

[3] N. A. Nekrasov, Adv. Theor. Math. Phys. **7**, 831 (2003).

[4] H. C. Kim, S. Kim, and J. Park, arXiv:1608.03919.

[5] J. J. Heckman, D. R. Morrison, and C. Vafa, J. High Energy Phys. 05 (2014) 028; 06 (2015) 017(E).

[6] J. J. Heckman, D. R. Morrison, T. Rudelius, and C. Vafa, Fortschr. Phys. **63**, 468 (2015).

[7] D. R. Morrison and C. Vafa, Nucl. Phys. **B473**, 74 (1996).

[8] D. R. Morrison and C. Vafa, Nucl. Phys. **B476**, 437 (1996).

[9] E. Witten, Nucl. Phys. **B471**, 195 (1996).

[10] D. R. Morrison and W. Taylor, Central Eur. J. Phys. **10**, 1072 (2012).

[11] J. Kim, S. Kim, K. Lee, J. Park, and C. Vafa, J. High Energy Phys. 09 (2017) 098.

[12] J. Kim, S. Kim, and K. Lee, arXiv:1510.03128.

[13] B. Haghighat, A. Iqbal, C. Kozaz, G. Lockhart, and C. Vafa, Commun. Math. Phys. **334**, 779 (2015); B. Haghighat, C. Kozcaz, G. Lockhart, and C. Vafa, Phys. Rev. D **89**, 046003 (2014).

[14] B. Haghighat, A. Klemm, G. Lockhart, and C. Vafa, Fortschr. Phys. **63**, 294 (2015).

[15] A. Gadde, B. Haghighat, J. Kim, S. Kim, G. Lockhart, and C. Vafa, J. High Energy Phys. 02 (2018) 143.

[16] H. Hayashi and K. Ohmori, J. High Energy Phys. 06 (2017) 078.

[17] M. Del Zotto and G. Lockhart, J. High Energy Phys. 09 (2017) 081.

[18] M. Del Zotto, J. Gu, M. x. Huang, A. K. Kashani-Poor, A. Klemm, and G. Lockhart, J. High Energy Phys. 03 (2018) 156.

[19] J. Kim, K. Lee, and J. Park, J. High Energy Phys. 10 (2018) 100.

[20] M. Del Zotto and G. Lockhart, J. High Energy Phys. 08 (2018) 173.

[21] N. Nekrasov and S. Shadchin, Commun. Math. Phys. **252**, 359 (2004).

[22] C. Hwang, J. Kim, S. Kim, and J. Park, J. High Energy Phys. 07 (2015) 063; 04 (2016) 094(E).

[23] S. Shadchin, arXiv:hep-th/0502180.

[24] D. Tong, J. High Energy Phys. 04 (2014) 193.

[25] E. Witten, Nucl. Phys. **B403**, 159 (1993).

[26] H. C. Kim, S. Kim, E. Koh, K. Lee, and S. Lee, J. High Energy Phys. 12 (2011) 031.

[27] K. Hori, H. Kim, and P. Yi, J. High Energy Phys. 01 (2015) 124.

[28] C. Cordova and S. H. Shao, arXiv:1406.7853.

[29] F. Benini, R. Eager, K. Hori, and Y. Tachikawa, Lett. Math. Phys. **104**, 465 (2014).

[30] F. Benini, R. Eager, K. Hori, and Y. Tachikawa, Commun. Math. Phys. **333**, 1241 (2015).

[31] S. Nakamura, Prog. Theor. Exp. Phys. (**2015**), 073B02.

[32] R. Flume and R. Poghossian, Int. J. Mod. Phys. A **18**, 2541 (2003).

[33] U. Bruzzo, F. Fucito, J. F. Morales, and A. Tanzini, J. High Energy Phys. 05 (2003) 054.

[34] K. A. Intriligator, D. R. Morrison, and N. Seiberg, Nucl. Phys. **B497**, 56 (1997).

[35] G. Zafrir, J. High Energy Phys. 07 (2015) 087.

[36] P. Jefferson, H. C. Kim, C. Vafa, and G. Zafrir, arXiv:1705.05836.

[37] Y. Yun, J. High Energy Phys. 12 (2016) 016.

[38] R. Feger and T. W. Kephart, Comput. Phys. Commun. **192**, 166 (2015).

[39] M. Bershadsky and C. Vafa, arXiv:hep-th/9703167.

[40] H. Shimizu and Y. Tachikawa, J. High Energy Phys. 11 (2016) 165.

[41] M. B. Green, J. H. Schwarz, and P. C. West, Nucl. Phys. **B254**, 327 (1985).

[42] A. Sagnotti, Phys. Lett. B **294**, 196 (1992).

[43] K. Intriligator, J. High Energy Phys. 10 (2014) 162.

[44] K. Ohmori, H. Shimizu, Y. Tachikawa, and K. Yonekura, Prog. Theor. Exp. Phys. (**2014**), 103B07.

[45] S. Cremonesi, G. Ferlito, A. Hanany, and N. Mekareeya, J. High Energy Phys. 12 (2014) 103.

[46] A. Hanany, N. Mekareeya, and S. S. Razamat, J. High Energy Phys. 01 (2013) 070.

[47] G. Zafrir, J. High Energy Phys. 03 (2016) 109.

[48] H. C. Kim, S. S. Kim, and K. Lee, J. High Energy Phys. 10 (2012) 142.

[49] H. Hayashi, H. C. Kim, and T. Nishinaka, J. High Energy Phys. 06 (2014) 014.

[50] L. Bao, V. Mitev, E. Pomoni, M. Taki, and F. Yagi, J. High Energy Phys. 01 (2014) 175.

[51] O. Bergman, D. Rodríguez-Gómez, and G. Zafrir, J. High Energy Phys. 01 (2014) 079; 03 (2014) 112.

[52] S. Benvenuti, A. Hanany, and N. Mekareeya, J. High Energy Phys. 06 (2010) 100.

[53] K. Ohmori, H. Shimizu, Y. Tachikawa, and K. Yonekura, J. High Energy Phys. 12 (2015) 131.

[54] J. Kim, S. Kim, and K. Lee, J. High Energy Phys. 02 (2016) 170.

[55] M. Del Zotto, C. Vafa, and D. Xie, J. High Energy Phys. 11 (2015) 123.

[56] H.-C. Kim (unpublished).

[57] M. Del Zotto, J. J. Heckman, and D. R. Morrison, J. High Energy Phys. 09 (2017) 147.

[58] D. R. Morrison and N. Seiberg, Nucl. Phys. **B483**, 229 (1997).

[59] M. Aganagic, A. Klemm, M. Marino, and C. Vafa, Commun. Math. Phys. **254**, 425 (2005).

[60] R. Gopakumar and C. Vafa, arXiv:hep-th/9812127.

[61] A. Hanany and A. Zaffaroni, Nucl. Phys. **B529**, 180 (1998).

[62] I. Brunner and A. Karch, J. High Energy Phys. 03 (1998) 003.

[63] A. Gadde, S. S. Razamat, and B. Willett, Phys. Rev. Lett. **115**, 171604 (2015); P. Putrov, J. Song, and W. Yan, J. High Energy Phys. 03 (2016) 185.

[64] K. Maruyoshi and J. Song, Phys. Rev. Lett. **118**, 151602 (2017); J. High Energy Phys. 02 (2017) 075; P. Agarwal, K. Maruyoshi, and J. Song, J. High Energy Phys. 12 (2016) 103; 04 (2017) 113(A); P. Agarwal, A. Sciarappa, and J. Song, J. High Energy Phys. 10 (2017) 211; S. Benvenuti and S. Giacomelli, J. High Energy Phys. 10 (2017) 106.

[65] H. C. Kim, J. High Energy Phys. 03 (2016) 199.

[66] D. Gaiotto and H. C. Kim, J. High Energy Phys. 10 (2016) 012.

[67] M. Bullimore, H. C. Kim, and P. Koroteev, J. High Energy Phys. 05 (2015) 095.

[68] D. Gaiotto and H. C. Kim, J. High Energy Phys. 01 (2017) 019.

[69] H. Hayashi, S. S. Kim, K. Lee, and F. Yagi, J. High Energy Phys. 03 (2018) 125.